Quasi Deterministic Radio Channel Generator User Manual and Documentation

Document Revision: v1.0.7-191

June 26, 2013

Fraunhofer Heinrich Hertz Institute
Wireless Communication and Networks
Einsteinufer 37, 10587 Berlin, Germany

e-mail: quadriga@hhi.fraunhofer.de
http://www.quadriga-channel-model.de

Fraunhofer
Heinrich Hertz Institute

Contributors

Editor:	Fraunhofer Heinrich Hertz Institute Wireless Communication and Networks Einsteinufer 37, 10587 Berlin, Germany
Contributing Authors:	Stephan Jaeckel, Leszek Raschkowski, Kai Börner and Lars Thiele *Fraunhofer Heinrich Hertz Institute* Frank Burkhardt and Ernst Eberlein *Fraunhofer Institute for Integrated Circuits IIS*

Grants and Funding

This work was supported by

- the European Space Agency (ESA) in the Advanced Research in Telecommunications Systems (ARTES) programme under contract AO/1-5985/09/08/NL/LvH (Acronym: MIMOSA), [EHB+13]
  http://telecom.esa.int/telecom/www/object/index.cfm?fobjectid=31061
- the German Federal Ministry of Economics and Technology (BMWi) in the national collaborative project IntelliSpektrum under contract 01ME11024
  http://www.intellispektrum.de

Acknowledgements

The authors thank G. Sommerkorn, C. Schneider, M. Kaeske [Ilmenau University of Technology (IUT), Ilmenau, Germany] and V. Jungnickel [Heinrich Hertz Institute (HHI), Berlin, Germany] for the fruitful discussions on the QuaDRiGa channel model and the manuscript of this document.

How to Cite this Document

[JRB+13] S. Jaeckel, L. Raschkowski, K. Börner, L. Thiele, F. Burkhardt and E. Eberlein, "QuaDRiGa - Quasi Deterministic Radio Channel Generator, User Manual and Documentation", Fraunhofer Heinrich Hertz Institute, Tech. Rep. v1.0.5-171, 2013.

Contents

eMail: quadriga@hhi.fraunhofer.de

List of Figures

List of Tables

List of Acronyms

AoA	angle of arrival. 58, 76
AoD	angle of departure. 58
BS	base station. 10, 58, 59, 79
CIR	channel impulse response. 35, 68, 70
DS	delay spread. 67–70, 80, 81
FIR	finite impulse response. 68
KF	Ricean K-factor. 67, 70, 71, 79
LBS	last bounce scatterer. 74, 75
LHCP	left hand circular polarized. 62
LOS	line of sight. 11, 21, 22, 24, 27–29, 32, 35–38, 40, 41, 44–46, 50–52, 58, 59, 71, 74–76, 78–80
LSP	large scale parameter. 11–15, 31, 35, 38, 40, 45, 50, 64, 67–69, 74, 80
MIMO	multiple-input multiple-output. 10, 60
MPC	multipath component. 58, 79
MT	mobile terminal. 10, 58, 59, 79, 80
NLOS	non line of sight. 21, 22, 24, 26, 28, 32, 33, 35, 38, 40, 42, 46, 48, 50–52, 64, 65, 70, 74, 77, 78
PDP	power delay profile. 70
PG	path gain. 79
PL	path loss. 64
RHCP	right hand circular polarized. 62
Rx	receiver. 71, 74–76, 79
SCM	spatial channel model. 11, 60, 74, 77
SF	shadow fading. 79
SISO	single input single output. 10
Tx	transmitter. 71, 74–76, 79
UML	unified modeling language. 54
WINNER	Wireless World Initiative for New Radio. 10, 11, 58, 67, 74, 78, 80
XPR	cross polarization ratio. 78

List of Symbols

γ	Polarization rotation angle derived from the NLOS XPD
$\hat{\phi}_m$	Offset angle of the m-th subpath relative to (ϕ, θ)
κ	Cross polarization power ratio
λ	Carrier wavelength
$\mathbf{a}$	Departure- or Arrival vector in Cartesian Coordinates
$\mathbf{B}$	Autocorrelation map of a large scale parameter
$\mathbf{e}_r$	Position of the r^{th} element in the receive array (relative to the array center)
$\mathbf{F}(\phi, \theta)$	Antenna field pattern
$\mathbf{G}_l$	Coefficient matrix of a tap between all n_t Tx antennas and n_r Rx antennas
$\mathbf{H}_{n,s}$	MIMO channel matrix for all n_t Tx antennas and n_r Rx antennas in frequency domain
$\mathbf{M}$	Polarization coupling matrix
$\mathbf{o}_{r/t}$	Antenna orientation vector for the receiver/transmitter
$\mathbf{p}_{r/t}$	Projection of the orientation vector $\mathbf{o}_{r/t}$ on the plane perpendicular to $\mathbf{r}$
$\mathbf{r}$	Wave travel direction in Cartesian coordinates
ϕ	Azimuth angle, ϕ^a for arrival (AoA), ϕ^d for departure (AoD)
ϕ_{LOS}	LOS direction seen from the receiver
$\psi_{l,m,s}$	Phase of the m^{th} subpath of the l^{th} cluster at snapshot position s
ρ	Correlation coefficient
σ_ϕ	Angular Spread
σ_τ	RMS delay spread
$\tau_{l,s}$	Delay of the l^{th} cluster at snapshot position s
PL	Path Loss (linear scale), $\text{PL}_{[\text{dB}]} = 10 \cdot \log_{10} \text{PL}$ is for logarithmic scale
SD	Sample Density in units of samples per half wave length
SF	Shadow Fading (linear scale), $\text{SF}_{[\text{dB}]} = 10 \cdot \log_{10} \text{SF}$ is for logarithmic scale
θ	Elevation angle, θ^a for arrival (EoA), θ^d for departure (EoD)
ϑ	Polarization rotation angle used for the coupling matrix $\mathbf{M}$
ζ	Per Cluster Shadow Fading
a_k, b_k	Filter coefficients
c	Speed of Light
$C_\phi(L, K)$	Correction function for the initial angles
$C_\tau(K)$	Correction function for the initial path delays
c_{AoA}	Cluster-wise azimuth spread of arrival
d	Distance; also used a path length
d_λ	Decorrelation distance
d_r	Total length of the wave travel direction vector $\mathbf{r}$
d_{LOS}	Distance between the receiver position and the scatterers for the LOS cluster
d_{px}	Distance (in m) between two adjacent pixels of the autocorrelation map $\mathbf{B}$
f_c	Carrier Frequency
f_S	Sampling Rate – in units of samples per meter
f_T	Sampling Rate – in units of samples per second
$g_{r,t,l}$	Complex amplitude of a tap between Tx antenna t and Rx antenna r
$h_{r,t,n}$	Channel coefficient in frequency domain
K	Ricean K-factor (linear scale), $K_{[\text{dB}]}$ is for logarithmic scale
k	Filter coefficient index
L	Number of clusters or paths

eMail: quadriga@hhi.fraunhofer.de

l	Cluster or path index, $l = 1...L$
m	Subpath index, $m = 1...20$
N	Number of carriers
n	Carrier index; $n = 1 \dots N$
n_r	Number of receive antennas
n_t	Number of transmit antennas
P_l	Cluster power
r	Receive antenna index; $t = 1 \dots n_r$
r_τ	Delay distribution proportionality factor
S	Number of snapshots in one segment
s	Snapshot index within one segment
t	Transmit antenna index; $t = 1 \dots n_t$
v	Speed
X,Y,Z	Random variables, e.g. $X \sim \mathrm{uni}(X_{\min}, X_{\max})$ for uniform or $X \sim \mathrm{N}(\mu, \sigma)$ for Normal distribution

eMail: quadriga@hhi.fraunhofer.de

References

[3GP05] 3GPP TDOC R4-050854. Spatial radio channel models for systems beyond 3G. Technical report, Elektrobit, Nokia, Siemens, Philips, Alcatel, Telefonica, Lucent, Ericsson, 8 2005.

[3GP11] 3GPP TR 25.996 v10.0.0. Spatial channel model for multiple input multiple output (MIMO) simulations. Technical report, 3 2011.

[BHS05] D.S. Baum, J. Hansen, and J. Salo. An interim channel model for beyond-3G systems. *Proc. IEEE VCT '05 Spring*, 5:3132–3136, 2005.

[CG03] Xiaodong Cai and Georgios B. Giannakis. A two-dimensional channel simulation model for shadowing processes. *IEEE Trans. Veh. Technol.*, 52(6):1558–1567, 2003.

[Cla05] H. Claussen. Efficient modelling of channel maps with correlated shadow fading in mobile radio systems. *Proc. IEEE PIMRC' 05*, 1:512 –516, 2005.

[EHB+13] Ernst Eberlein, Thomas Heyn, Frank Burkhardt, Stephan Jaeckel, Lars Thiele, Thomas Haustein, Gerd Sommerkorn, Martin Käske, Christian Schneider, Maria Dominguez, and Joel Grotz. Characterisation of the MIMO channel for mobile satellite systems (acronym: MIMOSA), TN8.2 – final report. Technical Report v1.0, Fraunhofer Institute for Integrated Circuits (IIS), 2013.

[Gud91] M. Gudmundson. Correlation model for shadow fading in mobile radio systems. *IET Electron Lett.*, 27(23):2145–2146, November 1991.

[Hat80] M. Hata. Empirical formula for propagation loss in land mobile radio services. *IEEE Trans. Veh. Technol.*, 29(3):317–325, 1980.

[HMK+10] Petteri Heino, Juha Meinilä, Pekka Kyösti, et al. CELTIC / CP5-026 D5.3: WINNER+ final channel models. Technical report, 2010.

[JRB+13] S. Jaeckel, L. Raschkowski, K. Börner, L. Thiele, F. Burkhardt, and E. Eberlein. QuaDRiGa - Quasi Deterministic Radio Channel Generator, User Manual and Documentation. Technical Report v1.0.5-171, Fraunhofer Heinrich Hertz Institute, 2013.

[KMH+07] Pekka Kyösti, Juha Meinilä, Lassi Hentilä, et al. IST-4-027756 WINNER II D1.1.2 v.1.1: WINNER II channel models. Technical report, 2007.

[MTIO09] L. Materum, J. Takada, I. Ida, and Y. Oishi. Mobile station spatio-temporal multipath clustering of an estimated wideband MIMO double-directional channel of a small urban 4.5 GHz macrocell. *EURASIP J. Wireless Commun. Netw.*, 2009.

[NKS+07] M. Narandzic, M. Käske, C. Schneider, M. Milojevic, M. Landmann, G. Sommerkorn, and R.S. Thomä. 3D-antenna array model for IST-WINNER channel simulations. *Proc. IEEE VTC '07 Spring*, pages 319–323, 2007.

[NSK+11] M. Narandzic, C. Schneider, M. Käske, S. Jaeckel, G. Sommerkorn, and R.S. Thomä. Large-scale parameters of wideband MIMO channel in urban multi-cell scenario. *Proc. EUCAP '11*, 2011.

[OCGD08] C. Oestges, B. Clerckx, M. Guillaud, and M. Debbah. Dual-polarized wireless communications: From propagation models to system performance evaluation. *IEEE Trans. Wireless Commun.*, 7(10):4019–4031, 2008.

[PB01] M.F. Pop and N.C. Beaulieu. Limitations of sum-of-sinusoids fading channel simulators. *IEEE Trans. Commun.*, 49(4):699–708, 2001.

eMail: quadriga@hhi.fraunhofer.de

[PHL+11] J. Poutanen, K. Haneda, Lingfeng Liu, C. Oestges, F. Tufvesson, and P. Vainikainen. Parameterization of the COST 2100 MIMO channel model in indoor scenarios. *Proc. EUCAP '11*, pages 3606–3610, 2011.

[PMF97] K.I. Pedersen, P.E. Mogensen, and B.H. Fleury. Power azimuth spectrum in outdoor environments. *Electronics Letters*, 33(18):1583–1584, 1997.

[QOHDD10] F. Quitin, C. Oestges, F. Horlin, and P. De Doncker. A polarized clustered channel model for indoor multiantenna systems at 3.6 GHz. *IEEE Trans. Veh. Technol.*, 59(8):3685–3693, 2010.

[Rap02] T.S. Rappaport. *Wireless Communications. Principles and Practice.* Prentice Hall, 2 edition, 2002.

[SNK+10] C. Schneider, M. Narandzic, M. Käske, G. Sommerkorn, and R.S. Thomä. Large scale parameter for the WINNER II channel model at 2.53 GHz in urban macro cell. *Proc. IEEE VTC '10 Spring*, 2010.

[Sva01] T. Svantesson. A physical MIMO radio channel model for multi-element multi-polarized antenna systems. *Proc. IEEE VTC' 01 Fall*, 2:1083–1087, 2001.

[SZM+06] M. Shafi, Min Zhang, A.L. Moustakas, P.J. Smith, A.F. Molisch, F. Tufvesson, and S.H. Simon. Polarized MIMO channels in 3-D: models, measurements and mutual information. *IEEE J. Sel. Areas Commun.*, 24:514–527, Mar. 2006.

[ZRP+05] Y. Zhou, S. Rondineau, D. Popovic, A. Sayeed, and Z. Popovic. Virtual channel space-time processing with dual-polarization discrete lens antenna arrays. *IEEE Trans. Antennas Propag.*, 53:2444–2455, Aug. 2005.

eMail: quadriga@hhi.fraunhofer.de

1 Introduction and Overview

1.1 General Remarks

This document gives a detailed overview of the QuaDRiGa channel model and its implementation details. The model has been evolved from the Wireless World Initiative for New Radio (WINNER) channel model described in WINNER II deliverable D1.1.2 v.1.1 [KMH+07]. This document covers only the model itself. Measurement campaigns covering the extraction of suitable parameters can be found in the WINNER documentation [KMH+07, HMK+10] or other publications such as [SNK+10, NSK+11]. Furthermore, the MIMOSA project [EHB+13] covers the model development and parameter extraction for land-mobile satellite channels.

The QuaDRiGa channel model follows a geometry-based stochastic channel modeling approach, which allows the creation of an arbitrary double directional radio channel. The channel model is antenna independent, i.e. different antenna configurations and different element patterns can be inserted. The channel parameters are determined stochastically, based on statistical distributions extracted from channel measurements. The distributions are defined for, e.g. delay spread, delay values, angle spread, shadow fading, and cross-polarization ratio. For each channel segment the channel parameters are calculated from the distributions. Specific channel realizations are generated by summing contributions of rays with specific channel parameters like delay, power, angle-of-arrival and angle-of- departure. Different scenarios are modeled by using the same approach, but different parameters. The basic features of the model approach can be summarized as follows:

- Support of freely configurable network layouts with multiple transmitters and receivers
- Scalability from a single input single output (SISO) or multiple-input multiple-output (MIMO) link to a multi-link MIMO scenario
- Same modeling approach for both indoor and outdoor environments as well as combinations of them
- Support of a frequency range of 2-6 GHz with up to 100 MHz RF bandwidth
- Support of multi-antenna technologies, polarization, multi-user, multi-cell, and multi-hop networks
- Smooth time evolution of large-scale and small-scale channel parameters including the transition between different scenarios
- High accuracy for the calculation of the polarization characteristics

The QuaDRiGa channel model largely extends the WINNER model to support several new features that were originally not included. These are

- Time evolution
  Short term time evolution of the channel coefficients is realized by updating the delays, the departure- and arrival angels, the polarization, the shadow fading and the K-Factor based on the position of the terminal.
- Scenario transitions
  When the mobile terminal (MT) moves through the fading channel, it may pass through several different scenarios. QuaDRiGa supports smooth transitions between adjacent channel segments. This is used to emulate long term time evolution and allows the simulation of e.g. handover scenarios.
- Variable speeds for mobile terminals
  QuaDRiGa supports variable speeds including accelerating and sowing down of mobile terminals.
- Common framework for LOS and NLOS simulations
  In WINNER, LOS and NLOS scenarios were treated differently. QuaDRiGa used the same method for both scenarios types. This reduces the model complexity and enables freely configurable multicell scenarios. E.g. one MT can see two base stations (BSs), one in LOS and another in NLOS.

- Geometric polarization
  The polarizations for the LOS and for the NLOS case is now calculated based on a ray-geometric approach.
- Improved method for calculating correlated large scale parameters (LSPs)
  The WINNER model calculates maps of correlated parameter values using filtered random numbers. `QuaDRiGa` uses the same method but extends the map generation algorithm to also consider diagonal movement directions and to create smoother outputs.
- New functions for modifying antenna patterns
  Antenna patterns can now be freely rotated in 3D-coordinates while maintaining the polarization properties.
- New MATLAB implementation
  The MATLAB code was completely rewritten. The implementations now fosters object oriented programming and object handles. This increases the performance significantly and lowers the memory usage.

The `QuaDRiGa` approach can be understood as a "statistical ray-tracing model." Unlike the classical ray tracing approach, it doesn't use an exact geometric representation of the environment but distributes the positions of the scattering clusters (the sources of indirect signals such as buildings or trees) randomly. A simplified overview of the model is depicted in Fig. 2. For each path, the model derives the angle of departure (the angle between the transmitter and the scatterer), the angle of arrival (the angle between the receiver and the scatterer) and the total path length d which results in a delay τ of the signal. For the sake of simplicity, only two paths are shown in the figure.

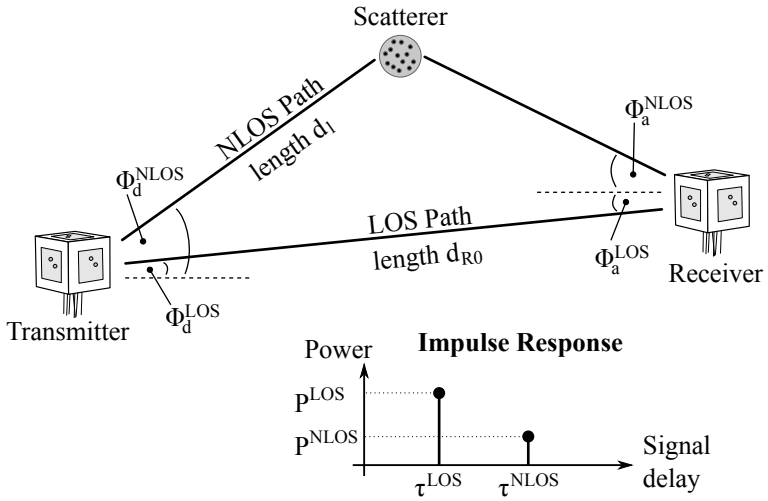

Figure 1: Simplified overview of the modeling approach used in `QuaDRiGa`

Normally, the spatial channel model (SCM) uses 6 clusters, the WINNER model up to 20 and `QuaDRiGa` supports a variable number of up to 42 clusters. The output is an ordered list of complex-valued Dirac-functions at a specific delay. If the simulation contains a line of sight (LOS) component, this signal component always arrives first at the receiver as the according path length is the shortest possible. When there are no obstructions, then that signal is also dominant in the impulse response.

The following section describes some of the Key features of the model using a real world example. A detailed introduction with a variety of tutorials, test cases and interface descriptions then follows in section 2. The later part of the document then focusses on the mathematical models behind the software and the assumptions made.

eMail: quadriga@hhi.fraunhofer.de

1.2 Description of modeling of different reception conditions by means of a typical drive course

This section shows how different reception conditions and their changes are modeled within the QuaDRiGa model. The description is done with the help of a typical driving course in a satellite scenario.

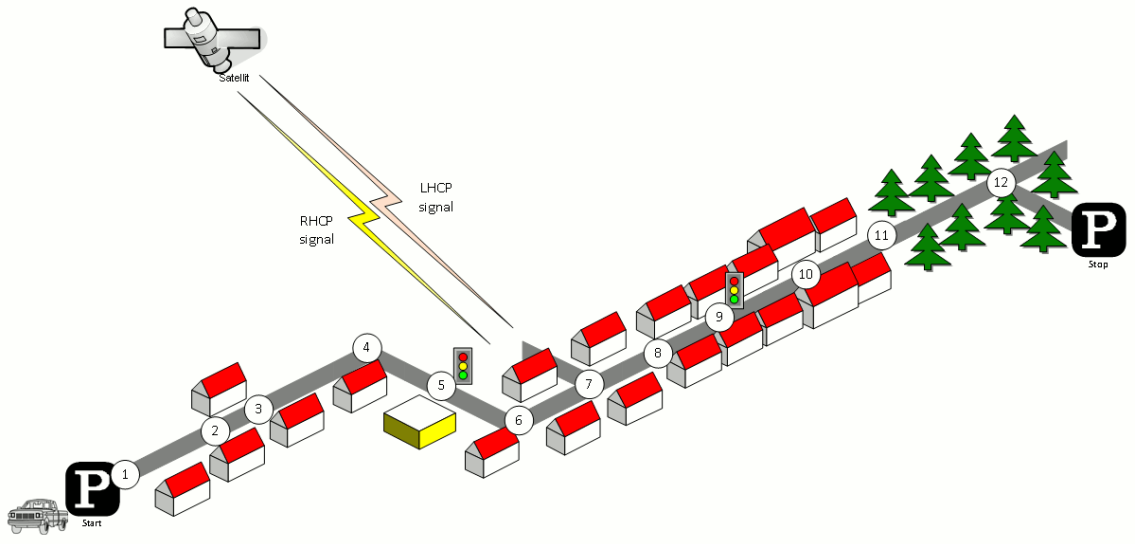

Figure 2: Typical driving course: From home to woodland parking site on the village outskirts

The different effects along the track can be summarized as follows:

1. Start Environment: Urban, LOS reception of satellite signal
2. LOS → NLOS Change
3. NLOS → LOS Change
4. Turning off without change in reception condition (LOS)
5. Stopping at traffic light (LOS)
6. Turning off with change of reception condition (LOS → NLOS)
7. Crossing side Street (NLOS → short LOS → NLOS)
8. Structural change in the environment without a change in the environment type (higher density of buildings but still the environment remains urban)
9. Stopping at traffic lights (NLOS)
10. Houses have the same characteristics as before but are further away from the street (urban environment with different reception characteristics)
11. Change of environment (Urban → Forest)
12. Turning off without change of environment (NLOS)

Each simulation run in QuaDRiGa is done in three (and an optional fourth) step.

1. Set up tracks, scenarios, antennas and network layout
2. Generate correlated LSPs
3. Calculate the channel coefficients
4. (optional) Post-processing

Those steps also need to be done for the above scenario. However, different aspects of the track are handled in different parts of the model. Additionally, the QuaDRiGa model supports two operating modes for handling the LSPs:

1. The first (default) mode generates the correlated LSPs automatically based on a scenario-specific parameter set. This is done in step 2 and involves so called parameter maps.

2. The manual mode does not generate LSPs automatically. Here, the user has to supply a list of parameters to the model. The step 2 thus to be implemented by the user.

Steps 1, 3 and 4 are identical for both modes. The following list describes the modeling of the observed effects along the track when using the automatic mode (1).

1. **Start Environment: Urban, LOS reception of satellite signal**
   Each segment along the track gets assigned an environment. In the QuaDRiGa terminology, this is called a scenario. E.g. the first segment on the track is in the "Satellite-LOS-Urban"-scenario. The selection of the scenario is done during the first step (set up tracks, scenarios, antennas and network layout). QuaDRiGa itself does not supply functions to perform the setting up of tracks and scenarios automatically. However, external scripts can be used to perform this task. An example can be found in section 2.2.3. A RHCP/LHCP signal is defined in the antenna setup.

   After the model setup, the "automatic mode" generates a set of LSPs for this segment. I.e. the second step of the model calculates one value for each of the 7 LSPs using the map-based method. Thus, a set of seven maps is created for the scenario "Satellite-LOS-Urban". Those maps cover the entire track. Thus, the same maps are used for all "Satellite-LOS-Urban"-segments of the track.

   The third step then calculates a time-series of fading coefficients for the first segment that have the properties of the LSPs from the map. E.g. if one calculates the RMS-DS from the coefficients, one gets the same value as generated by the map in step 2.

2. **LOS → NLOS Change**
   A scenario change is defined along the track. E.g. the second segment along the track gets assigned the scenario "Satellite-NLOS-Urban". Now, a second set of maps is generated for all "Satellite-NLOS-Urban"-segments. So in total, we now have 14 maps (seven for LOS and another seven for NLOS). The parameters for calculating the channel coefficients are drawn from the second seven maps.

   We get a set of channel coefficients with different properties (e.g. more multipath components, lower K-Factor etc.). A smooth transition between the coefficients from the first segment and the second is realized by the ramping down the powers of the clusters of the old segment and ramping up the power of the new. This is implemented in step 4 (Post-processing).

3. **NLOS → LOS Change**
   This is essentially the same as in point 2. However, since the third segment is also in the scenario "Satellite-LOS-Urban", no new maps are generated. The parameters are extracted from the same map as for the starting segment.

4. **Turning off without change in reception condition (LOS)**
   QuaDRiGa supports free 3D-trajectories for the receiver. Thus, no new segment is needed - the terminal stays in the same segment as in point 3. However, we assume that the receive antenna is fixed to the terminal. Thus, if the car turns around, so does the antenna. Hence, the arrival angles of all clusters, including the direct path, change. This is modeled by a time-continuous update of the angles, delays and phases of each multipath component, also known as drifting. Due the change of the arrival angles and the path-lengths, the terminal will also see a change in its Doppler-profile.

5. **Stopping at traffic light (LOS)**
   QuaDRiGa performs all internal calculations at a constant speed. However, a stop of the car at a traffic light is realized by interpolating the channel coefficients in an additional post processing step (step 4). Here, the user needs to supply a movement profile that defines all acceleration, deceleration or stopping points along the track. An example is given in section 2.2.6. Since the interpolation is an independent step, it makes no difference if the mobile terminal is in LOS or NLOS conditions.

eMail: quadriga@hhi.fraunhofer.de

6. **Turning off with change of reception condition (LOS → NLOS)**
   This is realized by combining the methods of point 2 (scenario change) and point 4 (turning without change). The scenario change is directly in the curve. Thus, the LOS and the NLOS segments have an overlapping part where the cluster powers of the LOS segment ramp down and the NLOS clusters ramp up. The update of the angles, delays and phases is done for both segments in parallel.

7. **Crossing side Street (NLOS → short LOS → NLOS)**
   This is modeled by two successive scenario changes (NLOS-LOS and LOS-NLOS). For both changes, a new set of clusters is generated. However, since the parameters for the two NLOS-segments are extracted from the same map, they will be highly correlated. Thus, the two NLOS segments will have similar properties.

8. **Structural change in the environment without a change in the environment type** (higher density of buildings but still the environment remains urban)
   This is not explicitly modeled. However, the "Satellite-NLOS-Urban"-map covers a typical range of parameters. E.g. in a light NLOS area, the received power can be some dB higher compared to an area with denser buildings. The placement of light/dense areas on the map is random. Thus, different characteristics of the same scenario are modeled implicit. They are covered by the model, but the user has no influence on where specific characteristics occur on the map when using the automatic mode. An alternative would be to manually overwrite the automatically generated parameters or use the manual mode.

   In order to update the LSPs and use a new set of parameters, a new segment needs to be created. I.e. here, an environment change from "Satellite-NLOS-Urban" to the same "Satellite-NLOS-Urban" has to be created. Thus, a new set of LSPs is read from the map and new clusters are generated accordingly.

9. **Stopping at traffic lights (NLOS)**
   This is the same as in point 5.

10. **Structural change in environment**. Houses have the same characteristics as before but are further away from the street (urban environment with different reception characteristics)
    Same as point 8.

11. **Change of environment (Urban → Forest)**
    This is the same as in point 2. The segment on the track gets assigned the scenario "Satellite-Forest" and a third set of maps (15-21) is generated for the "Satellite-Forest"-segment. The parameters are drawn from those maps, new channel coefficients are calculated and the powers of the clusters are ramped up/down.

12. **Turning off without change of environment (NLOS)**
    Same as in point 4.

2 Getting Started with QuaDRiGa

2.1 Installation and System Requirements

The installation is straightforward and it does not require any changes to your system settings. If you would like to use QuaDRiGa, just extract the ZIP-File containing the model files and add the "source"-folder from the extracted archive to you MATLAB-Path. This can be done by opening MATLAB and selecting "File" - "Set Path ..." from the menu. The you can use the "Add folder ..." button to add QuaDRiGa to your MATLAB-Path.

Table 1: Minimum System Requirements

Requirement	Value
Processing power	1 GHz Single Core
Memory	1 GB
Storage	50 MB
Operating System	Linux, Windows, Mac OS
MATLAB	7.12 (R2011a)

2.2 Tutorials

In the following, we provide a variety of tutorials that can get you started with QuaDRiGa. You can also use the MATLAB Help to access these files.

2.2.1 Network Setup and Parameter Generation

The channel model class 'parameter_set' generates correlated values for the LSPs. The channel builder then uses those values to create coefficients that have the specific properties defined in 'parameter_set'. One important question is therefore: Can the same properties which are defined in 'parameter_set' also be found in the generated coefficients? This is an important test to verify, if all components of the channel builder work correctly.

Channel model setup and coefficient generation We first set up the basic parameters. We do not need drifting here, since no time varying channels are generated.

```
close all
clear all

set(0,'defaultTextFontSize', 14)
set(0,'defaultAxesFontSize', 14)

s = simulation_parameters;
s.center_frequency = 2.53e9;
s.sample_density = 2;
s.use_absolute_delays = 1;
s.drifting_precision = 0;
```

We have one transmitter and 250 receiver positions. Each receiver gets a specific channel. However, the receivers LSPs will be correlated. We use omni directional antennas at all terminals.

```
l = layout( s );
l.no_rx = 250;
l.randomize_rx_positions( 200 , 1.5 , 1.5 , 1 );  % 200 m radius, 1.5 m Rx height
l.track.set_scenario('BERLIN_UMa_NLOS');

l.tx_position(3) = 25;                            % 25 m tx height
l.tx_array.generate( 'omni' );
l.rx_array = l.tx_array;

l.visualize([],[],0);
view(-33, 60);
```

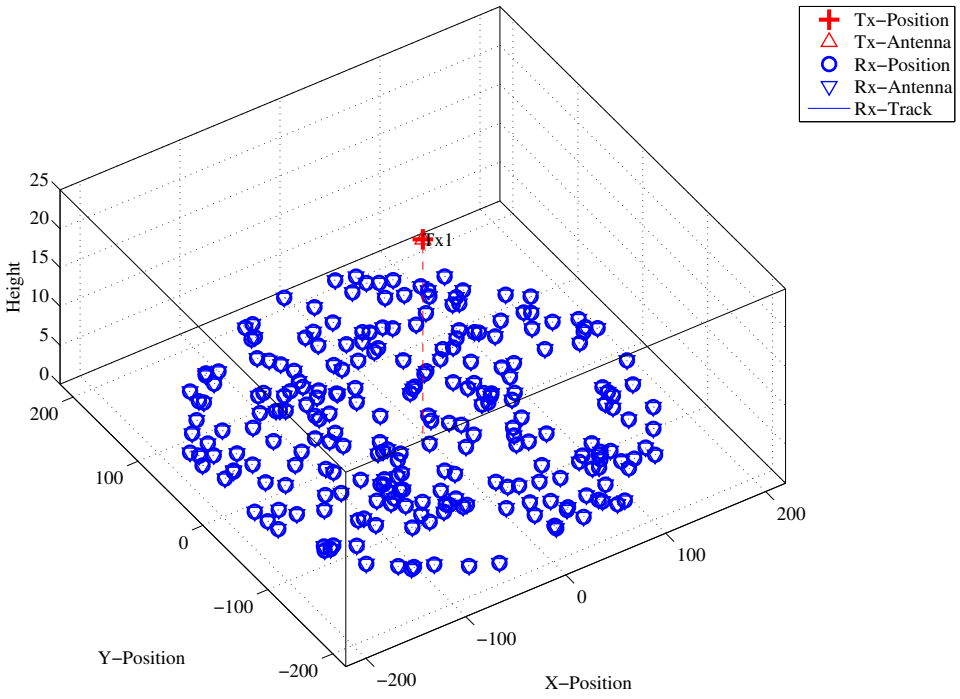

Figure 3: Distribution of the users in the scenario.

We set up the scenario such that there is no XPR. I.e. all vertical polarized paths will remain vertical after a reflection. The same result would be achieved with a perfectly X-polarized array at the receiver and summing up the power over all elements. We further increase the KF to have a wider spread. This allows us to study the parameters at a wider range when evaluating the results.

```
p = l.create_parameter_sets(0);
p.plpar = [];
p.scenpar.xpr_mu    = 100;              % Disable XPR
p.scenpar.xpr_sigma = 0;
p.scenpar.KF_mu     = 5;                % Increase KF-Range
p.scenpar.KF_sigma  = 15;
p.scenpar.DS_mu     = log10(0.6e-6);    % Median DS = 600 ns
p.scenpar.DS_sigma  = 0.3;              % 300-1200 ns range
p.update_parameters;

c = p.get_channels;

coeff = squeeze( cat( 1, c.coeff ) );
delay = permute( cat(3,c.delay) , [3,1,2] );
```

```
Parameters    [ooooooooooooooooooooooooooooooooooooooooooooooooooooo]     5 seconds
Channels      [ooooooooooooooooooooooooooooooooooooooooooooooooooooo]     8 seconds
```

Results and discussion In the following four plots, we extract parameters from the generated coefficients and compare them with the initial ones which were generated by the 'parameter_set' object (P). The values in (P) can be seen as a request to the channel builder and the values in the generated coefficients (C) as a delivery.

We first calculate the SF from the channel data by summing up the power over all 20 taps. We see, that the values are almost identical.

```
sf = sum(mean( abs(coeff).^2 ,3),2);

figure
plot(-35:35,-35:35,'k')
hold on
plot([-35:35]+3,-35:35,'--k')
plot([-35:35]-3,-35:35,'--k')
plot( 10*log10(p.sf') , 10*log10(sf) , '.'  )
hold off
axis([ -25 , 25 , -25, 25 ])

legend('Equal','+/- 3dB',4)
xlabel('SF_P [dB]');
ylabel('SF_C [dB]');
title('Shadow Fading - Requested vs. generated value');
```

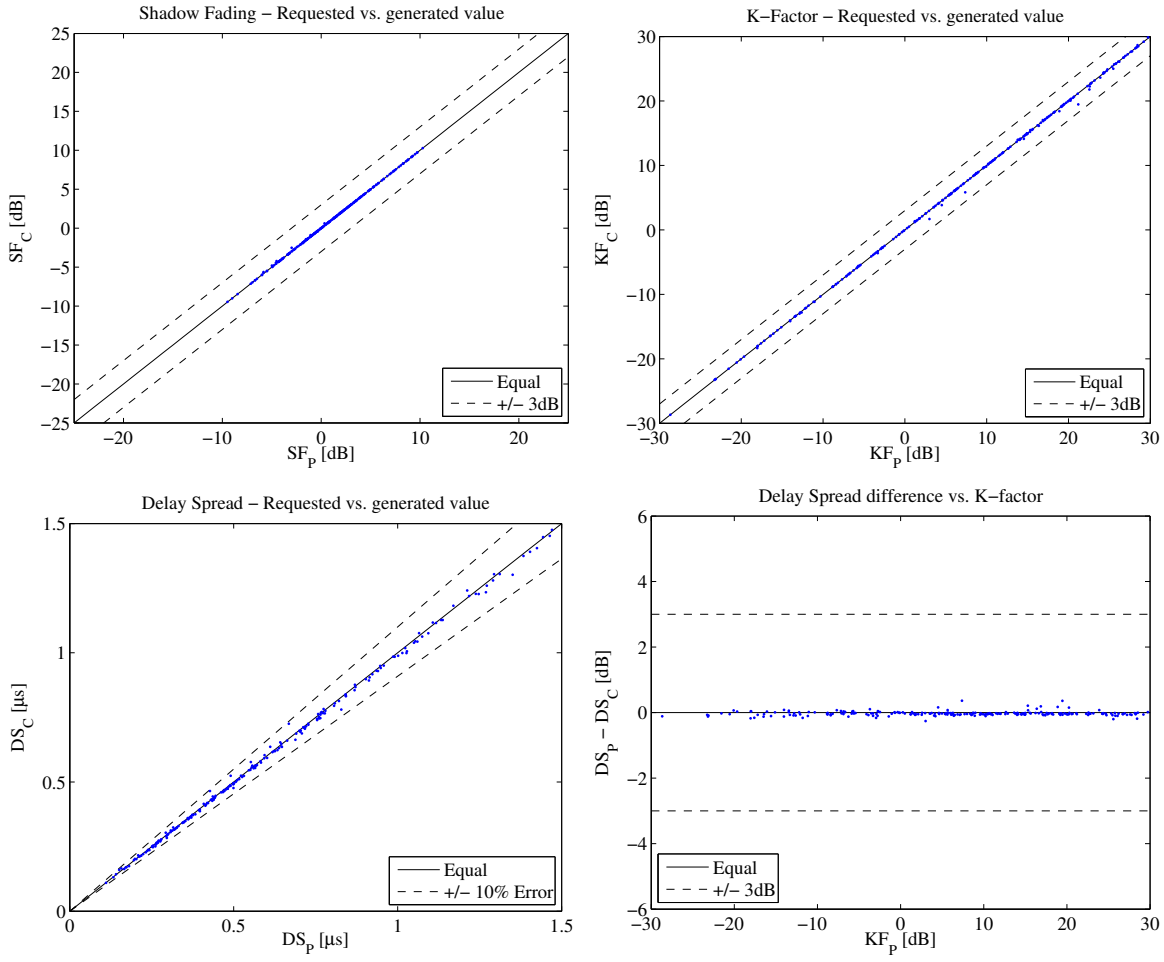

Figure 4: Comparison of input values and simulation results

Next, we repeat the same calculation for the K-Factor. Again, we see that the values are almost identical.

```
p_nlos = sum(mean( abs(coeff(:,2:end,:)).^2 ,3),2);
p_los  = mean( abs(coeff(:,1,:)).^2 ,3);
kf = p_los./p_nlos;

figure
plot(-35:35,-35:35,'k')
hold on
plot([-35:35]+3,-35:35,'--k')
plot([-35:35]-3,-35:35,'--k')
plot( 10*log10(p.kf') , 10*log10(kf) , '.'  )
hold off
axis([ -30 , 30 , -30, 30 ])

legend('Equal','+/- 3dB',4)
xlabel('KF_P [dB]');
ylabel('KF_C [dB]');
title('K-Factor - Requested vs. generated value');
```

Now we repeat the calculation for the RMS delays spread.

```
pow_tap = abs(coeff).^2;
pow_sum = sum(pow_tap,2);
mean_delay = sum( pow_tap.*delay,2) ./ pow_sum;
ds = sqrt( sum( pow_tap.*delay.^2 ,2)./ pow_sum - mean_delay.^2 );
ds = mean(ds,3);

figure
plot([0:0.1:2],[0:0.1:2],'k')
hold on
plot([0:0.1:2]*1.1,[0:0.1:2],'--k')
plot([0:0.1:2],[0:0.1:2]*1.1,'--k')
plot( p.ds'*1e6 , (ds')*1e6 , '.'  )
hold off
axis([ 0,1.5,0,1.5 ])

legend('Equal','+/- 10% Error',4)
xlabel('DS_P [\mus]');
ylabel('DS_C [\mus]');
title('Delay Spread - Requested vs. generated value');
```

The following plot shows the RMSDS of the requested and generated values (in dB) vs. the K-factor. A value of +3 means, that the RMSDS of the generated coefficients is twice a high as in the parameter_set (P). We see, that for a K-Factor of up to 30 dB, the DS difference is small (less than 3 dB).

```
figure
plot([-35,35],[0,0],'k')
hold on
plot([-35,35],[-3,-3],'--k')
plot([-35,35],[3,3],'--k')
plot( 10*log10(p.kf'), 10*log10(ds./p.ds') , '.' )
hold off
axis([ -30 , 30 , -6 6 ])

legend('Equal','+/- 3dB',3)
xlabel('KF_P [dB]');
ylabel('DS_P - DS_C [dB]');
title('Delay Spread difference vs. K-factor');
```

```
close all
disp(['QuaDRiGa Version: ',simulation_parameters.version])
```

```
QuaDRiGa Version: 1.0.1-145
```

2.2.2 Simulating a Measured Scenario

This script recreates a measured drive test from the Park Inn Hotel at Berlin Alexanderplatz. The transmitter was at the rooftop of the hotel while the mobile receiver was moving south on Grunerstraße. A simplified version of the scenario is recreated in the simulation where the scenarios along the track were classified by hand.

Channel model setup and coefficient generation First, we set up the channel model.

```
set(0,'defaultTextFontSize', 14)
set(0,'defaultAxesFontSize', 14)
RandStream.setGlobalStream(RandStream('mt19937ar','seed',1));

close all
clear all

s = simulation_parameters;                          % Basic simulation parameters
s.center_frequency = 2.185e9;
s.sample_density = 2;
s.use_absolute_delays = 1;

t = track('linear',500,-135*pi/180);                % Track with 500m length, direction SE
t.initial_position = [120;-120;0];                  % Start position
t.interpolate_positions( 1 );                       % Interpolate to 1 sample per meter

t.segment_index = [1    45   97   108  110  160  190  215  235  245 ...
    280  295  304  330  400  430 ];                  % Set segments (states)

Sl = 'MIMOSA_10-45_LOS';
Sn = 'MIMOSA_10-45_NLOS';
t.scenario      = {Sn,Sl,Sn,Sl,Sn,Sn,Sn,Sl,Sn,Sl,Sn,Sl,Sn,Sn,Sn,Sn};
t.interpolate_positions( 3 );

l = layout( s );
l.tx_position = [0;0;125];                          % Set the position of the Tx
l.track = t;                                        % Set the rx-track

l.tx_array = array('rhcp-lhcp-dipole');             % Generate Tx antenna
l.tx_array.rotate_pattern(30,'y');                  % 30 deg Tilt
l.tx_array.rotate_pattern(-90,'z');                 % point southwards

l.rx_array = array('rhcp-lhcp-dipole');             % Rx-Antenna
l.rx_array.rotate_pattern(-90,'y');                 % point skywards

l.visualize;
view(-33, 45);

lnk = [ l.tx_position, ...
    l.track.positions(:,l.track.segment_index(2))+l.track.initial_position ];

hold on
plot3( lnk(1,:),lnk(2,:),lnk(3,:) , '--' )
hold off
```

Generate channel coefficients Next, we calculate the channel coefficients.

```
[p,cb] = l.create_parameter_sets(0);
p(2).scenpar.NumClusters = 14;
p.update_parameters;

c = cb.get_channels;
cn = c.merge(0.2);
```

```
Parameters   [ooooooooooooooooooooooooooooooooooooooooooooooooooooo]    31 seconds
Channels     [ooooooooooooooooooooooooooooooooooooooooooooooooooooo]    15 seconds
Merging      [ooooooooooooooooooooooooooooooooooooooooooooooooooooo]     2 seconds
```

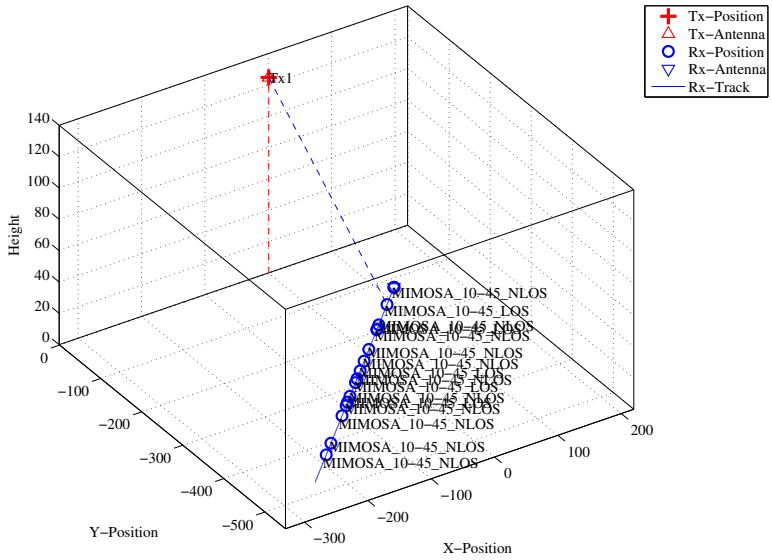

Figure 5: Scenario setup for the comparison of simulated and measured data

Results First, we plot the PDP vs distance from the start point (see Fig. 6).

```
h = cn(1).fr( 20e6,256 );
pdp = squeeze(sum(sum( abs(ifft(h,[],3)).^2 , 1),2));
pdp = 10*log10(pdp.');

figure
imagesc(pdp(end:-1:1,1:192));

cm = colormap('hot');
colormap(cm(end:-1:1,:));

caxis([ max(max(pdp))-60 max(max(pdp))-5 ]);
colorbar

title('Time variant power delay profile');

set(gca,'XTick',1:32:192);
set(gca,'XTickLabel',(0:32:192)/20e6*1e6);
xlabel('Delay [\mus]');

ind = sort( cn.no_snap : -cn(1).no_snap/10 : 1);
set(gca,'YTick', ind );
set(gca,'YTickLabel', round(sort(500-ind / 3,'descend')) );
ylabel('Distance [m]');
```

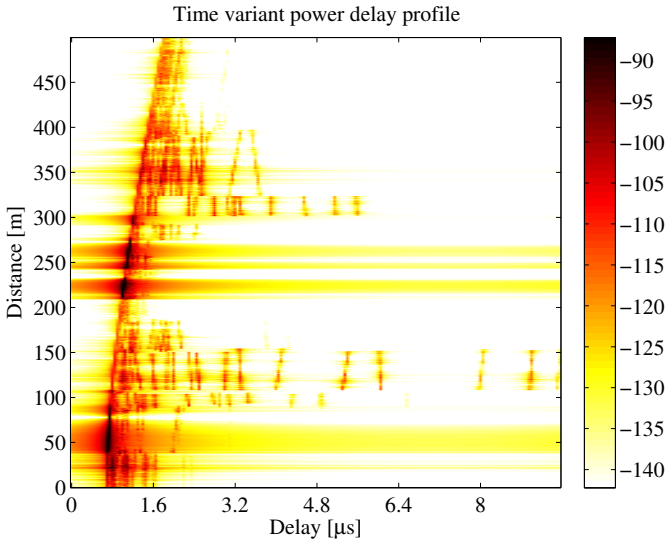

Figure 6: 2D PDP of the simulated track

The next plot shows the total received power along the path (Fig. 7, top left). Green shaded ares are LOS. The rest is non line of sight (NLOS).

```
dist = (1:cn.no_snap)*l.track.get_length/cn.no_snap;
ind  = find(strcmp(l.track.scenario,Sl));
los  = [];
for n = 1:numel(ind)
    los = [los l.track.segment_index(ind(n)) : l.track.segment_index(ind(n)+1)];
end

power = 10*log10( sum( reshape( abs(cn.coeff).^2 , [] , cn.no_snap ) ,1)/4 );
ar = zeros(1,cn.no_snap);
ar(los) = -200;

figure
a = area(dist,ar);
set(a(1),'FaceColor',[0.7 0.9 0.7]);
set(a,'LineStyle','none')

hold on
plot(dist,power)
hold off

title('Position dependent power')
xlabel('Track [m]');
ylabel('Power [dB]');
axis([0 500 min(power)-5 max(power)+5])
legend('LOS','P_{total}',4)
grid on
```

The following plot (Fig. 7, top right) shows the distribution (PDF) of the received power for both, the LOS and NLOS segments.

```
bins   = -150:2:-80;
p_los  = hist(power(los),bins)/cn.no_snap*100;
p_nlos = hist(power(setdiff(1:cn.no_snap,los)),bins)/cn.no_snap*100;

figure
bar(bins,[p_los;p_nlos]')
axis([-124.5,-83,0,ceil(max([p_los,p_nlos]))])
grid on
colormap('Cool')

title('Empirical PDF of the \ac{LOS} and NLOS power')
xlabel('P_{total} [dB]');
ylabel('Probability [%]');
legend('LOS','NLOS',1)
```

The next plot shows the RMS delay spread along the path. Again, shaded ares are for the LOS segments.

```
pow_tap = squeeze(sum(sum(abs(cn.coeff).^2,1),2));
pow_sum = sum( pow_tap,1 );
mean_delay = sum( pow_tap.*cn.delay ,1) ./ pow_sum;
ds = sqrt( sum( pow_tap.*cn.delay.^2 ,1)./ pow_sum - mean_delay.^2 );
ar = zeros(1,cn.no_snap);
ar(los) = 10;

figure
a = area(dist,ar);
set(a(1),'FaceColor',[0.7 0.9 0.7]);
set(a,'LineStyle','none')

hold on
plot( dist , ds*1e6  )
hold off

ma = 1e6*( max(ds)+0.1*max(ds) );
axis([0 500 0 ma])
title('Position dependant delay spread');
xlabel('Track [m]');
ylabel('Delay Spread [dB]');
legend('LOS','\sigma_\tau',1)
grid on
```

The final plot (Fig. 7, bottom right) shows the distribution (PDF) of the RMS delay spread for both, the LOS and NLOS segments.

```
bins = 0:0.03:3;
ds_los  = hist(ds(los)*1e6,bins)/cn.no_snap*100;
ds_nlos = hist(ds(setdiff(1:cn.no_snap,los))*1e6,bins)/cn.no_snap*100;

figure
bar(bins,[ds_los;ds_nlos]')
axis([0,1.5,0,ceil(max([ds_los,ds_nlos]))])
grid on
colormap('Cool')

title('Empirical PDF of the LOS and NLOS RMSDS')
xlabel('\sigma_\tau [\mus]');
ylabel('Probability [%]');
legend('LOS','NLOS',1)
```

```
close all
disp(['QuaDRiGa Version: ',simulation_parameters.version])
```

```
QuaDRiGa Version: 1.0.1-145
```

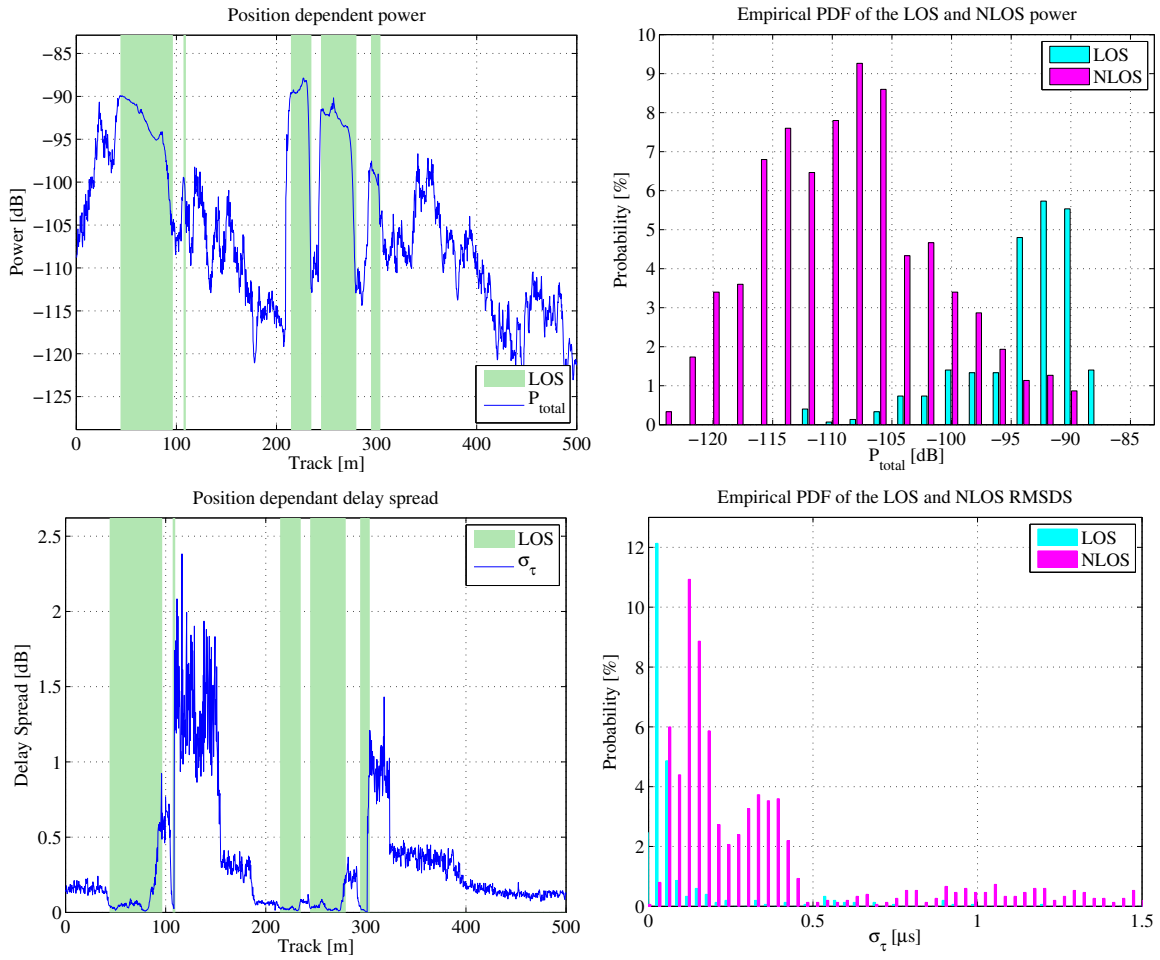

Figure 7: Results for the measurement based simulation tutorial

2.2.3 Generation of Satellite Channels

This script demonstrates the parametrization of the channel model to generate time-continuous sequences for a satellite scenario.

Setting up the Simulation Parameters First, we set up the general simulation parameters. We choose a center frequency of 2.1 GHz. We also want to use drifting in order to get the correct delays and angles for the time-continuous simulation. A sample density of 2.5 ensures that the channel coefficients can be interpolated to different playback speeds later on.

```
close all
clear all

s = simulation_parameters;          % Basic simulation parameters
s.center_frequency      = 2.185e9;
s.sample_density        = 0.25;

RandStream.setGlobalStream(RandStream('mt19937ar','seed',1));
```

Creating a random Track and defining states along the track Next, we generate a simulation track. A track describes the movement of a mobile terminal. It is composed of an ordered list of positions. During the simulation, one snapshot is generated for each position on the track. Later on, the generation of the track is done by the state sequence generator. Here, we implement a simple version of the sequence generator to generate a random track. We first create a set of streets with different length. We assume a normal distribution of the street length where the parameters mu and sigma were fitted from random distances between two crossings in central Berlin (measured with Google earth).

```
street_length_mu = 187;          % Average street length in m
street_length_sigma = 83;
min_street_length = 50;

turn_probability = 0.4;          % The prob. that the car turns at a crossing
curve_radius = 10;               % The curve radius in m
diro = rand * 2*pi;              % Random start direction
```

For the given parameters, we calculate a list of points along the track that resemble the street grid and the turns at crossings.

```
point = 0;                       % The start point (always at [0,0])
m = 1;                           % A counter for the points
for n = 1:3                      % We simulate 3 street segments

    % Get a random street length drawn from the distribution defined above
    street_length = randn*street_length_sigma + street_length_mu;
    while street_length < min_street_length
        street_length = randn*street_length_sigma + street_length_mu;
    end

    % Get 3 points along the street
    point(m+1) = point(m) + exp(1j*diro) * street_length*0.1;
    point(m+2) = point(m) + exp(1j*diro) * street_length*0.9;
    point(m+3) = point(m) + exp(1j*diro) * street_length;
    m=m+3;

    % At a crossing, the car could change its direction. This is
    % modeled here
    if rand < turn_probability
        dirn = diro + sign( rand-0.5 ) * pi/2 + randn*pi/12;
        point(m+1) = point(m) + curve_radius*( exp(1j*diro) + exp(1j*dirn) );
        diro = dirn;
        m=m+1;
    end
end
```

Next, we create a track object and pass the points along the track. We then use the internal interpolation functions to interpolate the track to 1 point per meter.

```
t = track;                          % Create a track object
t.positions = [ real(point) ; imag(point) ; zeros(1,numel(point))];
t.interpolate_positions( 1 );    % Interpolate to 1 point per meter
```

We now assemble a rudimentary state sequence generator that generates different states along the track. We first define the distribution parameters of the segment length and then calculate the segments themselves. The two possible states are "MIMOSA_10-45_LOS" which stands for LOS or good state and "MIMOSA_10-45_NLOS" for NLOS or bad state.

```
segment_length_mu = 30;          % Average segment length in m
segment_length_sigma = 12;       % Standard deviation in m
min_segment_length = 10;         % Minimum segment length in m

% Now we define the segments (the states) along the track
ind = 1;
while ind < t.no_snapshots

    % Each scenario has a 50% probability
    if rand < 0.5
        t.scenario{ t.no_segments } = 'MIMOSA_10-45_LOS' ;
    else
        t.scenario{ t.no_segments } = 'MIMOSA_10-45_NLOS' ;
    end

    % Get the length of the current segment
    segment_length = randn*segment_length_sigma + segment_length_mu;
    while segment_length<min_segment_length
        segment_length = randn*segment_length_sigma + segment_length_mu;
    end
    segment_length = round(segment_length);      % Segment length
    ind = ind + segment_length;                  % Start of next segment

    if ind < t.no_snapshots      % Exception for the last segment
        t.no_segments = t.no_segments + 1;
        t.segment_index( t.no_segments ) = ind;
    end
end
```

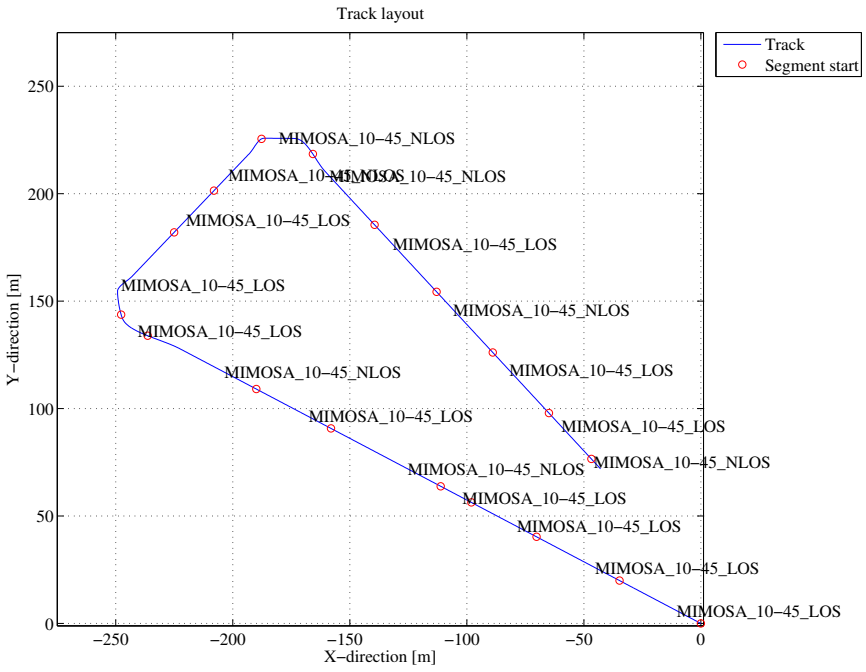

Figure 8: Receiver track for the satellite channel tutorial

Finally, we interpolate the track to the given sample density (2 samples per half-wave-length) and plot the track (see Fig. 8).

```
t.interpolate_positions( s.samples_per_meter );
t.visualize;
```

Defining Antenna Arrays In the third step, we set up our antenna arrays for the transmitter at the satellite and the receiver. We use synthetic dipole antennas for this case. Two dipoles are crossed by an angle of 90 degree. The signal is then split and fed with a 90 degree phase shift to both elements generating RHCP and LHCP signals.

```
% Create a patch antenna with 120 degree opening
a = array('custom',120,120,0);

% Copy element 1 to element 2 - the resulting antenna array has two
% elements, both dipoles.
a.copy_element(1,2);

% Rotate the second pattern by 90 degree around the x-axis.
a.rotate_pattern(90,'x',2);

% Set the coupling between the elements. The Tx-signal for the first
% element is shifted by +90 degree out of phase and put on the second element.
% The signal for the second element is shifted by -90 degree and copied to the
% first element. Both antennas thus radiate a RHCP and a LHCP wave.
a.coupling = 1/sqrt(2) * [1 1;1j -1j];

% Create a copy of the array for the receiver.
b = a.copy_objects;
b.coupling = 1/sqrt(2) * [1 1;1j -1j];

% Rotate the receive antenna array to face sky-wards.
b.rotate_pattern(-90,'y');

b.visualize;                    % Plot the pattern of the Rx-Antenna
```

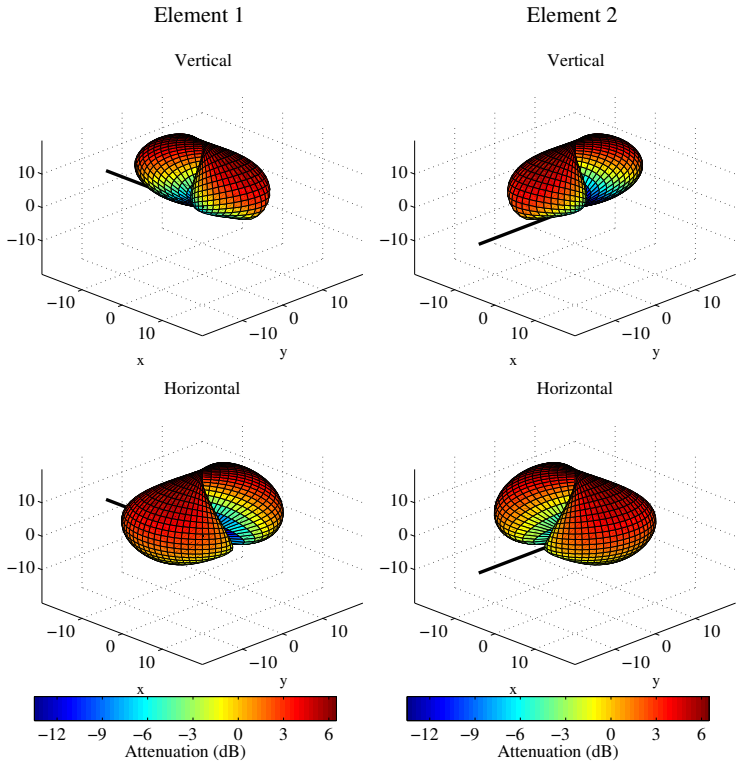

Figure 9: Antenna patterns for the satellite channel tutorial

Setting up the Layout In this step, we combine the track, the antennas and the position of the satellite into a simulation layout. A layout object contains all the geometric information that are necessary to run the simulation. First, we define the position of the satellite. Since the model uses Cartesian coordinates, we have to transform the position of the satellite first.

```
l = layout( s );                % Create a new layout

% Choose a random satellite position (Astra 2, seen from Berlin).
% The distance only needs to be big enough to ensure insignificant changes
% in the reception angle on the ground.

sat_el      = 28.4;             % Elevation angle
sat_az      = 161.6;            % Azimuth angle (South = 180 degree)
rx_latitude = 51;               % Latitude of the Rx

% Approximate the satelite distance for GEO orbit
dist_x      = 35786 + rx_latitude/90 * 6384;    % [km]
dist_y      = (1-rx_latitude/90) * 6384;        % [km]
sat_dist    = sqrt(dist_x^2 + dist_y^2);        % [km]
sat_dist    = sat_dist*1e3;                     % [m]

% Transform angles to Cartesian coordinates
sat_x = sat_dist * cosd(sat_el) * cosd( -sat_az+90 );
sat_y = sat_dist * cosd(sat_el) * sind( -sat_az+90 );
sat_z = sat_dist * sind(sat_el);

% We also turn the antenna of the satellite so it points to the receiver.
a.rotate_pattern( sat_el , 'y' );
a.rotate_pattern( 270-sat_az , 'z' );

% Set the satellite position in the layout
l.tx_position = [ sat_x ; sat_y ; sat_z ];

l.track = t;                    % Set the track for the receiver
l.tx_array = a;                 % Set the tx_array
l.rx_array = b;                 % Set the rx_array
```

Setting up scenario parameters Next, the large scale parameters are set. The first line calls "l.create_parameter_sets", a built-in function that processes the data in the layout and returns a new "parameter_set" object "p". "p" is an array with two elements. One of them contains all the parameters for the good state (LOS) and one for the bad state (NLOS).

```
p = l.create_parameter_sets(0);
```

Each parameter set has two different kinds of parameters. One for the scenario and one for the current state. For example, a scenario might have an average RMS Delay spread of 158 ns plus a certain variance which defines a range for the RMSDS. In addition to that, there are cross-correlations with other parameters such as the angular spread at the transmitter. All those parameters are stored in the "scenpar" property. For the good state, that parameters are:

```
Sl = strcmp( { p(1).name , p(2).name } ,'MIMOSA-10-45-LOS_Tx1' );  % Select good state
p(Sl).scenpar                                                      % Show parameter list
```

```

ans =

           NumClusters: 8
                   r_DS: 2.5000
         PerClusterAS_D: 6.2000e-07
         PerClusterAS_A: 12
         PerClusterES_D: 1.9000e-07
         PerClusterES_A: 7
    LOS_scatter_radius: 0.1000
               LNS_ksi: 3
                xpr_mu: 11.9000
             xpr_sigma: 5.5000
```

```
                DS_mu: -7.5000
             DS_sigma: 0.3000
                AS_D_mu: -4.6000
          AS_D_sigma: 0.1000
             AS_A_mu: 1.5000
          AS_A_sigma: 0.2000
             ES_D_mu: -5.1200
          ES_D_sigma: 0.1000
             ES_A_mu: 1.4000
          ES_A_sigma: 0.1000
            SF_sigma: 3.6000
               KF_mu: 15.5000
            KF_sigma: 5.9000
           DS_lambda: 30.5000
        AS_D_lambda: 1000
        AS_A_lambda: 31.5000
        ES_D_lambda: 1000
        ES_A_lambda: 6
          SF_lambda: 35
          KF_lambda: 4.5000
             asD_ds: 0
             asA_ds: 0.6100
             asA_sf: 0.5600
             asD_sf: 0
              ds_sf: 0.4300
            asD_asA: 0
             asD_kf: 0
             asA_kf: -0.4400
              ds_kf: -0.4600
              sf_kf: -0.3000
             esD_ds: 0
             esA_ds: -0.0500
             esA_sf: 0.1800
             esD_sf: 0
            esD_esA: 0
            esD_asD: 0
            esD_asA: 0
            esA_asD: 0
            esA_asA: 0.1500
             esD_kf: 0
             esA_kf: -0.0300
```

Note here, that the values are given for a log-normal distribution. Thus, the RMSDS in nanoseconds follows from

```
10^( p(S1).scenpar.DS_mu ) * 1e9
```

```

ans =

   31.6228
```

Each parameter on that list can be changed by just assigning it a new value. Here, we set the number of clusters for the LOS scenario to 7. Note that the default settings are stored in files in the sub-folder "config" of the channel model folder. Here, the default settings can be permanently set. After a change, the parameters of the segments need to be updated. This is done by calling the "update_parameters" method.

```
p(S1).scenpar.NumClusters = 7;
p.update_parameters;
```

```
Parameters   [oooooooooooooooooooooooooooooooooooooooooooooooooooo]    24 seconds
```

When "update_parameter" is called, the specific parameters for each segment are generated. E.g. each segment gets assigned a RMS Delay Spread and other values which are drawn from the statistics defined in scenpar. For the LOS segments, the individual RMSDS values for each segment are:

```
rmsds = p(S1).ds*1e9
average = mean(p(S1).ds*1e9)
```

```
rmsds =

  Columns 1 through 7

   48.8391    6.8370   55.2154   48.7273   25.9658   29.7929   22.2436

  Columns 8 through 11

   68.7237   13.3159   85.5425  121.5296


average =

   47.8848
```

Generate channel coefficients Next, we generate the channel coefficients. This is a lengthy task. The next line then combines the channels of the individual segments into a time-continuous channel. Here, the parameter (0.2) sets the length of the overlap region between two segments. In this case, it is 20%.

```
c = p.get_channels;                                % Generate coefficients
cn = c.merge(0.2);                                 % Combine segments
```

```
Channels      [ooooooooooooooooooooooooooooooooooooooooooooooooooo]    21 seconds
Merging       [ooooooooooooooooooooooooooooooooooooooooooooooooooo]     1 seconds
```

Evaluation of the data The next two plots show some basic evaluations of the generated coefficients. The first plot shows the received power for the 4 MIMO links along the track. The plot shows the differences between the LOS and NLOS segments and the cross-pol discrimination between the MIMO links. The average path loss for LOS was set to -95 dB and for NLOS -113 dB.

```
dist = (1:cn.no_snap)*t.get_length/cn.no_snap;
ind  = find(strcmp(t.scenario,'MIMOSA_10-45_LOS'));
los  = [];
for n = 1:numel(ind)
    start = t.segment_index(ind(n));
    if n==numel(ind)
        try
            stop =  t.segment_index(ind(n)+1);
        catch
            stop = t.no_snapshots;
        end
    else
        stop =  t.segment_index(ind(n)+1);
    end
    los = [los start:stop];
end

power = reshape( 10*log10( squeeze(sum( abs(cn.coeff).^2 , 3 )) ) , 4,[]);

mi = min(reshape(power,[],1)) - 5;
ma = max(reshape(power,[],1)) + 5;

ar = ones(1,cn.no_snap) * ma;
ar(los) = mi;

figure('Position',[ 100 , 100 , 1000 , 700]);
a = area(dist,ar);
set(a(1),'FaceColor',[0.7 0.9 0.7]);
set(a,'LineStyle','none')

hold on
plot(dist,power')
hold off

```

```
xlabel('Track [m]');
ylabel('Received Power per MIMO LINK [dB]');
axis([0 t.get_length mi ma])
legend('LOS','P_{11}','P_{12}','P_{21}','P_{22}',4)
box on

title('Received power along the track')
```

The next plot shows the RMS delay spread along the path for the first MIMO element. Again, shaded ares are for the LOS segments.

```
pow_tap = abs(squeeze(cn.coeff(1,1,:,:))).^2;
pow_sum = sum( pow_tap,1 );
mean_delay = sum( pow_tap.*cn.delay ,1) ./ pow_sum;
ds = sqrt( sum( pow_tap.*cn.delay.^2 ,1)./ pow_sum - mean_delay.^2 );
ar = zeros(1,cn.no_snap);
ar(los) = 10000;

figure('Position',[ 100 , 100 , 1000 , 700]);
a = area(dist,ar);
set(a(1),'FaceColor',[0.7 0.9 0.7]);
set(a,'LineStyle','none')

hold on
plot( dist , ds*1e9  )
hold off

ma = 1e9*( max(ds)+0.1*max(ds) );

axis([0 t.get_length 0 ma])
xlabel('Track [m]');
ylabel('Delay Spread [ns]');
legend('LOS','\sigma_\tau',1)
title('Position dependant delay spread');
```

```
close all
disp(['QuaDRiGa Version: ',simulation_parameters.version])
```

```
QuaDRiGa Version: 1.0.1-145
```

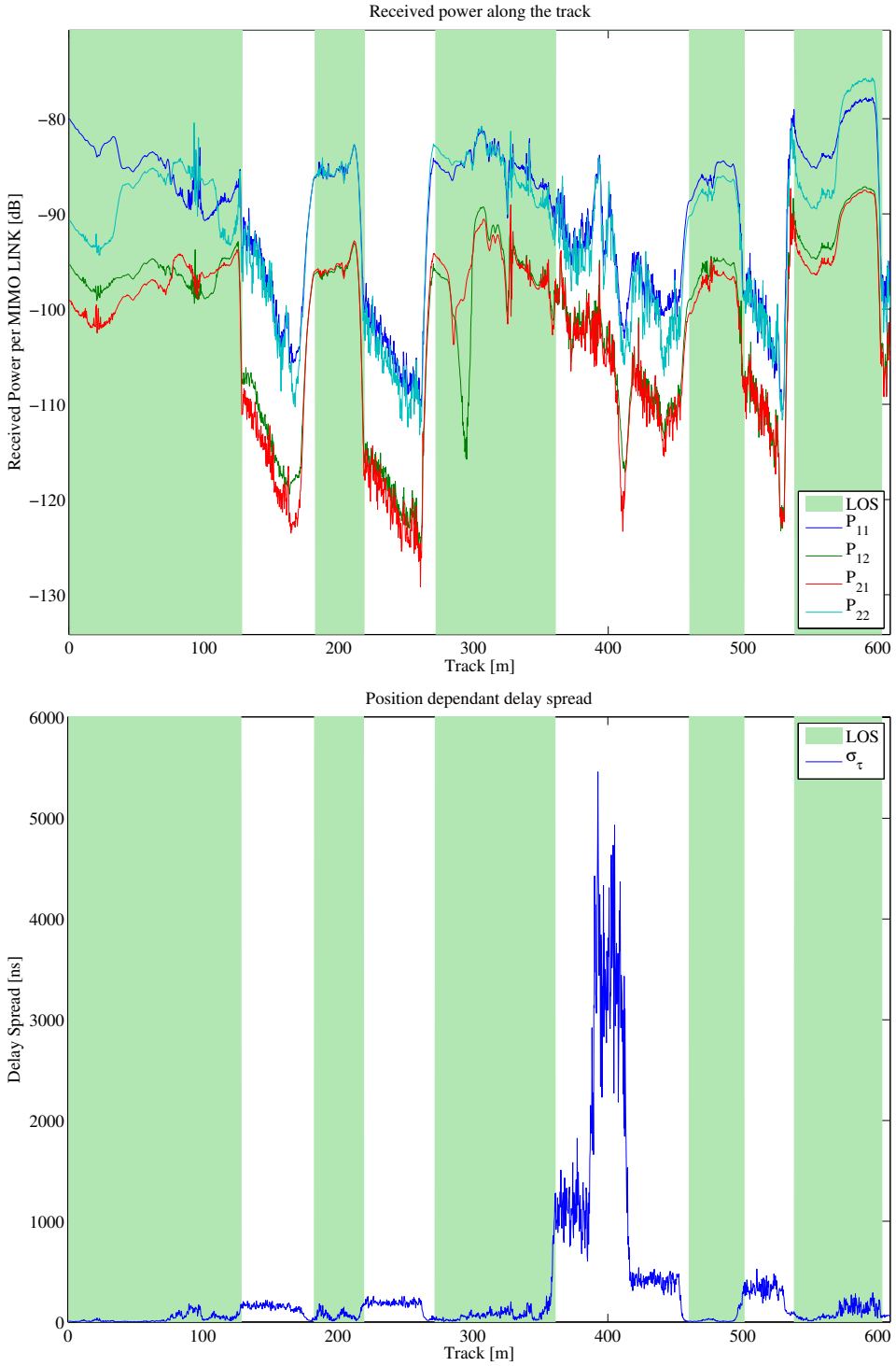

Figure 10: Results for the satellite channel tutorial

2.2.4 Drifting Phases and Delays

Drifting is an essential feature of the channel model. Drifting enables a continuous time evolution of the path delays, the path phases, the departure- and arrival angles and the LSPs. It is thus the enabling feature for time continuous channel simulations. Although drifting was already available in the SCME branch of the WINNER channel model, it did not make it into the main branch. Thus, drifting is not available in the WIM1, WIM2 or WIM+ model. Here the functionality is implemented again. This script focuses on the delay and the phase component of the drifting functionality.

Channel model setup and coefficient generation First, we parameterize the channel model. We start with the basic simulation parameters. For the desired output, we need two additional options: we want to evaluate absolute delays and we need to get all 20 subpaths. Normally, the subpaths are added already in the channel builder.

```
s = simulation_parameters;
s.center_frequency = 2.53e9;
s.sample_density = 4;
s.use_subpath_output = 1;
s.use_absolute_delays = 1;
```

Second, we define a user track. Here we choose a linear track with a length of 30 m. The track start 20 m east of the transmitter and runs in east direction, thus linearly increasing the distance from the receiver.

```
l = layout( s );
l.tx_position(3) = 25;
l.track.generate('linear',30,0);
l.track.initial_position = [20;0;0];
l.track.scenario = 'WINNER_UMa_C2_LOS';
l.track.interpolate_positions( s.samples_per_meter );
l.visualize;
```

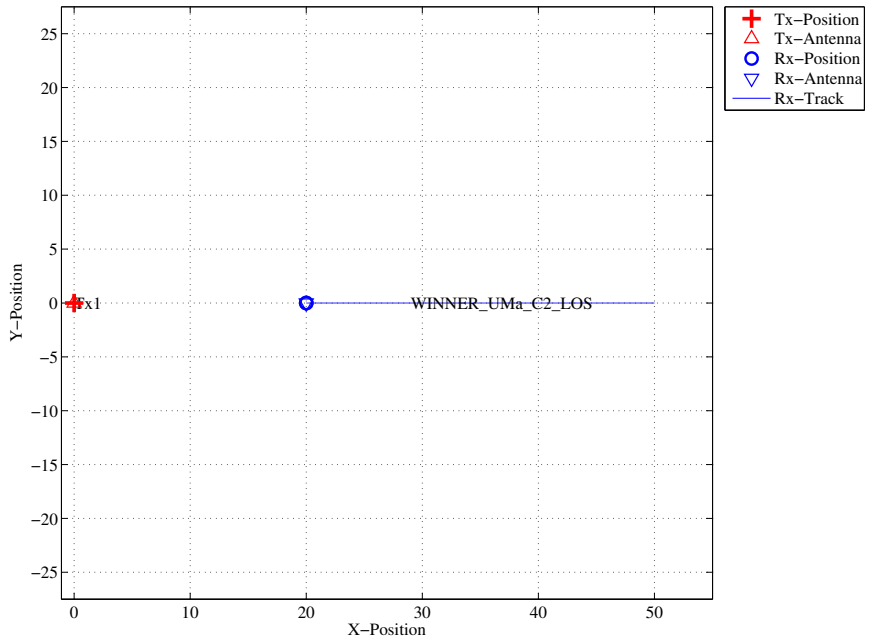

Figure 11: Scenario setup for the drifting phases tutorial

Now, we generate the LSPs. In order to get repeatable results, we set a specific random seed. This is a MATLAB internal function and is not a feature of the channel model. We also set the shadow fading and K-factor to 1 and disable the path loss model.

```
RandStream.setGlobalStream(RandStream('mt19937ar','seed',5));
p = l.create_parameter_sets;
p.parameter_maps(:,:,[2 3]) = 0;            % Fix SF and KF to 0
p.plpar = [];                               % Disable path loss model
p.update_parameters;
```

```
Parameters    [ooooooooooooooooooooooooooooooooooooooooooooooooooo]     1 seconds
```

Now, we generate the channel coefficients. The first run uses the new drifting module, the second run disables it. Note that drifting needs significantly more computing resources. In some scenarios it might thus be useful to disable the feature to get quicker simulation results.

```
s.drifting_precision = 1;
RandStream.setGlobalStream(RandStream('mt19937ar','seed',2));
c = p.get_channels;

s.drifting_precision = 0;
RandStream.setGlobalStream(RandStream('mt19937ar','seed',2));
d = p.get_channels;
```

```
Channels      [ooooooooooooooooooooooooooooooooooooooooooooooooooo]    12 seconds
Channels      [ooooooooooooooooooooooooooooooooooooooooooooooooooo]     7 seconds
```

Results and discussion The following plots represent the results of the test.

```
figure
distance = 20+(1:c.no_snap)*l.track.get_length/c.no_snap;
plot( distance, c.delay(1,:)*1e9 , '-b' )
hold on
plot( distance, d.delay(1,:)*1e9 , '-.b' )
plot( distance, c.delay(2,:)*1e9 , '-r' )
plot( distance, d.delay(2,:)*1e9 , '-.r' )
hold off
xlabel('Distance from track start point')
ylabel('Delay [ns] ')
```

The first plot (Fig. 12) shows the delay of the LOS tap (blue) and the delay of the first NLOS tap (red) vs. distance. The solid lines are from the channel with drifting, the dashed lines are from the channel without. The LOS delay is always increasing since the Rx is moving away from the Tx. However, the increase is not linear due to the 25 m height of the Tx. Without drifting, the delays are not updated and stay constant during the segment. The position of the first scatterer is in close distance to the Rx (only some m away).

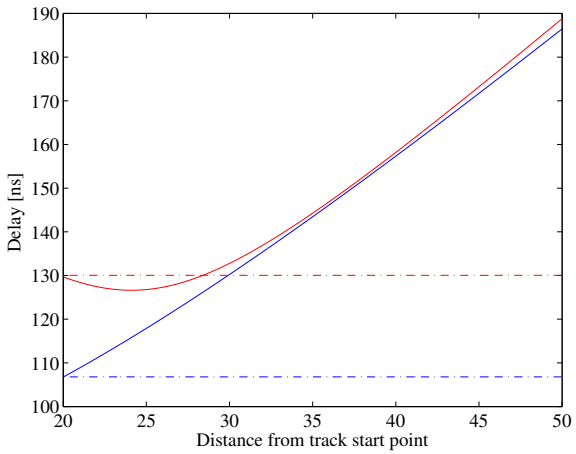

Figure 12: Cluster delays vs. Rx position (drifting phases tutorial)

When moving, the Rx first approaches the scatterer (delay gets a bit smaller) and then the distance increases again.

```
phase = unwrap(angle(squeeze((c.coeff(1,1,2,:,:)))));
plot( distance,phase )
xlabel('Distance from track start point')
ylabel('Continuous phase')
```

The second plot (Fig. 13, left) shows the phases of the 20 subpaths of the first NLOS tap for the drifting case. Note that the phases are not linear. This comes from the close proximity of the scatterer to the initial Rx position. The position of all 20 reflection points are calculated by the channel model. Those position mark the position of the last bounce scatterer (LBS). When moving the Rx, the distance to the LBS changes for each subpath and so does the phase. Here, the phase of each of the subpaths is calculated from the length of the path.

```
pow = abs(squeeze(sum( c.coeff(1,1,2,:,:) , 5 ))).^2;
plot( distance,10*log10(pow),'-r' )
xlabel('Distance from track start point')
ylabel('Tap power (dB)')
```

This plot shows the power of the first NLOS tap along the track. The fading is significantly higher in the beginning and becomes much less strong towards the end.

```
phase = unwrap(angle(squeeze((d.coeff(1,1,2,:,:)))));
plot( distance,phase )
xlabel('Distance from track start point')
ylabel('Continuous phase')
```

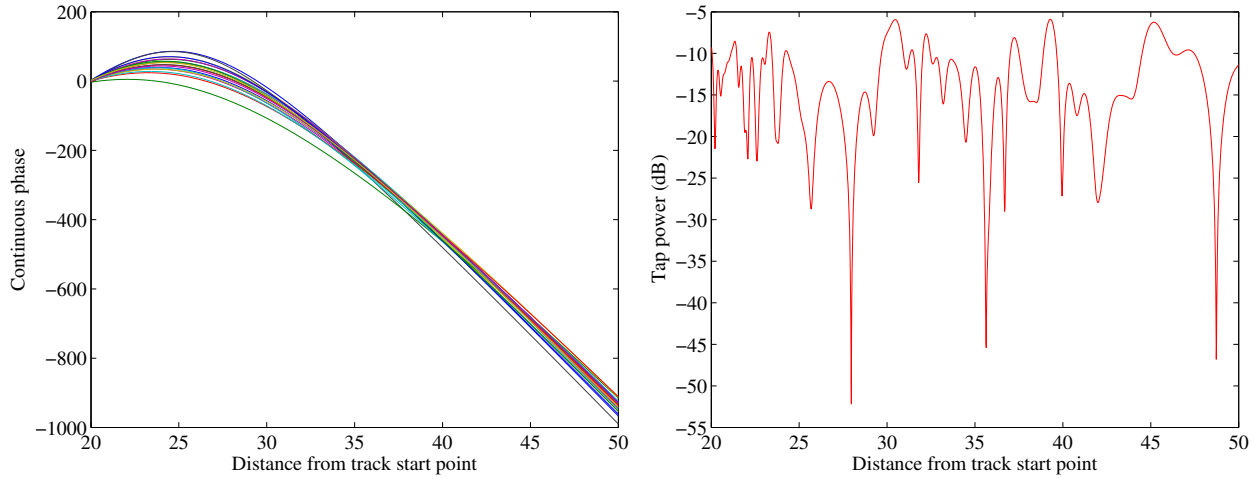

Figure 13: Drifting phases and Tx power vs. Rx position (drifting phases tutorial)

Without drifting, the phases of the subpaths are approximated by assuming that the angles to the LBSs do not change. However, this only holds when the distance to the LBS is large. Here, the initial distance is small (ca. 5 m). When the initial angles are kept fixed along the track, the error is significant. Here, the phase ramp is negative, indicating a movement direction towards the scatterer and thus a higher Doppler frequency. However, when the scatterer is passed, the Rx moves away from the scatterer and the Doppler frequency becomes lower. This is not reflected when drifting is turned off.

Note here, that with shorter delay spreads (as e.g. in satellite channels), the scatterers are placed closer to the Rxs initial position. This will amplify this effect. Hence, for correct time evolution results, drifting needs to be turned on.

```
pow = abs(squeeze(sum( d.coeff(1,1,2,:,:) , 5 ))).^2;
plot( distance,10*log10(pow),'-r' )
xlabel('Distance from track start point')
ylabel('Tap power (dB)')
```

```
close all
disp(['QuaDRiGa Version: ',simulation_parameters.version])
```

```
QuaDRiGa Version: 1.0.1-145
```

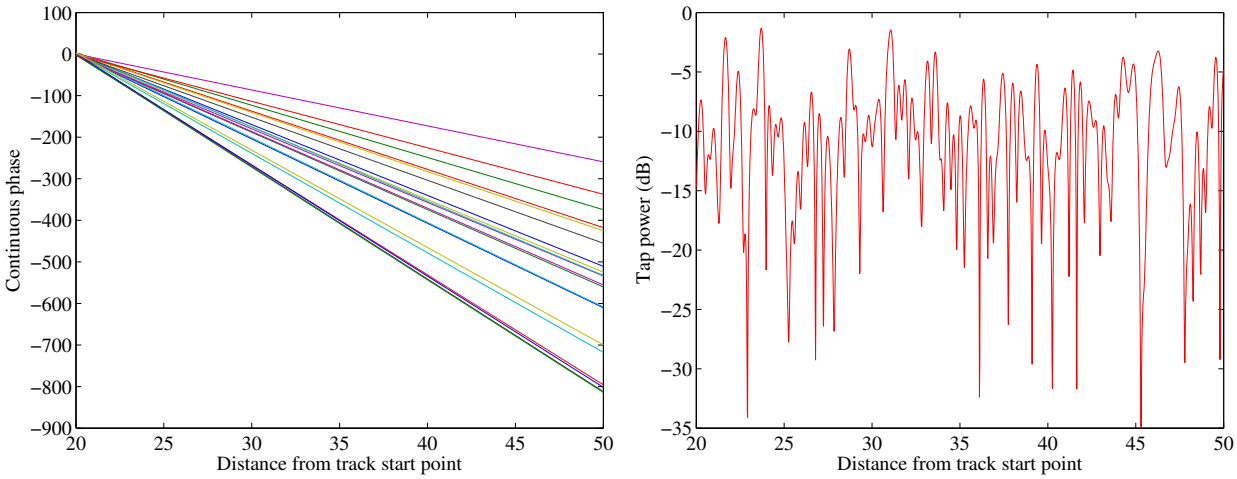

Figure 14: Phases and Tx power vs. Rx position without drifting (drifting phases tutorial)

2.2.5 Time Evolution and Scenario Transitions

The channel model generates the coefficients separately for each segment. In order to get a time-continuous output, these coefficients have to be combined. This is a feature which is originally described in the documentation of the WIM2 channel model, but which was never implemented. Since this component is needed for time-continuous simulations, it was implemented here. This script sets up the simulation and creates such time-continuous channel impulse responses (CIRs).

Channel model setup and coefficient generation First, we set up the channel model.

```
close all
clear all

set(0,'defaultTextFontSize', 14)
set(0,'defaultAxesFontSize', 14)

s = simulation_parameters;
s.center_frequency = 2.53e9;
s.sample_density = 4;
s.use_absolute_delays = 1;
```

Second, we create a more complex network layout featuring an elevated transmitter (25 m) and two receivers at 1.5 m height. The first Rx moves along a circular track around the receiver. The second receiver moves away from the Tx. Both start at the same point.

Note here, that each track is split into three segments. The first Rx goes from an LOS area to a shaded area and back. The second track also start in the LOS area. Here, the scenario changes to another LOS segment and then to an NLOS segment. The LOS-LOS change will create new small-scale fading parameters, but the LSPs will be highly correlated between those two segments.

```
l = layout( s );                                % New layout
l.no_rx = 2;                                    % Two receivers

l.tx_array.generate('dipole');                  % Dipola antennas at all Rx and Tx
l.rx_array = l.tx_array;

l.tx_position(3) = 25;                          % Elevate Tx to 25 m

UMal = 'BERLIN_UMa_LOS';
UMan = 'BERLIN_UMa_NLOS';

l.track(1).generate('circular',20*pi,0);        % Circular track with 10m radius
l.track(1).initial_position    = [10;0;1.5];    % Start east, running nord
l.track(1).segment_index       = [1,40,90];     % Segments
l.track(1).scenario            = { UMal , UMan , UMal };

l.track(2).generate('linear',20,0);             % Linear track, 20 m length
l.track(2).initial_position    = [10;0;1.5];    % Same start point
l.track(2).interpolate_positions( 128/20 );
l.track(2).segment_index       = [1,40,90];
l.track(2).scenario            = { UMal , UMal , UMan };

l.visualize;                                    % Plot all tracks

l.track.interpolate_positions( s.samples_per_meter );
l.track.compute_directions;
```

Now we create the channel coefficients. The fixing the random seed guarantees repeatable results (i.e. the taps will be at the same positions for both runs). Also not the significantly longer computing time when drifting is enabled.

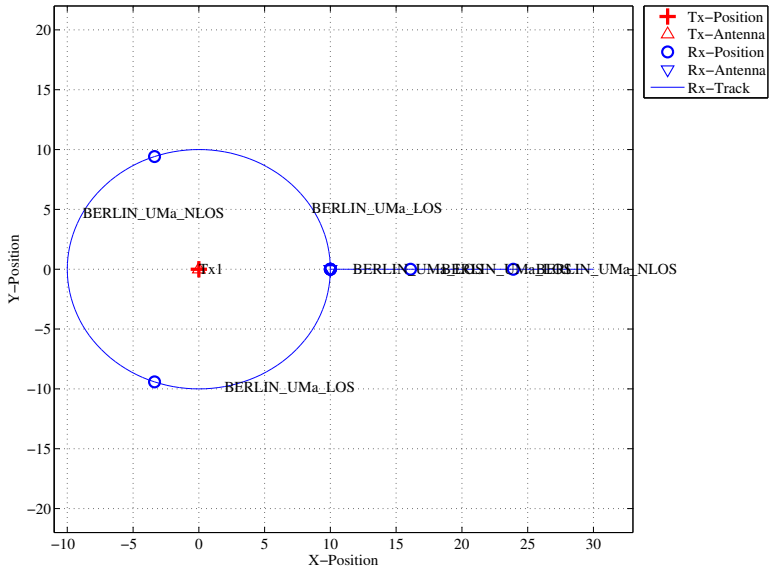

Figure 15: Scenario setup for the time evolution tutorial

```
RandStream.setGlobalStream(RandStream('mt19937ar','seed',2));
p = l.create_parameter_sets;

disp('Drifting enabled:');
s.drifting_precision = 1;
RandStream.setGlobalStream(RandStream('mt19937ar','seed',1));
c = p.get_channels;
cn = c.merge;

disp('Drifting disabled:');
s.drifting_precision = 0;
RandStream.setGlobalStream(RandStream('mt19937ar','seed',1));
d = p.get_channels;
dn = d.merge;
```

```
Parameters   [ooooooooooooooooooooooooooooooooooooooooooooooooooo]     1 seconds
Drifting enabled:
Channels     [ooooooooooooooooooooooooooooooooooooooooooooooooooo]    36 seconds
Drifting disabled:
Channels     [ooooooooooooooooooooooooooooooooooooooooooooooooooo]     5 seconds
```

Results and discussion Now we plot the and discuss the results. We start with the power of the LOS tap along the circular track and compare the outcome with and without drifting (Fig. 16, left).

```
degrees = (0:cn(1).no_snap-1)/cn(1).no_snap * 360;
los_pwr_drift = 10*log10(squeeze(abs(cn(1).coeff(1,1,1,:))).^2);
los_pwr_nodrift = 10*log10(squeeze(abs(dn(1).coeff(1,1,1,:))).^2);

figure
plot( degrees,los_pwr_drift )
hold on
plot(degrees,los_pwr_nodrift ,'-.r')
hold off

a = axis;
axis( [0 360 a(3:4) ] );

xlabel('Position on circle [\degree\]');
ylabel('Power of the LOS component');
title('Power of the LOS component for the circular track');
legend('Drifting','No drifting',4);
```

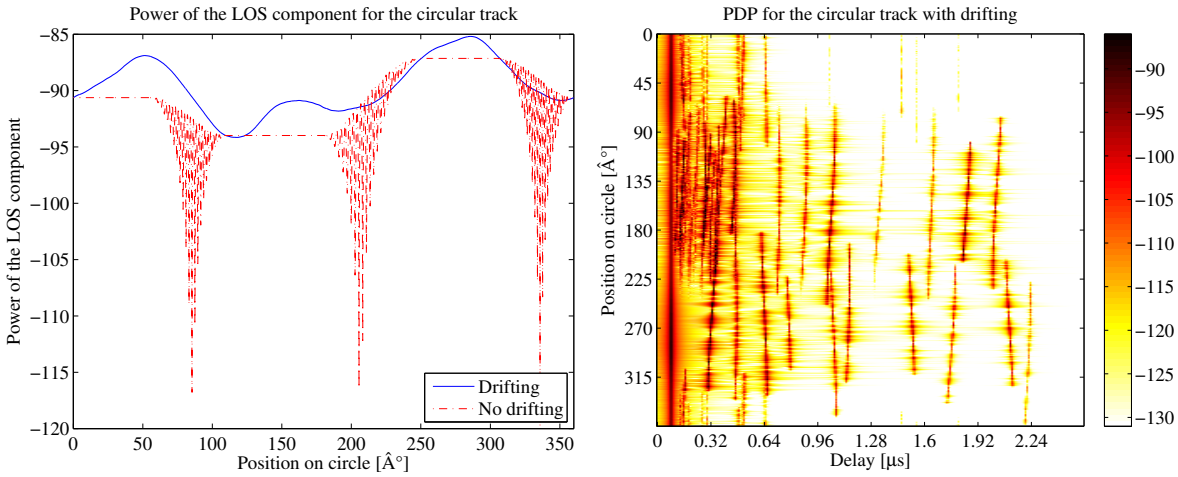

Figure 16: Received power on the circular track (time evolution tutorial)

When drifting is enabled (Fig. 16, left, blue curve), the channel output after merging is time-continuous. The variations along the track come from the drifting K-Factor and the drifting shadow fading. When drifting is disabled, these parameters are not updated and kept fixed at their initial value.

At the and of each segment, both channels are cross-faded. I.e. the power of the output of the first segment ramps down and the power of the second segment ramps up. Since drifting guarantees a time-continuous evolution of the phase, this ramping process is also time continuous and no artifacts are visible in the blue curve.

Without drifting, however, the phases are approximated based on their initial values, the initial arrival- and departure angles and the traveled distance from the start point. However, since the Rx moves along a circular track, the angles change continuously which is not correctly modeled. The phase at the end of the first segment does not match the phase at the beginning of the second. When adding both components, artifacts appear as can be seen in the red curve.

Next, we plot the power-delay profiles for both tracks. We calculate the frequency response of the channel and transform it back to time domain by an IFFT. Then, we create a 2D image of the received power at each position of the track. We start with the circular track.

```
h = cn(1).fr( 100e6,512 );
h = squeeze(h);
pdp = 10*log10(abs(ifft(h,[],1).').^2);

figure
imagesc(pdp(:,1:256));
caxis([ max(max(pdp))-50 max(max(pdp))-5 ]);
colorbar

cm = colormap('hot');
colormap(cm(end:-1:1,:));

set(gca,'XTick',1:32:255);
set(gca,'XTickLabel',(0:32:256)/100e6*1e6);
xlabel('Delay [\mus]');

set(gca,'YTick',1:cn(1).no_snap/8:cn(1).no_snap);
set(gca,'YTickLabel', (0:cn(1).no_snap/8:cn(1).no_snap)/cn(1).no_snap * 360 );
ylabel('Position on circle [\degree\]');

title('PDP for the circular track with drifting');
```

The X-axis (Fig. 16, right) shows the delay in microseconds and the Y-axis shows the position on the circle. For easier navigation, the position is given in degrees. 0° means east (starting point), 90° means north, 180° west and 270° south. The LOS delay stays constant since the distance to the Tx is also constant.

However, the power of the LOS changes according to the scenario. Also note, that the NLOS segment has significantly more taps due to the longer delay spread. Next, we create the same plot for the linear track (Fig. 17). Note the slight increase in the LOS delay and the high similarity of the first two LOS segments due to the correlated LSPs. Segment change is at around 6 m.

```
h = cn(2).fr( 100e6,512 );
h = squeeze(h);
pdp = 10*log10(abs(ifft(h,[],1).').^2);

figure
imagesc(pdp(:,1:256));
caxis([ max(max(pdp))-50 max(max(pdp))-5 ])
colorbar

cm = colormap('hot');
colormap(cm(end:-1:1,:));

set(gca,'XTick',1:32:255);
set(gca,'XTickLabel',(0:32:256)/100e6*1e6);
xlabel('Delay [\mus]');

set(gca,'YTick',1:cn(2).no_snap/8:cn(2).no_snap);
set(gca,'YTickLabel', (0:cn(2).no_snap/8:cn(2).no_snap)/cn(2).no_snap * 20 );
ylabel('Distance from start point [m]');

title('PDP for the linear track with drifting');
```

Last, we plot the same results for the linear track without drifting (Fig. 17, right). Note here, that the LOS delay is not smooth during segment change. There are two jumps at 6 m and again at 13.5 m.

```
h = dn(2).fr( 100e6,512 );
h = squeeze(h);
pdp = 10*log10(abs(ifft(h,[],1).').^2);

figure
imagesc(pdp(:,1:256));
caxis([ max(max(pdp))-50 max(max(pdp))-5 ])
colorbar

cm = colormap('hot');
colormap(cm(end:-1:1,:));

set(gca,'XTick',1:32:255);
set(gca,'XTickLabel',(0:32:256)/100e6*1e6);
xlabel('Delay [\mus]');

set(gca,'YTick',1:cn(2).no_snap/8:cn(2).no_snap);
set(gca,'YTickLabel', (0:cn(2).no_snap/8:cn(2).no_snap)/cn(2).no_snap * 20 );
ylabel('Distance from start point [m]');

title('PDP for the linear track without drifting');
```

```
close all
disp(['QuaDRiGa Version: ',simulation_parameters.version])
```

```
QuaDRiGa Version: 1.0.1-145
```

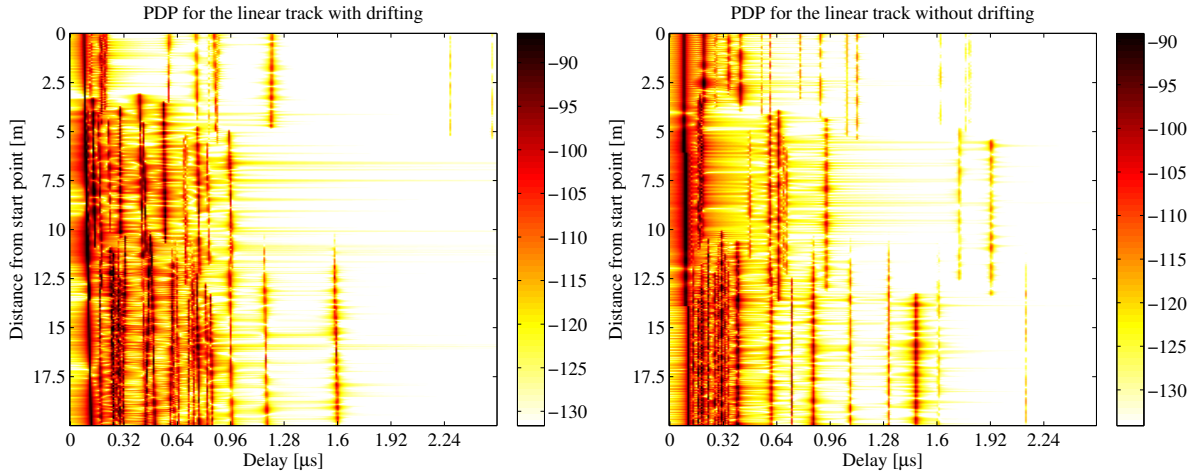

Figure 17: Received power on the linear track (time evolution tutorial)

2.2.6 Applying Varying Speeds (Channel Interpolation)

One new feature that makes the simulations more realistic is the function to apply arbitrary speed- and movement profiles, e.g. accelerating, breaking or moving at any chosen speed. These profiles are defined in the track class. The profiles are then converted in to effective sampling points which aid the interpolation of the channel coefficients.

Channel model setup First, we set up the simulation parameters. Note the sample density of 2.5 which enables very fast simulations even with drifting.

```
s = simulation_parameters;
s.center_frequency = 2.53e9;
s.sample_density = 2.5;
s.use_absolute_delays = 1;
```

Second, we define a track. It has a length of 20 m, starts at 10 m east of the transmitter and consists of three segments (LOS, NLOS, LOS). The positions are interpolated to match the sample density defined above. The track is then plugged into a network layout with one transmitter at position (0,0,25). Both, transmitter and receiver are equipped with dipole antennas. The last three lines create the LSPs.

```
t = track('linear',20,0);
t.initial_position = [60;0;1.5];
t.interpolate_positions( 128/20 );
t.segment_index       = [1,40,90];
t.scenario            = { 'WINNER_UMa_C2_LOS' , 'WINNER_UMa_C2_NLOS' ,...
    'WINNER_UMa_C2_LOS' };
t.interpolate_positions( s.samples_per_meter );

l = layout( s );
l.tx_array.generate('dipole');
l.rx_array = l.tx_array;
l.tx_position(3) = 25;
l.track = t;

l.visualize;

RandStream.setGlobalStream(RandStream('mt19937ar','seed',5));
p = l.create_parameter_sets;
```

```
Parameters    [ooooooooooooooooooooooooooooooooooooooooooooooooooo]     2 seconds
```

Channel generation and results Next, we generate the channel coefficients. Note that here, the initial sample density is 2.5. We then interpolate the sample density to 20. It would take ten times as long to achieve the same result with setting the initial sample density to 20. The interpolation is significantly faster. It is done by first setting the speed to 1 m/s (default setting) and then creating a distance vector which contains a list of effective sampling points along the track.

```
c = p.get_channels;
cn = c.merge;

t.set_speed( 1 );
dist = t.interpolate_movement( s.wavelength/(2*20) );
ci = cn.interpolate( dist , t.get_length , 'spline' );
```

```
Channels      [ooooooooooooooooooooooooooooooooooooooooooooooooooo]     5 seconds
```

The next plot shows the power of the first three taps from both, the original and the interpolated channel, plotted on top of each other. The values are identical except for the fact, that the interpolated values (blue line) have 5 times as many sample points.

eMail: quadriga@hhi.fraunhofer.de

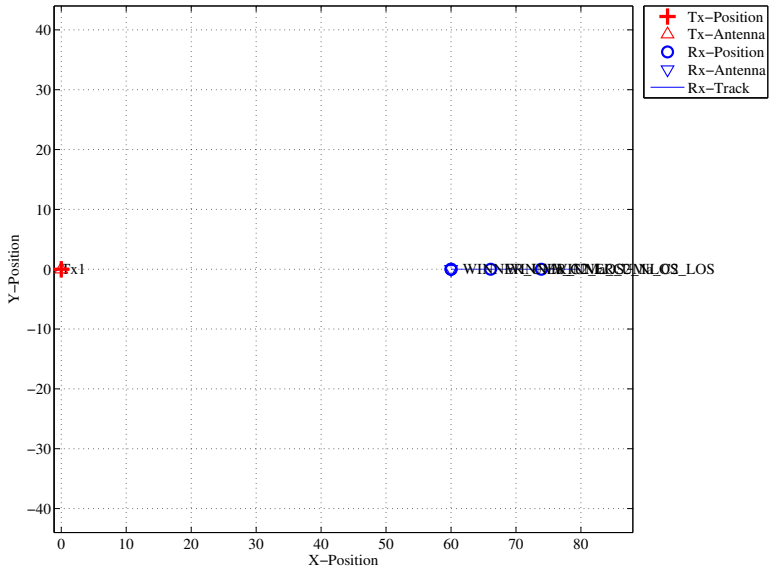

Figure 18: Scenario setup for the speed profile tutorial

```
pwr_orig = 10*log10(squeeze(abs(cn.coeff(1,1,1:3,:))).^2);
nsnap = cn.no_snap;
dist_orig = (0:nsnap-1) * t.get_length/(nsnap-1);
pwr_int = 10*log10(squeeze(abs(ci.coeff(1,1,1:3,:))).^2);

figure
plot( dist_orig,pwr_orig , 'r','Linewidth',2 )
hold on
plot( dist,pwr_int ,'b' )
hold off
axis(  [ min(dist) , max(dist) ,...
    min( pwr_orig( pwr_orig>-Inf ) ) , ...
    max( pwr_orig( pwr_orig>-Inf ) )+10 ] )

xlabel('Distance from start point [m]');
ylabel('Power [dB]');
```

Fig. 19 (right) shows the power delay profile (PDP) for the interpolated channel. As defined in the track object, it starts with a LOS segment, going into a shaded area with significantly more multipath fading at around 4 seconds and then back to LOS at around 13 sec.

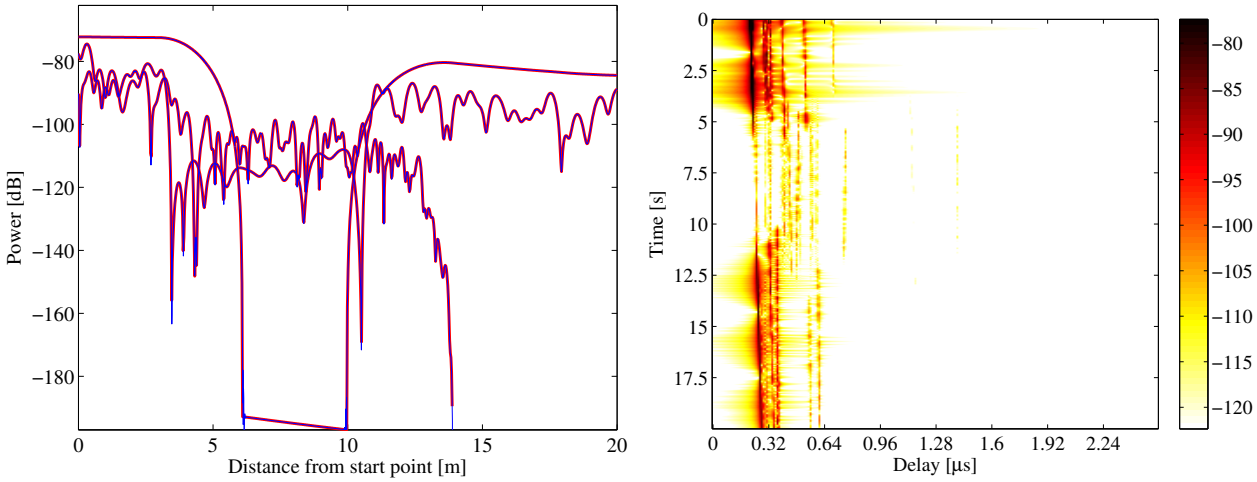

Figure 19: Received power and 2D PDP for the speed profile tutorial

```
h = ci.fr( 100e6,512 );
h = squeeze(h);
pdp = 10*log10(abs(ifft(h,[],1).').^2);

figure
imagesc(pdp(:,1:256));
caxis([ max(max(pdp))-50 max(max(pdp))-5 ])
colorbar

cm = colormap('hot');
colormap(cm(end:-1:1,:));

set(gca,'XTick',1:32:255);
set(gca,'XTickLabel',(0:32:256)/100e6*1e6);
xlabel('Delay [\mus]');

set(gca,'YTick',1:ci.no_snap/8:ci.no_snap);
set(gca,'YTickLabel', (0:ci.no_snap/8:ci.no_snap)/ci.no_snap * 20 );
ylabel('Time [s]');
```

Now, we create a movement profile. It is defined by a set of value pairs in track.movement_profile. The first value represents the time in seconds, the second value the position on the track. Here, we start at a position of 7 m, i.e. in the second (NLOS) segment. We then go back to the beginning of the track. This takes 5 seconds. Then, we wait there for 1 second and go to the end of the track, which we reach after additional 14 seconds.

The next step is to interpolate the sample points. This is done by the interpolate_movement method. It requires the sample interval (in s) as an input argument. Here, we choose an interval of 1 ms which gives us 1000 samples per second. Fig. 20 (left) illustrates the results.

```
t.movement_profile = [ 0,7 ; 5,0 ; 6,0 ; 20,20  ]';
dist = t.interpolate_movement( 1e-3 );
ci = cn.interpolate( dist , t.get_length );

nsnap = ci.no_snap;
time = (0:nsnap-1) * t.movement_profile(1,end)/(nsnap-1);

figure
plot( time,dist , 'r' )

xlabel('Time [s]');
ylabel('Position on track [m]');
```

The last plot (Fig. 20, right) shows the PDP of the interpolated channel with the movement profile applied. The channel starts in the second segment with a lot of fading, goes back to the first while slowing down at the same time. After staying constant for one second, the channel starts running again, speeding up towards the end of the track.

```
h = ci.fr( 100e6,512 );
h = squeeze(h);
pdp = 10*log10(abs(ifft(h,[],1).').^2);

figure
imagesc(pdp(:,1:256));
caxis([ max(max(pdp))-50 max(max(pdp))-5 ])
colorbar

cm = colormap('hot');
colormap(cm(end:-1:1,:));

set(gca,'XTick',1:32:255);
set(gca,'XTickLabel',(0:32:256)/100e6*1e6);
xlabel('Delay [\mus]');

set(gca,'YTick',1:ci.no_snap/8:ci.no_snap);
set(gca,'YTickLabel', (0:ci.no_snap/8:ci.no_snap)/ci.no_snap * 20 );
ylabel('Time [s]');
```

```
close all
disp(['QuaDRiGa Version: ',simulation_parameters.version])
```

```
QuaDRiGa Version: 1.0.1-145
```

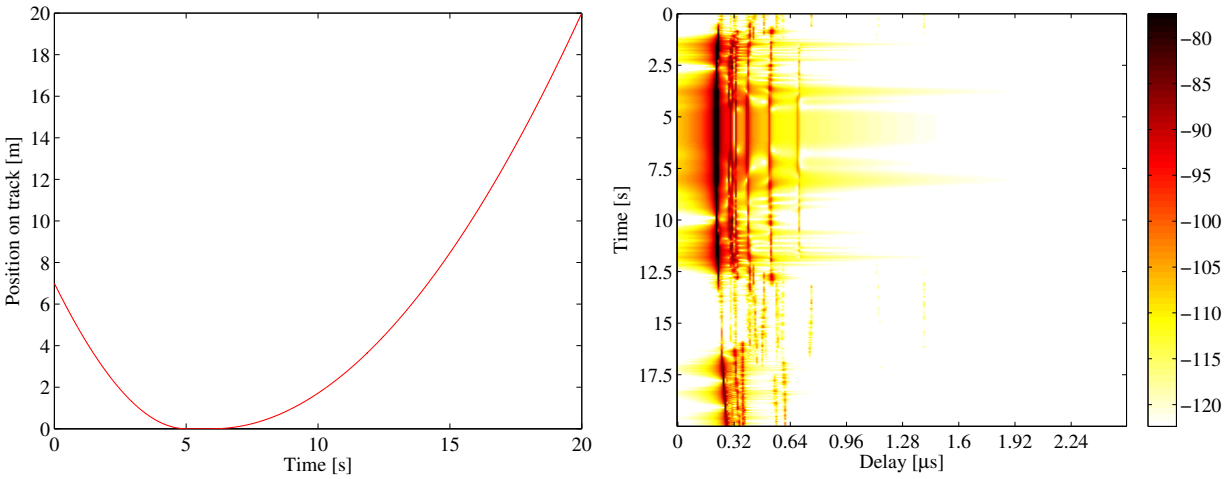

Figure 20: Movement profile (left) and interpolated PDP (right)

2.2.7 Geometric Polarization

Here, we demonstrate the polarization rotation model that calculates the path power for polarized antenna arrays. We do this by setting up the simulation with different H/V polarized antennas at the transmitter and at the receiver. Then we define a circular track around the receiver. When the receiver moves around the transmitter, it changes its antenna orientation according to the movement direction. In this way, all possible departure and elevation angles are sampled. Depending on the antenna orientation, the polarizations are either aligned (e.g. the Tx is V-polarized and the Rx is V-polarized), they are crossed (e.g. the Tx is V-polarized and the Rx is H-polarized) or the polarization orientation is in between those two. The generated channel coefficients should reflect this behavior.

Setting up the simulation environment First, we have to set up the simulator with some default settings. Here, we choose a center frequency of 2.1 GHz. We also want to use drifting in order to get the correct angles for the LOS component and we set the number of transmitters and receivers to one.

```
close all
clear all

set(0,'defaultTextFontSize', 14)
set(0,'defaultAxesFontSize', 14)

s = simulation_parameters;                  % Set the simulation parameters
s.center_frequency = 2.1e9;                 % Center-frequency: 2.1 GHz
s.use_polarization_rotation = 1;
s.samples_per_meter = 360/(40*pi);          % One sample per degree
s.drifting_precision = 1;
```

Setting up the antenna arrays In the second step, we set up our antenna arrays. We use the synthetic dipole antennas for this case. Those antennas show perfect polarization characteristics. First, we generate a

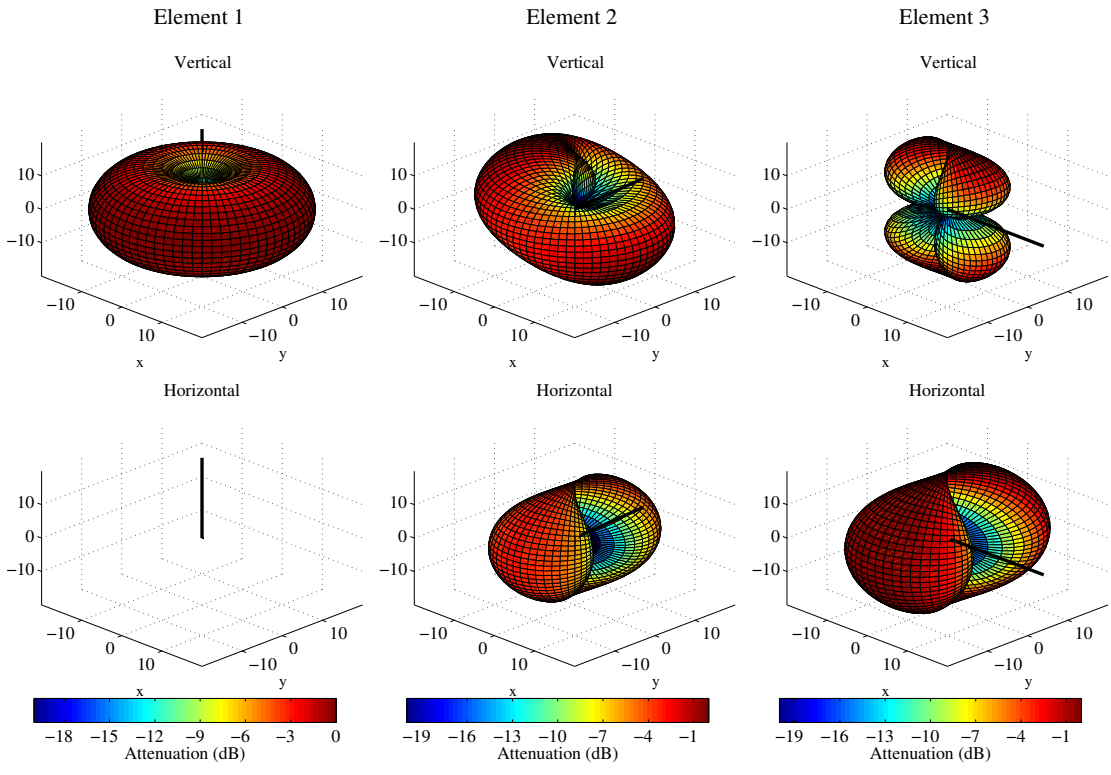

Figure 21: Polarimetric Dipole antenna patterns for different orientations

single dipole with V-polarization. Then, we create multiple copies of this antenna element and rotate them by 45 and 90 degrees, respectively. We then use the same array for the receiver.

```
l = layout( s );                                % Create a new Layout
l.tx_array.generate('dipole');                  % create V-polarized dipole
l.tx_array.set_grid( (-180:10:180)*pi/180 , (-90:10:90)*pi/180 );

l.tx_array.field_pattern_vertical = ...         % Normalize
    l.tx_array.field_pattern_vertical / max(max(l.tx_array.field_pattern_vertical));

l.tx_array.set_grid( (-180:5:180)*pi/180 , (-90:5:90)*pi/180 );
l.tx_array.copy_element(1,2:3);                 % Duplicate the element two more times
l.tx_array.rotate_pattern(45,'y',2);            % 45\degree\ polarization
l.tx_array.rotate_pattern(90,'y',3);            % 90\degree\ polarization
l.tx_array.visualize;                           % Plot the array
l.rx_array = l.tx_array;                        % Use the same array for the Rx
```

Defining a track The third step defines the track. Here, we use a circle with 20 m diameter starting in the east, traveling north. We also choose a LOS scenario since we want to study the LOS polarization. The transmitter is located 8 m north of the center of the circle at an elevation of 2 m.

```
l.tx_position = [ 0 ; 12 ; 6 ];                 % Tx position
l.rx_position = [ 20 ; 0 ; 0 ];                 % Start position for the Rx track
l.track.generate('circular',40*pi,0);           % A circular track with radius 10 m
l.track.scenario = 'BERLIN_UMa_LOS';            % Chosse the Urban Macro LOS scenario
l.track.interpolate_positions( s.samples_per_meter );     % Interpolate positions
l.visualize;                                    % Plot the track
```

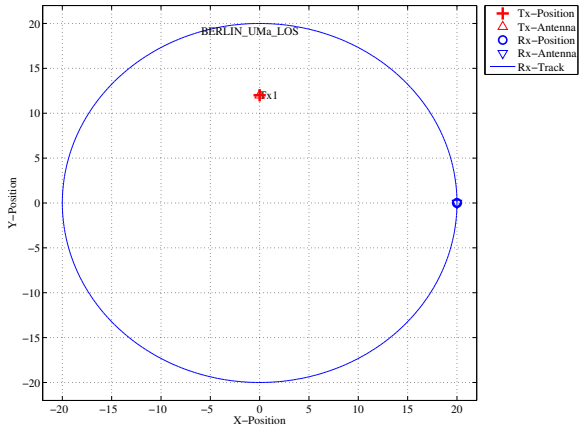

Figure 22: geometric_polarization_04

Generating channel coefficients Now, we have finished the parametrization of the simulation and we can generate the parameters. We thus create a new set of correlated LSPs and the fix the shadow fading and the K-factor to some default values. This disables the drifting for those parameters. We need to do that since otherwise, drifting and polarization would interfere with each other.

```
RandStream.setGlobalStream(RandStream('mt19937ar','seed',1));

p = l.create_parameter_sets;                    % Create parameter sets
p.parameter_maps(:,:,2) = 3;                    % Fix KF to 3 dB
p.parameter_maps(:,:,3) = 0;                    % Fix SF to 0 dB
p.plpar = [];                                   % Disable path loss model
p.update_parameters;

[c,cb] = p.get_channels;                        % Get the channel coefficients
```

```
Parameters    [ooooooooooooooooooooooooooooooooooooooooooooooooooooooooo]     1 seconds
Channels      [ooooooooooooooooooooooooooooooooooooooooooooooooooooooooo]     3 seconds
```

Results and Evaluation We now check the results and confirm, if they are plausible or not. We start with the two vertically polarized dipoles at the Tx and at the Rx side.

The model creates 8 taps, which is the default for the Urban-Macro LOS scenario. Without path-loss and shadow fading (SF=1), the power is normalized such that the sum over all taps is 1W and with a K-Factor of 3 dB, we get a received power of 0.67W for the LOS component. The remaining 0.33W are in the NLOS components. The results can be seen in Fig. 23 (top left).

```
figure                                              % New figure
plot(abs(squeeze( c.coeff(1,1,:,:) )').^2);         % Plot the graph
axis([0 360 -0.1 1]);                               % Set the axis
xlabel('Position [degrees]');                       % Add description
ylabel('LOS Power, linear scale');
title('Tx: Vertical , Rx: Vertical');               % Add title

disp(['LOS power:  ',num2str(mean( abs(c.coeff(1,1,1,:)).^2 , 4))])
disp(['NLOS power: ',num2str(mean( sum(abs(c.coeff(1,1,2:end,:)).^2,3) , 4))])
```

```
LOS power:  0.52851
NLOS power: 0.22249
```

The LOS power is almost constant when the Rx is south of the Tx. However, in close proximity (at 90°), the power is lowered significantly. This comes from the 2 m elevation of the Tx. When the Rx is almost under the Tx, the radiated power of the Dipole is much smaller compared to the broadside direction. The average power of the LOS is thus also lowered to 0.56 W. The average sum-power if the 7 NLOS components

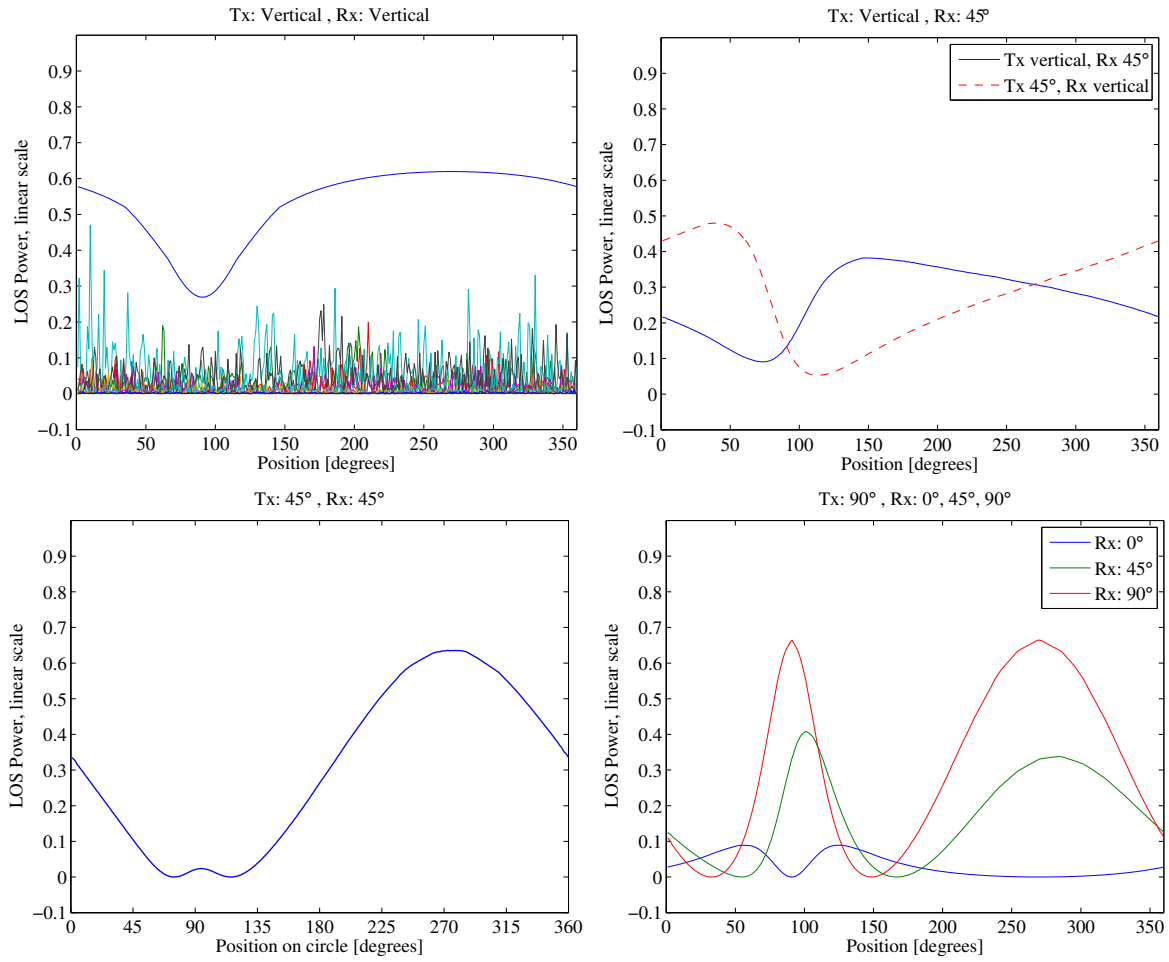

Figure 23: Results from the geometric polarization tutorial

is 0.26 W. This mainly come from the XPR which leakes some power from the vertical- into the horizontal polarization and thus reduces the received power on the vertically polarized Dipole.

Next, we study two cases. Either the Tx is vertical polarized and the Rx is at 45° or vise versa (Fig. 23, top right).

```
figure                                              % New figure
plot(abs(squeeze( c.coeff(2,1,1,:) )).^2);          % Tx vertical, Rx 45\degree\
hold on
plot(abs(squeeze( c.coeff(1,2,1,:) )).^2,'--r');    % Tx 45\degree\, Rx vertical
hold off
axis([0 360 -0.1 1]);
legend('Tx vertical, Rx 45\circ', 'Tx 45\circ, Rx vertical')
xlabel('Position [degrees]');
ylabel('LOS Power, linear scale');
title('Tx: Vertical , Rx: 45\circ');
```

The receiver changes its direction in a way that it always has the same orientation towards the Tx. However, due to the displacement of the Tx, the radiated power towards the Tx becomes minimal at around 90°Ṫhis minimum is visible in both curves (blue and red). However, the pole of the 45° slanted dipole now points to a different direction which explains the difference in the two lines. When the Rx is at 45° and the Tx is vertical, the pole is in the right half if the circle - resulting in a lower received power. When the Rx is Vertical and the Tx is 45° the minimum power is achieved in the left half of the circle.

Next, we evaluate the two dipoles which are rotated by 45°Ẇhen moving around the circle, the Tx stays fixed and the Rx rotates. Subsequently, at one position, we will have both dipoles aligned and at another position, both will be crossed. When they are crossed, the received power will be 0 and when they are aligned, the power will match the first plot (two vertical dipoles). This can be seen in the following figure.

```
figure                                              % New figure
plot(abs(squeeze( c.coeff(2,2,1,:) )).^2 , 'Linewidth',1);
axis([0 360 -0.1 1]);
set(gca,'XTick',0:45:360)
xlabel('Position on circle [degrees]');
ylabel('LOS Power, linear scale');
title('Tx: 45\circ , Rx: 45\circ');
```

In the last figure, we have the Tx-antenna turned by 90°İt is thus lying on the side and it is horizontally polarized. For the Rx, we consider three setups: Vertical (blue line), 45° (green line) and 90° (red line). Note that the Tx is rotated around the y-axis. At the initial position (0°), the Rx (45 and 90°) is rotated around the x-axis. This is because the movement direction.

```
figure                                              % New figure
plot(abs(squeeze( c.coeff(:,3,1,:) ))'.^2);
axis([0 360 -0.1 1]);
legend('Rx: 0\circ','Rx: 45\circ','Rx: 90\circ' )
xlabel('Position [degrees]');
ylabel('LOS Power, linear scale');
title('Tx: 90\circ , Rx: 0\circ, 45\circ, 90\circ');
```

When the receiver is vertical (blue line), both antennas are always crossed. There is no position around the circle where a good link can be established. When the receiver is horizontal (red line), however, there are two points where the two dipoles are aligned. For the 45° dipole, the same behavior can be observed but with roughly half the power.

```
close all
disp(['QuaDRiGa Version: ',simulation_parameters.version])
```

```
QuaDRiGa Version: 1.0.1-145
```


eMail: quadriga@hhi.fraunhofer.de

2.2.8 Visualizing RHCP/LHCP Patterns

The internal algorithms of the channel model only work with linear polarization. The antenna patterns are thus only stored in H/V polarization. This script defines two circular patch antennas and places them in an environment. It then rotates the transmit antenna degree by degree and thus samples all azimuth and elevation angles. The channel model is set up to record the channel response and thus record the RHCP/LHCP response like in a measurement in an anechoic chamber.

Set up the array We set up a patch antenna with an opening angle of 120°Ẇe then copy that patch and rotate it by 90° around the x-axis to create an X-Pol array. We then set the coupling to +/- 90° phase to transmit circular polarized waves.

```
resolution = 10;        % in Degrees

a = array('custom',120,120,0);
a.set_grid( (-180:resolution:180)*pi/180 , (-90:resolution:90)*pi/180 );
a.copy_element(1,2);

b = a.copy_objects;

a.rotate_pattern(90,'x',2);
a.coupling = 1/sqrt(2) * [1 1;1j -1j];

b.rotate_pattern(90,'x',2);
b.coupling = 1/sqrt(2) * [1 1;1j -1j];
```

Place arrays in layout We place two of those arrays in a layout. The scenario 'LOSonly' has no NLOS scattering. One can see this setup as a perfect anechoic chamber.

```
l = layout;
l.simpar.show_progress_bars = 0;
l.simpar.drifting_precision = 0;

l.rx_position = [11;0;0];
l.track.no_snapshots = 1;
l.track.ground_direction = pi;
l.track.scenario = 'LOSonly';
l.tx_array = a;
l.rx_array = b;

p = l.create_parameter_sets;
[~,cb] = p.get_channels;
cb.pin = zeros( size(cb.pin) );
```

Get array response We now sample the array response for each degree in the antenna array.

```
pat = zeros( a.no_el , a.no_az , 2 , 2 );

values = a.no_az;
fprintf('Calculating  ['); m0=0; tStart = clock;  % A Status message
for n = 1:a.no_az
    m1=ceil(n/values*50); if m1>m0; for m2=1:m1-m0; fprintf('o'); end; m0=m1; end;

    a1 = a.copy_objects;
    a1.rotate_pattern( a.azimuth_grid(n)*180/pi , 'z');

    for m=1:a.no_el
        a2 = a1.copy_objects;
        a2.rotate_pattern( a.elevation_grid(m)*180/pi,'y');
        cb.tx_array = a2;
        c = cb.get_channels;
        pat(m,n,:,:) = c.coeff;
    end
end
fprintf('] %5.0f seconds\n',round( etime(clock, tStart) ));
```

```
Calculating  [oooooooooooooooooooooooooooooooooooooooooooooooooo]    17 seconds
```

Plot For plotting we use the internal function of the array class. We adjust the title of the figures accordingly.

```
d = a.copy_objects;
d.field_pattern_vertical =  pat(:,:,:,1) ;
d.field_pattern_horizontal = pat(:,:,:,2) ;
x = d.visualize;

set(x(1,11),'String','RHCP-RHCP')
set(x(1,12),'String','RHCP-LHCP')

set(x(2,11),'String','LHCP-RHCP')
set(x(2,12),'String','LHCP-LHCP')
```

```
close all
disp(['QuaDRiGa Version: ',simulation_parameters.version])
```

```
QuaDRiGa Version: 1.0.1-145
```

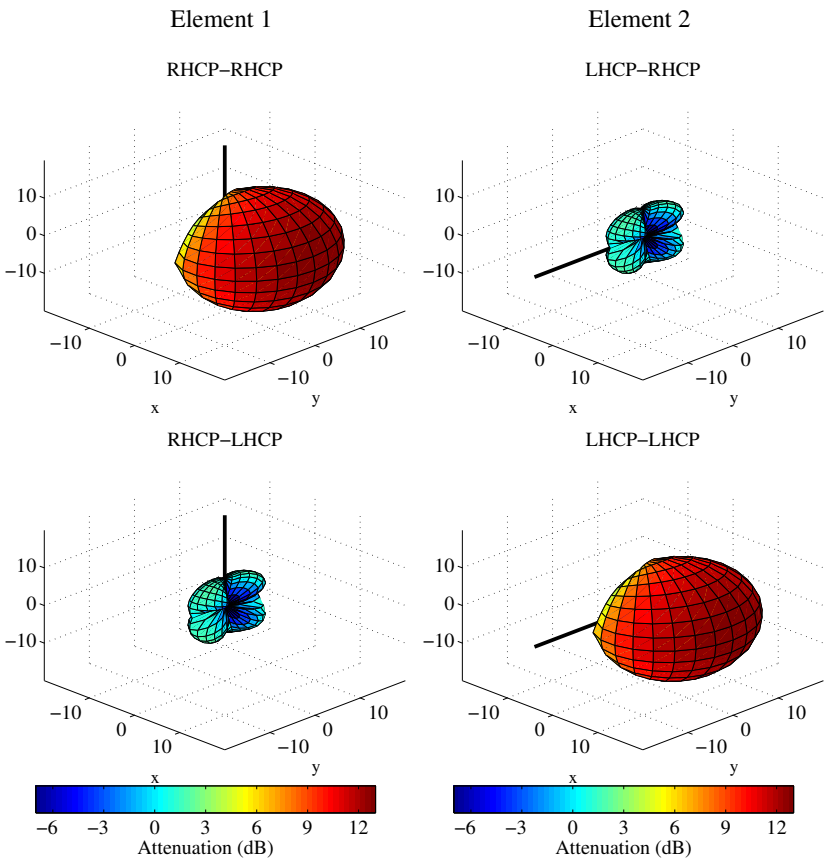

Figure 24: RHCP / LHCP antenna patterns

2.2.9 How to manually set LSPs in QuaDRiGa

This tutorial explains, how to generate a time-series of channel coefficients with manual selection of LSPs.

Setting general parameters We set up some basic parameters such as center frequency, sample density and the position of the transmitter.

```
close all
clear all

set(0,'defaultTextFontSize', 14)    % Set default font size for the plots
set(0,'defaultAxesFontSize', 14)

s = simulation_parameters;          % Basic simulation parameters
s.center_frequency      = 2.185e9;  % Center Frequency
s.sample_density        = 4;        % 4 samples / half wave length

l = layout(s);                      % Create Layout
```

Setting up a user track QuaDRiGa needs the positions of transmitter and receiver, e.g. for calculating the polarization or the arrival and departure angels. The positioning information of the Tx and Rx is essential also when the LSPs are not calculated. The following generates a linear track with 20 m length having a direction. The track is further split into 4 segments of 5 m length.

The splitting is done by calling the method 'split_segment' of the track object. The the first two arguments of that function are the minimum length of a segment (1 m) and the maximum length of the segment (6 m). Each existing segment that is longer then the maximum length is split into subsegments. The length of those segments is random where the third and fourth parameter determine the mean and the STD of the length of new subsegment. Hence, 't.split_segment(1,6,5,0)' splits all segment longer than 6 m into subsegments of 5 m length.

Each segment gets assigned a scenario. This is also essential since many parameters (such as the number of clusters, the XPR etc.) are scenario-specific. Hence, they are the same for the entire scenario. Here, we set the first the segments to NLOS, the third to LOS and the last to NLOS.

Last, we set a random starting position for the track in the layout.

```
l.tx_position = [0;0;25];                       % Set Tx-position

t = track('linear',20);                         % Linear track, 20 m length
t.interpolate_positions( s.samples_per_meter);  % Interpolate to sample density
t.split_segment( 1,6,5,0 )                      % Split in 4 segments

Un = 'WINNER_UMa_C2_NLOS';
Ul = 'WINNER_UMa_C2_LOS';
t.scenario = {Un,Un,Ul,Un};                     % Set scenarios

l.randomize_rx_positions( 500,0,0,0 );          % Random start position
tmp = l.rx_position;
l.track = t;
l.rx_position = tmp;

l.visualize;
```

Manual setting of the parameters Now we initialize the parameter-set objects.

The method "l.create_parameter_sets" splits the track into smaller sub-tracks, one for each segment. It further extracts the scenario informations. Each scenario gets its own parameter-set object. So we get an

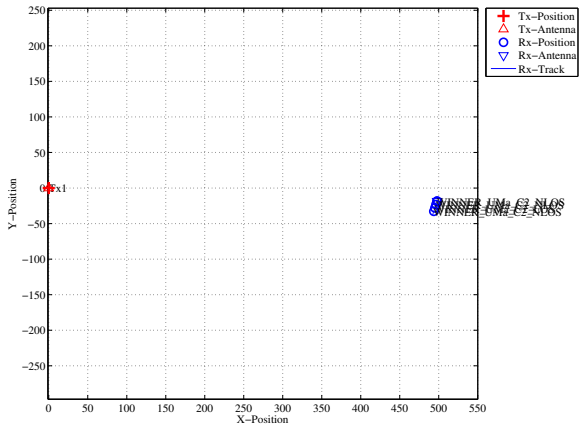

Figure 25: Scenario overview (manual parameter selection)

array of two parameter sets. The first element p(1) has three positions (NLOS segments) and the second has one position (LOS segment).

```
p = l.create_parameter_sets(1);

p(1).name
p(1).no_positions

p(2).name
p(2).no_positions
```

```
Parameters   [oooooooooooooooooooooooooooooooooooooooooooooooooooo]     5 seconds

ans =

WINNER-UMa-C2-NLOS_Tx1


ans =

     3


ans =

WINNER-UMa-C2-LOS_Tx1


ans =

     1
```

We set the number of clusters for the NLOS segments to 14. Currently, it is not possible to have a different number of clusters for each segment, i.e. it is not possible for the first NLOS segment to have 14 clusters and for the second to have only 10.

```
p(1).scenpar.NumClusters = 14;
```

In order to manually set the parameters, we have to overwrite the original settings. We do this here for the delay spread. The automatically generated values are:

```
[p(1).ds(1) p(1).ds(2) p(2).ds(1) p(1).ds(3) ]*1e6
```

```

ans =

    0.2696    0.2433    0.0948    0.2094
```

We want to set the values of the four segments to 0.45, 0.33, 0.12 and 0.60 microseconds. This is done by:

```
p(1).ds(1) = 0.45e-6;
p(1).ds(2) = 0.33e-6;
p(2).ds(1) = 0.12e-6;
p(1).ds(3) = 0.60e-6;
```

The K-Factor and the shadow fading are read from the map during the generation of channel coefficients. This would overwrite any manual values. However, this could be deactivated. A drawback is that in this case the KF, SF and PL are only updated once per segment. This will result in a step-like function of the output power. There is currently no method the set the power manually on a per-snapshot basis.

In the following example, we want to fix the received power to -102, -97, -82 and -99 dBm. K-Factors are taken from the map.

```
p(1).plpar = [];                        % Disable path loss for NLOS
p(2).plpar = [];                        % Disable path loss for LOS

p(1).sf = 10.^(0.1*[-102, -97, -99]);   % Set power for NLOS segments
p(2).sf = 10.^(0.1*[-82]);              % Set power for LOS segments

p(1).map_valid = false;                 % Disable automatic overwrite for NLOS
p(2).map_valid = false;                 % Disable automatic overwrite for LOS
```

Calculate channel coefficients Now we calculate the coefficients and the received power along the path. The following command calculate the channel coefficients. We then check the number of clusters that have been produced for each segment.

```
cm = p.get_channels;                    % Calculate the channel coefficients
cat( 1, cm.no_path )                    % Display the number of paths
```

```
Channels     [ooooooooooooooooooooooooooooooooooooooooooooooooooo]     7 seconds

ans =

    14
    14
    14
     8
```

The first three segments have 14 clusters. This has been set earlier. The last LOS segment has 15 clusters. One can see, that the three NLOS segment come first, followed by the LOS segment. The order has been scrambled. The following command sorts and combines the segments into one fading sequence.

```
c = cm.merge;
```

We now plot the power along the path. You can see the power levels of around -102, -97, -82 and -99 dBm which have been set earlier. Each segment has a transition area (e.g. from 2.5m to 5m, from 7.5m to 10m and from 12.5m to 15m) where the merging took place. In those areas, the power is scaled linearly. That means that, for example, in between 7.5 and 10m, the power ramps up from -97 to -82 dBm.

```
power = squeeze(sum(abs(c.coeff).^2,3));
power = 10*log10(power);

figure
[~,dist] = t.get_length;
plot(dist,power)
title('Simulated Power')
xlabel('Distance from start point [m]')
ylabel('Received Power [dBm]')
axis([0,20,-110,-80])
grid on
```

Figure 26: Power along the track (manual parameter selection)

The last plot shows the DS along the path. The results reflect the settings of 0.45, 0.33, 0.12 and 0.60 quiet well. As for the power, there is an overlap in between the segments. For example, in between 7.5 and 10m the DS drops from 0.33 to 0.12 microseconds. Additional fluctuations are caused by small scale fading.

```
coeff = squeeze( c.coeff );
delay = c.delay;

pow_tap = abs(coeff).^2;
pow_sum = sum(pow_tap);
mean_delay = sum( pow_tap.*delay) ./ pow_sum;
ds = sqrt( sum( pow_tap.*delay.^2)./ pow_sum - mean_delay.^2 );

figure
plot(dist,ds*1e6)
title('Simulated Delay Spread')
xlabel('Distance from start point [m]')
ylabel('RMS DS [\mus]')
axis([0,20,0,1])
grid on
```

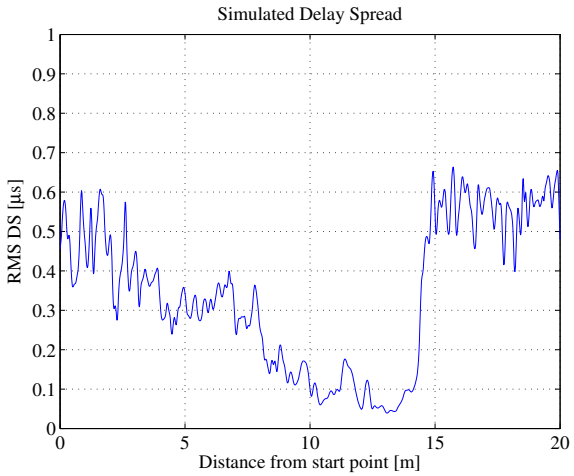

Figure 27: DS along the track (manual parameter selection)

```
close all
disp(['QuaDRiGa Version: ',simulation_parameters.version])
```

```
QuaDRiGa Version: 1.0.1-145
```

2.3 Overview of the Software Structure

An overview of the model software is depicted in Fig. 28. The unified modeling language (UML) class diagram of the `QuaDRiGa` channel model gives an overview of all the classes, methods and properties of the model. The class diagram serves as a reference for the following descriptions which also lists the methods that implement a specific functionality.

A detailed help for each method or property is given as MATLAB help. To get help for "array.interpolate" you can type in the MATLAB console:

```
help array.interpolate
```

The result will be:

```
%INTERPOLATE Interpolates the field pattern
%
%   [V,H] = INTERPOLATE( azimuth,elevation ) Interpolates the field pattern to the
%   given azimuth and elevation values. Azimuth and elevation are angles in the
%   spheric coordinate system. Azimuth can range from -Pi to Pi and elevation can
%   have values in between -Pi/2 and Pi/2. Values outside this range will be
%   converted accordingly. Important: All angles must be given in radians!
%
%   [V,H] = INTERPOLATE( azimuth,elevation,element ) also specifies the element
%   range for which the pattern will be interpolated.
%
%   [V,H,dist] = INTERPOLATE( azimuth,elevation,element ) also returns the
%   effective distances between the antenna elements when seen from the
%   direction of the incident path. The distance is calculated by an
%   projection of the array positions on the normale plane of the incident
%   path.
%
%   Note: Interpolation of the beam patterns is very (!!!) computing intensive. It
%   must be performed several thousands of times during a simulation run. It is
%   highly recommended to use nearest-neighbor interpolation for this task since
%   this method is optimized for speed. Linear and spline interpolation call the
%   MATLAB internal interpolation function which is more than 10 times slower.
%   To enable nearest-neighbor interpolation, set the 'interpolation_method'
%   property of the array object to 'nearest'.
%
% Stephan Jaeckel
% Fraunhofer Heinrich Hertz Institute
% Wireless Communication and Networks
% Einsteinufer 37, 10587 Berlin, Germany
% e-mail: stephan.jaeckel@hhi.fraunhofer.de
```

Alternatively, you can read the help files using the MATLAB browser. In this case, open the MATLAB Help and navigate to the menu item "QuaDRiGa Toolbox" on the left hand side. The item "QuaDRiGa Class Overview" now gives access to all the help files.

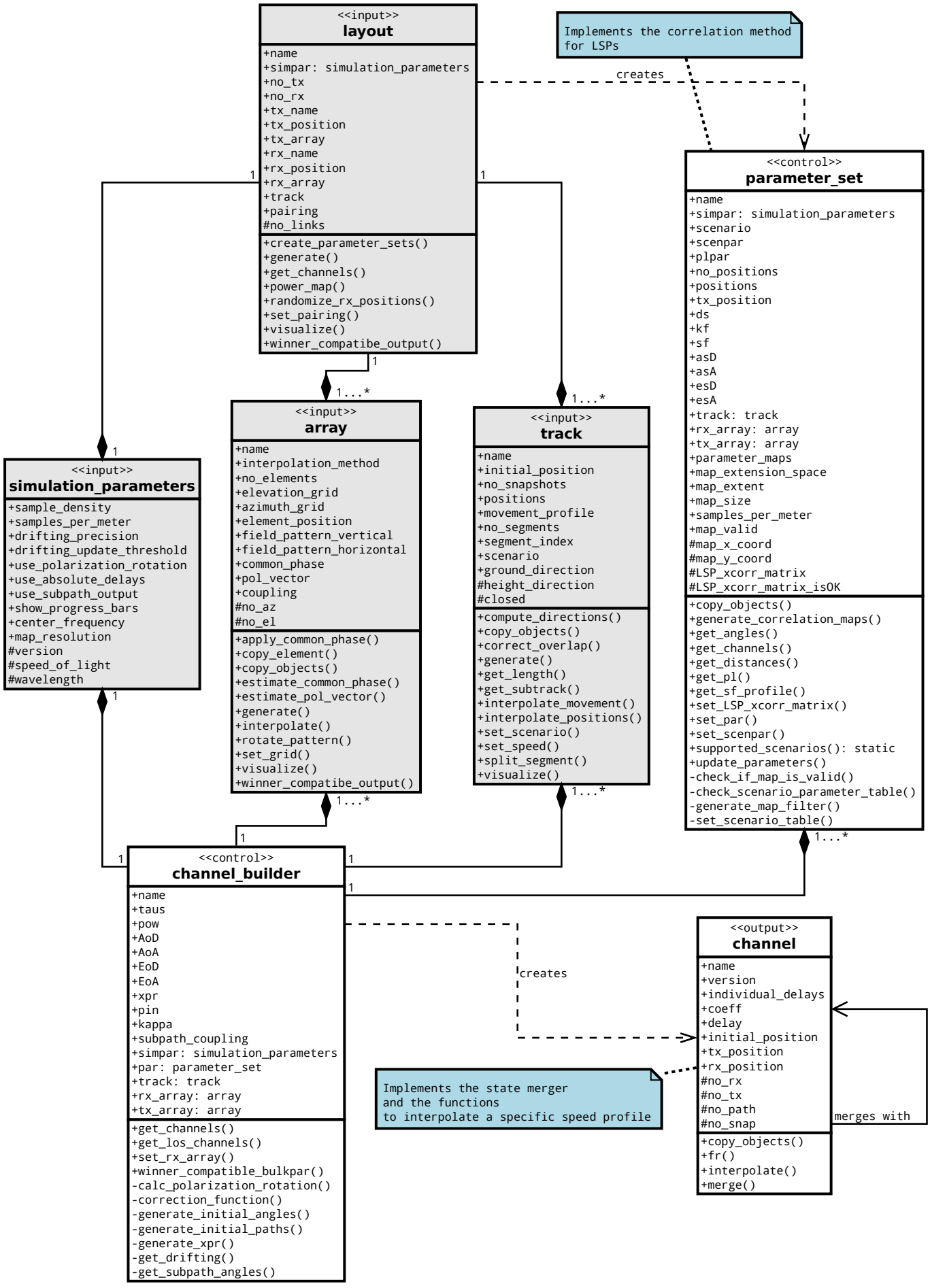

Figure 28: UML class diagram of the model software.

2.4 Adding New Scenarios

The scenario parameters are set in "parameter_set.scenpar". Here, you also have the option to change individual parameters by assigning new values. The scenario "UMal", for example, uses by default 8 clusters. When the simulations should be done with 15 clusters, one can change the settings by

```
p = parameter_set('BERLIN_UMa_LOS');          % New parameter set
p.scenpar.NumClusters = 15;                   % Set new number of clusters
```

A list of currently supported scenarios is generated by:

```
parameter_set.supported_scenarios
```

The default settings of those scenarios are stored in config files which are located in the "config"-folder of the QuaDRiGa source path. The "UMal" config file for example looks like this:

```
% Config File for scenario "UMal"
% WINNER+ Urban Macro LOS
% See: CELTIC / CP5-026 D5.3: WINNER+ Final Channel Models
% and: IST-4-027756 WINNER II D1.1.2 v.1.1: WINNER II Channel Models
%
% Stephan Jaeckel
% Fraunhofer Heinrich Hertz Institute
% Wireless Communication and Networks
% Einsteinufer 37, 10587 Berlin, Germany
% e-mail: stephan.jaeckel@hhi.fraunhofer.de

NumClusters = 8
r_DS        = 2.5

SF_sigma    = 5
SF_lambda   = 45
LNS_ksi     = 3

KF_mu       = 7
KF_sigma    = 3
KF_lambda   = 12

DS_mu       = -7.39
DS_sigma    = 0.63
DS_lambda   = 40

AS_D_mu     = 1
AS_D_sigma  = 0.25
AS_D_lambda = 15
PerClusterAS_D = 6

AS_A_mu     = 1.7
AS_A_sigma  = 0.19
AS_A_lambda = 15
PerClusterAS_A = 12

ES_D_mu     = 0.7
ES_D_sigma  = 0.2
ES_D_lambda = 15    % D5.3 pp. 73
PerClusterES_D = 3

ES_A_mu     = 0.95
ES_A_sigma  = 0.16
ES_A_lambda = 15    % D5.3 pp. 73
PerClusterES_A = 7

xpr_mu      = 8
xpr_sigma   = 4

% Adjustments have been made to keep xcorr-matrix positive definite
asD_ds  =  0.4
asA_ds  =  0.7 % 0.8
asA_sf  = -0.5
asD_sf  = -0.4 % 0.5
```

```
ds_sf    = -0.4
asD_asA =  0.3
asD_kf   =  0.1
asA_kf   = -0.2
ds_kf    = -0.4
sf_kf    =  0.3
esD_ds   = -0.4 % -0.5
esD_asD =  0.4 % 0.5
esA_sf   = -0.8
esA_asA =  0.4

% A * log10 d + B + C * log10 f + D * log10 hBS + E * log10 hMS
% Two different values (first before breakpoint, last after breakpoint)
% Different SF coefficients

PL_model = winner_los

PL_A1    = 26
PL_B1    = 25
PL_C1    = 20
PL_D1    = 0
PL_E1    = 0
PL_sig1 = 4

PL_A2    = 40
PL_B2    = 9.27
PL_C2    = 6
PL_D2    = -14
PL_E2    = -14
PL_sig2 = 6
```

You can create you own scenario by editing this file and saving it under a new filename in the "config"-Folder. The file ending must be ".conf". The filename then is also the scenario name and the settings can be accessed from inside MATLAB as described above.

3 Technical Documentation

An overview of the modeling steps is given in Fig. 29. The user provides the network layout, i.e. the positions of the BSs, antenna configurations, downtilts, the positions and trajectories of the MTs and the propagation scenarios. The channel coefficients are then calculated in seven steps which are described in sections 3.2 and 3.3.

Much of the modeling approach is inspired by the WINNER model [KMH+07]. Major extensions concerning the time evolution have been made in steps D and G. In order to make those extension work properly, changes were also required in the other parts. For example, time evolution requires a more detailed description of the mobility of the terminals which is solved by assigning tracks, i.e. ordered lists of positions, to the MTs. Updates of the channel coefficients are then triggered at fixed snapshot positions.

The WINNER model only allows constant speeds via a continuous rotation of the phases of the multipath components (MPCs). However, realistic scenarios would also include accelerations, decelerations and MTs with different speeds, e.g. pedestrian and vehicular users. However, to minimize the computational overhead and memory requirements, we generate the channel coefficients at a constant sample rate which fulfills the sampling theorem, i.e. updates are triggered at least twice per half wave length. A time-series for varying speeds is then obtained by interpolating the coefficients in a separate postprocessing step.

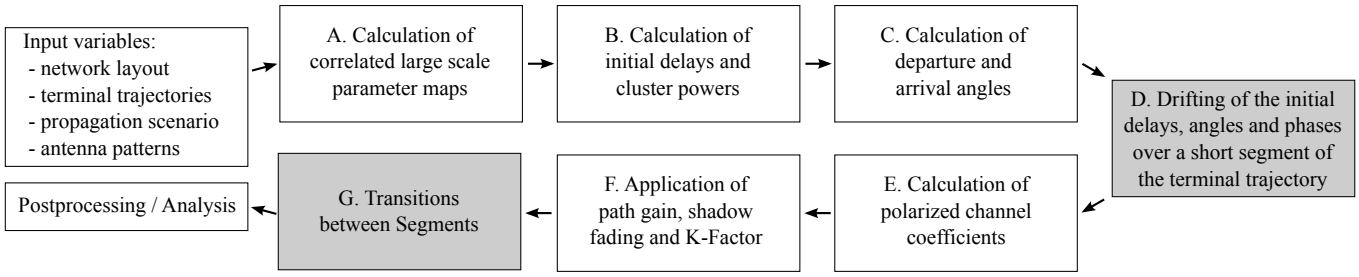

Figure 29: Essential steps for the calculation of time evolving channel coefficients

3.1 Tracks, Scenarios, Antennas and Network Layout

3.1.1 Drops and Segments

The concept of segments and drops is already described in [KMH+07]. See also Fig. 30. Channel segments represent a period of quasi-stationarity during which probability distributions of low-level parameters are not changed noticeably. During this period all large-scale parameters are practically constant. To be physically feasible, the channel segment must be confined in distance. The size of the segments depends on the environment, but it can be at maximum a few dozen meters. The decorrelation distances of different parameters describe roughly the proper size of the channel segment. These decorrelation distances can be extracted from measurements and are scenario dependent.

In the WINNER terminology, a drop is defined as a segment with zero-length. In order to extend the length of a drop, short-term time-variability of some channel parameters is added within the drops. This method is known as drifting and was first described in [BHS05]. The current model uses drifting to enable time continuous simulations. Here, two types of drifting need to distinguished:

1. Drifting of Path Delays and Angles and Polarization
   It is assumed that the positions of scatterers are fixed during a drop. As a consequence, the angle of departures (AoDs) of the scatters as seen from the BS do not change, with the exception of the LOS AoD. However, based on the fixed-geometry assumption, the angle of arrivals (AoAs) of the scatters

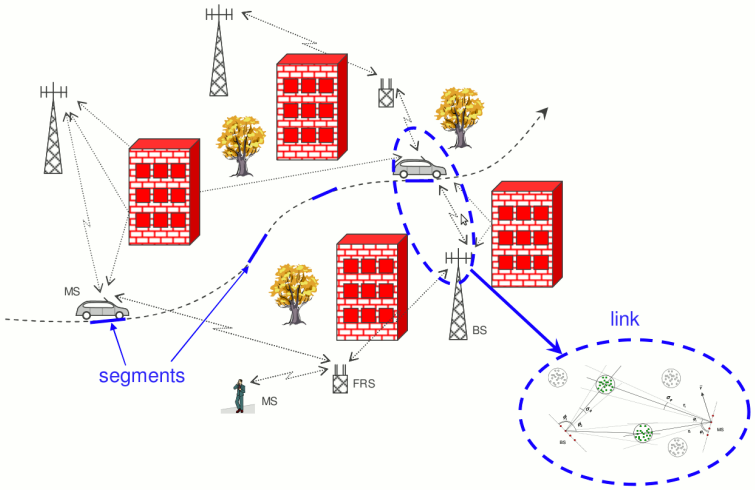

Figure 30: WINNER system level approach showing several segments (drops). Source: [KMH+07]

as seen from the MT as well as the subpath delays change during a drop due to the MT movement. Similarly, the LOS directions between BS and MT and the polarization characteristics vary in time. Implementation details of the drifting can be found in Section 3.3.3.

2. Drifting of Shadow Fading and K-Factor
   The time-evolution of shadow fading is determined by its spatial autocorrelation function. References show that an exponential function fits well and the drifting can thus be modeled by a first order autoregressive process. This is realized by calculating maps containing the correlated large scale parameters. The drifting is then implemented by reading the map values along the segments track and interpolating the data.

3.1.2 Sample Density vs. Sample Rate

If you consider moving receivers, choosing the right sampling rate depends directly on the Doppler spectrum. In order to successfully reconstruct the impulse response, you need a sample rate f_T fulfilling the sampling theorem.

$$f_T \geq 2B_D = 4 \max |\Delta f_D| = 4 \frac{\max |v|}{\lambda_c} \tag{1}$$

with B_D being the width of the Doppler spectrum, Δf_D the frequency change due to velocity v and λ_c being the carrier wavelength. Thus the appropriate sampling rate is proportional to the maximal velocity of the receivers. Since it is sometimes useful to examine algorithm behavior for different user velocities, it is unfortunate to fix the sampling rate in advance as the max speed is fixed as well. To overcome this problem it is advantageous to sample the channel in the spatial domain rather than in the time domain.

$$f_S = \frac{f_T}{\max |v|} \geq \frac{4}{\lambda_c} \tag{2}$$

Here f_S denotes the spatial sampling rate in samples per meter. In its normalized form it is also known as sample density SD

$$\mathrm{SD} = \frac{f_S}{\lambda_c / 2} \geq 2 \tag{3}$$

Another advantage of sampling in the spatial domain is the reduction of required storage, since the number of samples is reduced in case the maximum speed is greater than 1 meter per second (3.6 kilometers per hour).

3.1.3 The Antenna Model

One feature of `QuaDRiGa` is that it allows the separations of propagation- and antenna effects. An antenna is defined by its directional response F, also known as field pattern. The original SCM considers only 2D propagation. Thus, F is a function of the azimuth angle ϕ which is also indicated in Fig. 2. Later extensions [SZM+06] also consider the elevation direction θ. The complex amplitude g of one tap between a transmit antenna t and a receive antenna r notes

$$g_{r,t} = \sqrt{P} \cdot \mathbf{F}_r(\phi^a, \theta^a)^T \cdot \mathbf{M} \cdot \mathbf{F}_t(\phi^d, \theta^d) \cdot e^{-j\frac{2\pi}{\lambda} \cdot d} \tag{4}$$

where $\mathbf{F}_r$ and $\mathbf{F}_t$ are the patterns at the receiver and transmitter, respectively. λ is the wavelength and P is the power of the tap. Note here, that the patterns $\mathbf{F}(\phi, \theta)$ are two-element vectors which contain the vertically (F_V) and horizontally (F_H) polarized component of the antenna response

$$\mathbf{F}(\phi, \theta) = \begin{pmatrix} F_V(\phi, \theta) \\ F_H(\phi, \theta) \end{pmatrix} \tag{5}$$

$\mathbf{M}$ is the 2×2 polarization coupling matrix. This matrix describes how the polarization changes on the way from the transmitter to the receiver. It is important to note here, that in a MIMO configuration, which uses multiple antennas at the transmitter and receiver, the physical propagations effects such as the angles of departure and arrival, the path powers, the delays and the polarization coupling stay the same for all antennas. The only difference is that each antenna element has a different field pattern.

Changing the orientation of antennas Here we describe how the orientation of an antenna can be changed (e.g. when moving the receiver along a street, or turning a mobile phone in the hands of the user). This is done in two steps. First, the field patterns for both polarizations F_{V} and F_{H} are rotated and interpolated separately. The second step then includes the effects of the polarization.

An antenna pattern (5) is given in spherical coordinates as a function of the azimuth angle ϕ and elevation angle θ. When the orientation of the antenna element changes, the field pattern has to be read at different

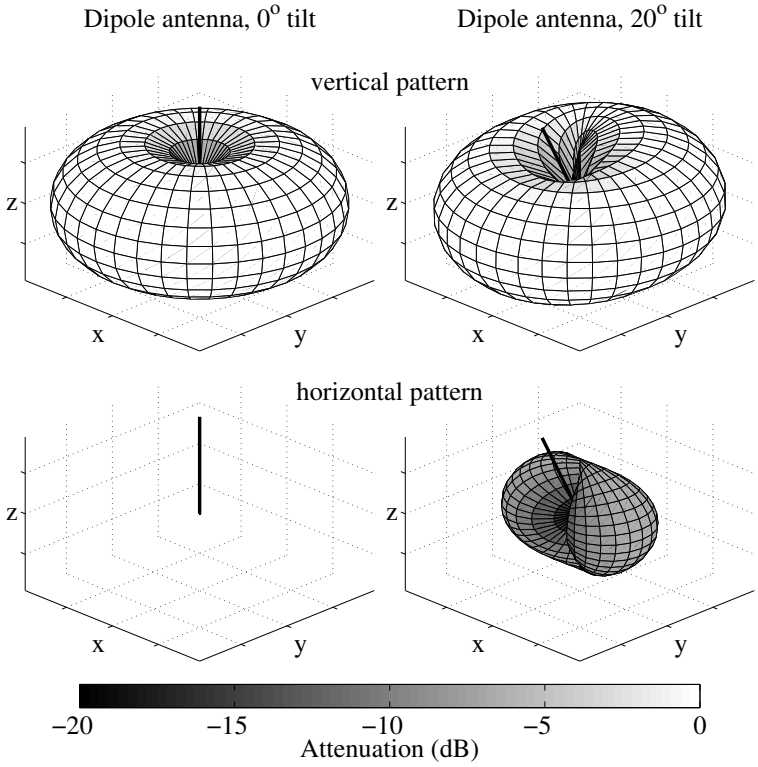

Figure 31: Example patterns for a dipole antenna.

angles (Φ, Θ) which include the effect of the orientation change. Rotations in 3D are easier in Cartesian coordinates. We therefore transform the original angle pair (ϕ, θ) into a vector $\mathbf{a}$ that describes the arrival- or departure angles in Cartesian coordinates. The three vector elements represent the x,y and z-component.

$$\mathbf{a}(\phi, \theta) = \begin{pmatrix} \cos\phi \cdot \cos\theta \\ \sin\phi \cdot \cos\theta \\ \sin\theta \end{pmatrix} \tag{6}$$

We now use a 3×3 matrix $\mathbf{Q}$ to describe the orientation change in 3D space. In principal, we can calculate $\mathbf{Q}^T$ for any arbitrary rotation axis and angle. The example in Fig. 31 was tilted by 20° around the x-axis of the coordinate system. The corresponding matrix is

$$\mathbf{Q}_x(20^\circ) = \begin{pmatrix} 1 & 0 & 0 \\ 0 & \cos(20^\circ) & -\sin(20^\circ) \\ 0 & \sin(20^\circ) & \cos(20^\circ) \end{pmatrix} \tag{7}$$

By multiplying $\mathbf{Q}$ with (6), we include the orientation change in the vector

$$\mathbf{a}^+(\phi, \theta) = \mathbf{Q}^T \cdot \mathbf{a}(\phi, \theta) \tag{8}$$

Since $\mathbf{a}^+$ is now also in Cartesian coordinates and we need the transformed pattern $\tilde{\mathbf{F}}$ in spherical coordinates, we have to transform $\mathbf{a}^+$ back to spherical coordinates. This results in the new angles (Φ, Θ).

$$\Phi(\phi, \theta) = \arctan_2\left[a_y^+(\phi, \theta), a_x^+(\phi, \theta)\right] \tag{9}$$

$$\Theta(\phi, \theta) = \arcsin\left[a_z^+(\phi, \theta)\right] \tag{10}$$

a_x^+, a_y^+ and a_z^+ are the x, y and z component of $\mathbf{a}^+$, respectively. We now get the coefficients of the rotated pattern by reading the original pattern $\mathbf{F}$ at the transformed angles

$$\hat{F}_{\mathrm{V/H}}(\phi, \theta) = F_{\mathrm{V/H}}(\Phi, \Theta) \tag{11}$$

Since the patterns are sampled at a fixed angular grid, this involves an interpolation step. As a standard computationally inexpensive procedure, we use linear interpolation. Alternatively, more advanced techniques based on the effective aperture distribution function (EADF) can be used [NKS+07].

The second step of the transformation takes the polarization into account. We first take the antenna orientation vector $\mathbf{o}$ and apply the rotation matrix $\mathbf{Q}$ to obtain $\tilde{\mathbf{o}}$

$$\tilde{\mathbf{o}} = \mathbf{Q} \cdot \mathbf{o} \tag{12}$$

This vector $\tilde{\mathbf{o}}$ is the new orientation vector of the transformed pattern. Next, we calculate a rotation matrix that accounts for the changed polarization characteristics of the rotated antenna pattern. In principal, the following procedure emulates an antenna measurement like in an anechoic chamber. The virtual transmitter is placed south of our test antenna. The wave travel direction $\mathbf{r}$ thus lies in y direction. We thus rotate the orientation vector of our antenna so that it matches the wave travel direction. The polarization vector $\mathbf{p}_r$ results from a projection of the orientation vector $\mathbf{o}_r$ on the plane perpendicular to the travel direction (see Fig. 38 for details).

1. We rotate the orientation vector $\tilde{\mathbf{o}}$ by $p = -\phi - \pi/2$ in azimuth direction and $q = \theta$ in elevation direction to match the orientation of the transmitter.

$$\mathbf{o}^+ = \begin{pmatrix} \cos p & -\sin p & 0 \\ \cos q \cdot \sin p & \cos q \cdot \cos p & -\sin q \\ \sin q \cdot \sin p & \sin q \cdot \cos p & \cos q \end{pmatrix} \cdot \tilde{\mathbf{o}} \tag{13}$$

2. We calculate the projection of the orientation vector on the projection plane. Since the projection plane lies in the x-z-plane due to the placement of the transmitter, we simply omit the y component of $\mathbf{o}^+$, switch

the x and z component and normalize the resulting vector to unit length. The switching is done to obtain the same orientation as in (5).

$$\mathbf{p}_r = \begin{pmatrix} o_z^+ \\ o_x^+ \end{pmatrix} / \left| \begin{pmatrix} o_z^+ \\ o_x^+ \end{pmatrix} \right| \tag{14}$$

3. We define the transmitter to be either perfectly vertical $\left(\mathbf{p}_t = [1,0]^T\right)$ or perfectly horizontal $\left(\mathbf{p}_t = [0,1]^T\right)$. As a consequence, the product $\mathbf{p}_r^T \cdot \mathbf{p}_t$ selects either the vertical or horizontal component of $\mathbf{p}_r$ and α can be calculated to

$$\alpha = \arctan_2\left(p_{ry}, p_{rx}\right) = \arctan_2\left(o_x^+, o_z^+\right) \tag{15}$$

4. α is the angle between the projection of the orientation vector and the E_x component of the transmit polarization. Since the transmitter is vertically polarized, β_t is 0. The angle β_r comes from the rotated field pattern response (11).

$$\beta_r = \arctan_2\left\{\hat{F}_H(\phi,\theta), \hat{F}_V(\phi,\theta)\right\} \tag{16}$$

5. The difference between α and β_r is the rotation angle ϑ which is used to calculate the polarization effects on the pattern. The rotated pattern then notes

$$\begin{aligned} \vartheta &= -\beta_r - \alpha \\ \tilde{\mathbf{F}}(\phi,\theta) &= \begin{pmatrix} \cos\vartheta & -\sin\vartheta \\ \sin\vartheta & \cos\vartheta \end{pmatrix} \cdot \begin{pmatrix} \hat{F}_{\mathrm{V}}(\phi,\theta) \\ \hat{F}_{\mathrm{H}}(\phi,\theta) \end{pmatrix} \end{aligned} \tag{17}$$

Modeling circularly polarized antennas In many applications, such as satellite communications, circular polarization is needed. A straight forward extension would use complex coefficients in the field patterns where

$$\mathbf{F}_{\mathrm{R}} = \frac{1}{\sqrt{2}} \begin{pmatrix} 1 \\ i \end{pmatrix} \quad \mathbf{F}_{\mathrm{L}} = \frac{1}{\sqrt{2}} \begin{pmatrix} 1 \\ -i \end{pmatrix} \tag{18}$$

are the Jones vectors for the right hand circular polarized (RHCP) and left hand circular polarized (LHCP) signal, respectively. However, an essential component of the polarization model is the orientation vector $\mathbf{o}$ which is not unique for circular polarized patterns. A solutions is to virtually assemble a circular polarized antenna out of two linear elements. These elements need to be crossed in a way that the transmission axes of both elements are perpendicular to each other. Both elements are fed with the same signal, but one of them is shifted by 90° out of phase. This is modeled by using the channel coefficients (4) for each of the two elements and assembling them in a channel matrix $\mathbf{G}$. In order to get circular polarized coefficient matrix $\mathbf{G}^\circ$, we use the Jones vectors (18) as coupling matrices.

$$\begin{aligned} \mathbf{G}^\circ &= \begin{pmatrix} g_{\mathrm{RR}} & g_{\mathrm{RL}} \\ g_{\mathrm{LR}} & g_{\mathrm{LL}} \end{pmatrix} = \mathbf{C}^H \mathbf{G} \mathbf{C} \\ &= \frac{1}{2} \begin{pmatrix} 1 & -i \\ 1 & i \end{pmatrix} \begin{pmatrix} g_{\mathrm{VV}} & g_{\mathrm{VH}} \\ g_{\mathrm{HV}} & g_{\mathrm{HH}} \end{pmatrix} \begin{pmatrix} 1 & 1 \\ i & -i \end{pmatrix} \end{aligned} \tag{19}$$

3.1.4 Data Flow

The data flow of the QuaDRiGa channel model is depicted in Fig. 32. This figure shows how each of the processing steps, which are described in detail in the following sections, are linked together. The lines show, which parameters are exchanged and how often they are updated. Black lines are for parameters that are either provided by the model users or which are given in the parameter table. Those values are constant. Blue values are updated once per segment and red values are updated once per snapshot.

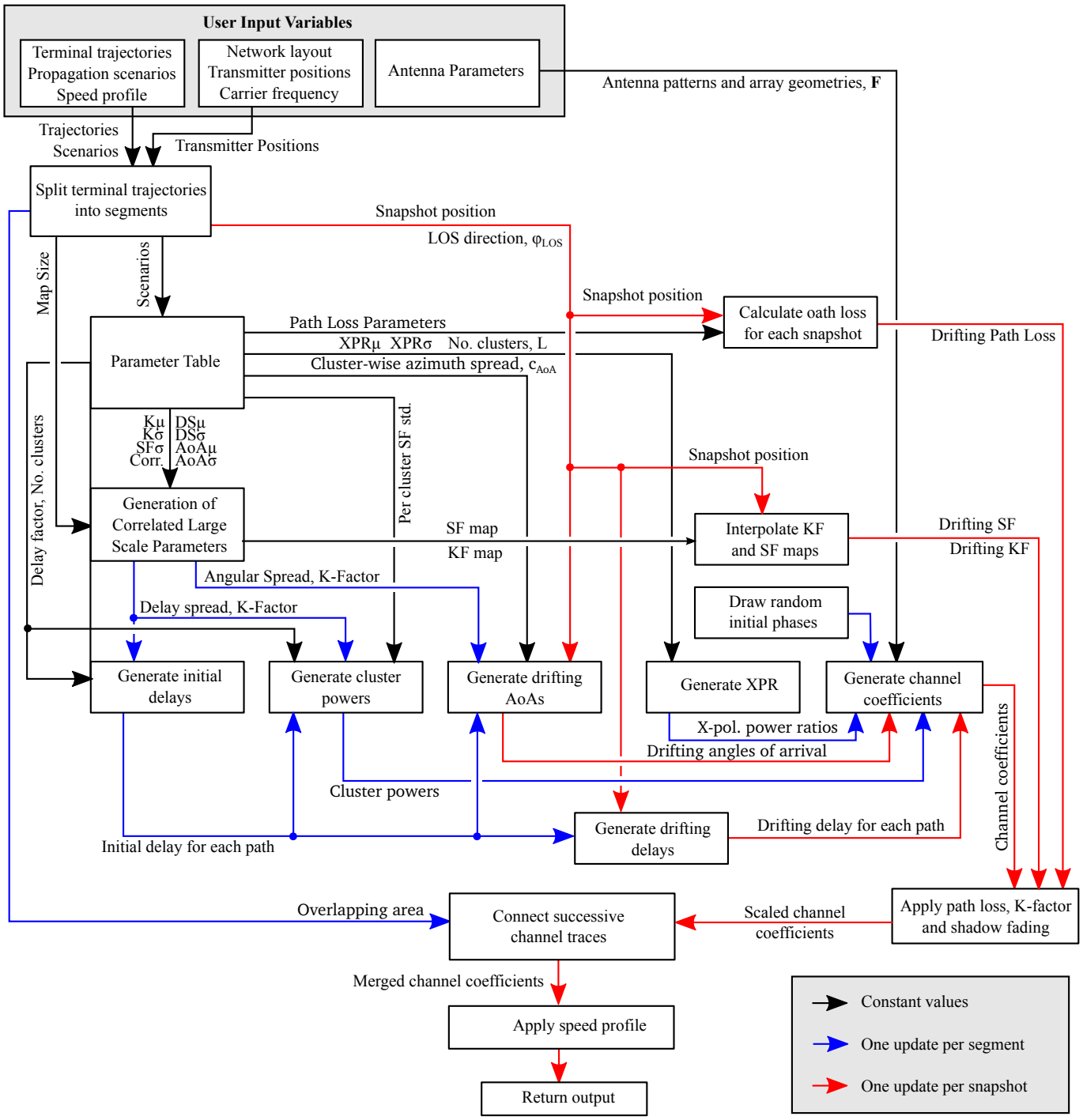

Figure 32: QuaDRiGa Data Flow

3.2 Scenario Specific Parameters

3.2.1 Description of the Parameter Table

The QuaDRiGa channel model is a generic model. That means, that it uses the same method for generating channel coefficients in different environments. E.g. the principal approach is exactly the same in a cellular network and in a satellite network. The only difference is the parametrization for both cases. Each environment is described by 55 individual parameters. These parameters are stored in configuration files that can be found in the subfolder named "config" in the main channel model folder. A typical parameter table describing the LSPs is given in Tab. 2. A second table 3 then describes the cross-correlations between those parameters. The parameters and values can be describes as follows:

- **No. Clusters**
  This value describes the number of clusters. Each cluster is the source of a reflected or scattered wave arriving at the receiver. Typically there are less clusters in a LOS scenario then in a NLOS scenario. Note that the number of clusters directly influences the time needed to calculate the coefficients.

- **Path Loss (PL)**
  A common path loss (PL) model for cellular systems is the log-distance model

$$\mathrm{PL}_{[\mathrm{dB}]} = A \cdot \log_{10} d + B \tag{20}$$

  where A and B are scenario-specific coefficients. The path-loss exponent A typically varies between 2 and 4, depending on the propagation conditions, the base station height and other influences. They are typically determined by measurements. d is the distance (in units of meters) between the transmitter and the receiver. Note that in Tab. 2, a factor of 10 is applied to the PL-exponent. In other environments such as in satellite systems, the PL does not depend on the distance but has a constant value. In this case, A would be 0.

- **Shadow Fading (SF)**
  Shadow fading occurs when an obstacle gets positioned between the wireless device and the signal transmitter. This interference causes significant reduction in signal strength because the wave is shadowed or blocked by the obstacle. It is modeled as log-normal distributed with two parameters: The standard deviation σ defines the width of the distribution, i.e. the power value (in dB) above or below the distance dependent PL and the decorrelation distance λ. This parameter defines how fast the SF varies when the terminal moves through the environment. E.g. a value of 87 means that when the terminal moves 87 m in any given direction, then the correlation of the value at this distance with the value at the initial position is $e^{-1} = 0.37$.

- **Delay Spread (DS)**
  The root-mean-square (RMS) delay spread is probably the most important single measure for the delay time extent of a multipath radio channel. The RMS delay spread is the square root of the second central moment of the power delay profile and is defined to be

$$\sigma_\tau = \sqrt{\frac{1}{P_i} \cdot \sum_{l=1}^{L} P_l \cdot (\tau_l)^2 - \left(\frac{1}{P_i} \cdot \sum_{l=1}^{L} P_l \cdot \tau_l \right)^2} \tag{21}$$

  with P_i is the total received power, P_l the cluster-power and τ_l the cluster delay.

  In order to generate the coefficients, QuaDRiGa has to generate delays for each of the multipath clusters. I.e. the total lengths of scattered paths have to be defined. This generation of delays is governed by value of the DS in a specific environment. The DS is assumed to be log-normal distributed and defined by two parameters: Its median value μ and its STD σ. Thus, a values of DS_μ

of -6.69 corresponds to 204 ns. σ then defines the range of possible values. E.g. $\mathrm{DS}_\sigma = 0.3$ leads to typical values in the range of $10^{-6.69-0.3} = 102$ ns to $10^{-6.69+0.3} = 407$ ns. As for the shadow fading, the decorrelation distance DS_λ defines how fast the DS varies when the terminal moves through the environment.

The delay spread σ_τ is calculated from both, the delays τ_l and the path powers P_l. I.e. lager delay spreads σ_τ can either be achieved by increasing the values of τ_l and keeping P_l fixed or adjusting P_l and keeping τ_l fixed. In order to avoid this ambiguity, an additional proportionality factor (delay factor) r_τ is introduced to scale the width of the distribution of τ_l. r_τ is calculated from measurement data. See Sec. 3.3.1 for more details.

- **Ricean K-Factor (KF)**
  Rician fading occurs when one of the paths, typically a line of sight signal, is much stronger than the others. The KF K is the ratio between the power in the direct path and the power in the other, scattered, paths. As for the DS, the KF is assumed to be log-normal distributed. The distribution is defined by its median value KF_μ and its STD KF_σ. The decorrelation distance KF_λ defines how fast the KF varies when the terminal moves through the environment.

- **Angular Spread**
  The angular spread defines the distribution of the departure- and arrival angles of each multipath component in 3D space seen by the transmitter and receiver, respectively. Each path gets assigned an azimuth angle in the horizontal plane and an elevation angle in the vertical plane. Thus we have four values for the angular spread:

  1. Azimuth spread of Departure (AsD)
  2. Azimuth spread of Arrival (AsA)
  3. Elevation spread of Departure (EsD)
  4. Elevation spread of Arrival (EsA)

  Each one of them is assumed to be log-normal distributed. Hence, we need the parameters μ, σ and λ to define the distributions. These spreads are translated into specific angles for each multipath cluster. Additionally, we assume that clusters are the source of several multipath components that are not resolvable in the delay domain. Thus, these sub-paths do not have specific delays, but they have different departure- and arrival angles. Thus, we need an additional parameter c_ϕ for each of the four angles that scales the dimensions of the clusters in 3D-space. See Sec. 3.3.2 for details.

- **Cross-polarization Ratio (XPR)**
  The XPR defines how the polarization changes for a multipath component. I.e. the initial polarization of a path is defined by the transmit antenna. However, for the NLOS components, the transmitted signal undergoes some diffraction, reflection or scattering before reaching the receiver.

  The XPR (in dB) is assumed to be normal distributed where μ and σ define the distribution. We translate the XPR in a polarization rotation angle which turns the polarization direction. A XPR value where a value of +Inf means that the axis remains the same for all NLOS paths. I.e. vertically polarized waves remain vertically polarized after scattering. On the other hand, a value of -Inf dB means that the polarization is turned by 90°. In case of 0 dB, the axis is turned by 45°, i.e. the power of a vertically polarized wave is split equally into a H- and V component.

eMail: quadriga@hhi.fraunhofer.de

Table 2: Large Scale Parameters

Parameter		Ul	Un
No. Clusters	L	15	25
PL	A	21.0	28.5
	B	47.5	38.0
SF (dB)	σ	3.7	4.0
autocorr. [m]	λ	87	36
DS	μ	-6.69	-6.47
($\log_{10}$s)	σ	0.30	0.20
autocorr. [m]	λ	65	44
Delay factor	r_τ	2.5	2.0
K-factor	μ	2.70	-6.30
(dB)	σ	2.30	3.70
autocorr. [m]	λ	22	22
ASD	μ	0.65	0.65
($\log_{10}^\circ$)	σ	0.23	0.22
autocorr. [m]	λ	8	25
per cluster	c_ϕ	2	6
ESD	μ	0.70	0.90
($\log_{10}^\circ$)	σ	0.20	0.20
autocorr. [m]	λ	15	30
per cluster	c_ϕ	3	3
ASA	μ	1.61	1.50
($\log_{10}^\circ$)	σ	0.17	0.16
autocorr. [m]	λ	11	45
per cluster	c_ϕ	12	15
ESA	μ	1.16	1.25
($\log_{10}^\circ$)	σ	0.14	0.14
autocorr. [m]	λ	11	25
per cluster	c_ϕ	3	8
XPR	μ	9.00	7.75
(dB)	σ	4.30	4.30

Table 3: Cross-Correlation Settings for the Urban Macrocell Scenario

Cross-correlation		LOS						
		DS	K	SF	ASD	ASA	ESD	ESA
	DS	1.0	-0.4	-0.5	0.0	0.2	-0.4	0.0
	K	-0.4	1.0	0.6	0.0	-0.2	0.0	-0.3
N	SF	-0.2	0.6	1.0	-0.2	-0.4	0.0	-0.6
L	ASD	0.1	0.0	0.0	1.0	0.5	0.5	-0.3
O	ASA	0.0	-0.2	-0.2	0.5	1.0	0.0	0.3
S	ESD	-0.4	0.0	0.0	0.5	0.0	1.0	0.0
	ESA	-0.2	-0.2	-0.5	-0.3	0.3	0.0	1.0

eMail: quadriga@hhi.fraunhofer.de

3.2.2 Generation of Correlated Large Scale Parameters

QuaDRiGa models the auto- and cross correlation properties of the LSPs by creating 2D maps for each of the following parameters.

1. RMS Delay Spread (DS)
2. Ricean K-Factor (KF)
3. Shadow Fading (SF)
4. Azimuth spread of Departure (AsD)
5. Azimuth spread of Arrival (AsA)
6. Elevation spread of Departure (EsD)
7. Elevation spread of Arrival (EsA)

The map-based method is already part of the WINNER implementation [KMH+07, HMK+10] where the maps are generated by filtering random, normal distributed numbers along the x and y axis of the map. Alternative approaches [CG03, Cla05] are known to have better autocorrelation properties at close distances. I.e. they are better in modeling the distance-dependent exponential decay of the correlation. However, the resulting map is difficult to interpolate since neighboring pixels can have large differences in magnitude. We thus extend the WINNER idea by filtering the maps also in the diagonal directions. This significantly increases the smoothness of the parameters along a random user trajectory which is an important feature for the time evolution of the channel coefficients. The principle of the map based correlation procedure is shown in Fig. 33 for an example using the delay spread (DS) in an urban cellular scenario. The granularity of each parameter can be described on three levels: the scenario level, the link level and the path level.

Scenario Level The magnitude, variance and the correlation of a parameter in a specific scenario (e.g. urban macrocell, indoor hotspot or urban satellite) are calculated from measurement data. Normally, parameters are assumed to be log-normal distributed. For example, the median log-normal delay spread DS_μ in an urban cellular scenario is -6.89 which corresponds to a delay spread (DS) of $\bar{\sigma}_\tau = 128$ ns (see Fig. 33, top). With a standard deviation of $\mathrm{DS}_\sigma = 0.5$, typical values may lie in between 40 and 407 ns. The same principle applies for the other six parameters. The decorrelation distance (e.g. $\mathrm{DS}_\lambda = 40$ m) describes the distance-dependent correlation of the LSP. If e.g. two mobile terminals in the above example are 40 m apart of each other, their DS is correlated with a correlation coefficient of $e^{-1} = 0.37$. Additionally, all parameters are cross correlated. A typical example is the dependance of the angular spread (e.g. the azimuth spread of arrival) on the Ricean K-factor (KF). With a large KF (e.g. 10 dB), a significant amount of energy comes from a single direction. Thus, the angular spread gets smaller which leads to a negative correlation between the DS and the KF.

Link Level When a user terminal is placed in a scenario (black dot on the map in Fig. 33), it experiences a radio channel which is determined by the specific values of the seven parameters at this position. Due to the autocorrelation properties, small distances between users also lead to high correlations in the channel

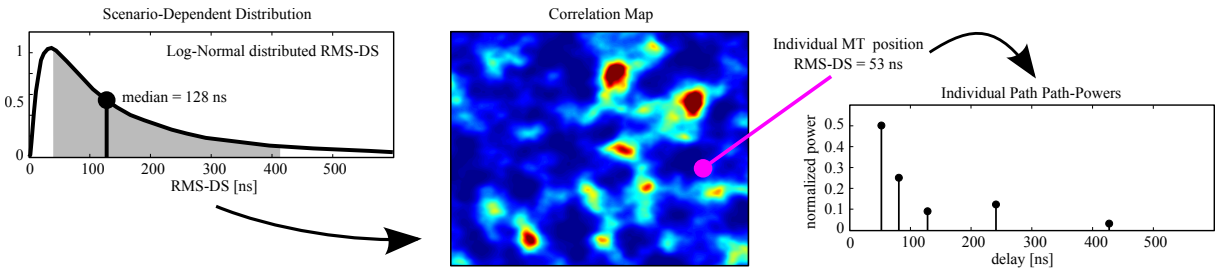

Figure 33: Principle of the generation of correlated LSPs

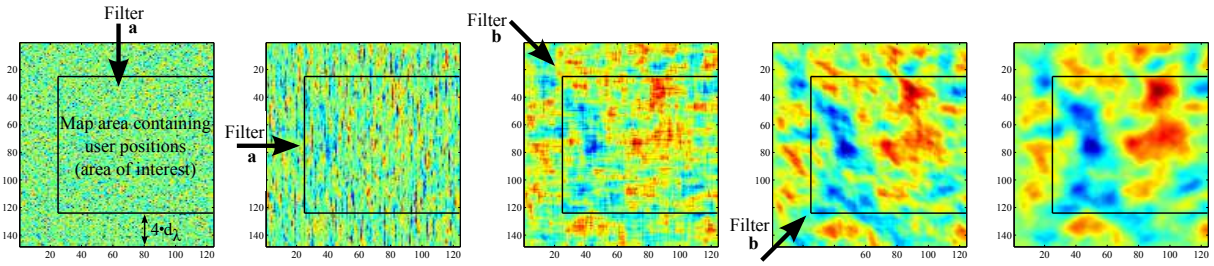

Figure 34: Principle of the map generation

statistics (e.g. a second terminal right next to the current user will experience a similar DS). The second granularity of the large scale parameters are thus the specific values of the LSPs for each user in the scenario. Generating those values can be seen as going backwards from the distribution μ, σ of a parameter to individual "measurement"-values. At the example position in the map, the DS is 53 ns.

Path Level Last, the individual components of the CIR are calculated. This procedure takes the values of the LSPs into account and calculates the power and the delay of the channel coefficients.

The correlation maps are generated at a fixed sampling grid by successively filtering a random, normal distributed sequence of numbers with a finite impulse response (FIR) filter. The principle is depicted in Fig. 34. The map is represented by a matrix $\mathbf{B}$ and one pixel of that matrix is $B_{y,x}$ where y is the row index and x is the column index. The first pixel $B_{1,1}$ is in the top left (or north-west) corner of the map. The FIR filter coefficients are calculated from the decorrelation distance d_λ (in units of m). The distance dependent correlation coefficient follows an exponential function

$$\rho(d) = e^{-\frac{d}{d_\lambda}} \tag{22}$$

with d as the distance between two positions [Gud91]. We now calculate two sets of filter coefficients, one for the horizontal and vertical directions and one for the diagonal elements. This is done by taking (22) and substituting the distance d by the relative distance d_{px} of two pixels.

$$a_k = \frac{1}{\sqrt{d_\lambda}} \cdot \exp\left(-\frac{k \cdot d_{\mathrm{px}}}{d_\lambda}\right) \tag{23}$$

$$b_k = \frac{1}{\sqrt{d_\lambda}} \cdot \exp\left(-\frac{k \cdot \sqrt{2} d_{\mathrm{px}}}{d_\lambda}\right) \tag{24}$$

k is the running filter coefficient index. We cut the exponential decay function a at maximum distance of $4d_\lambda$ and normalize it with $\sqrt{d_\lambda}$. The map size is determined by the distribution of the users in the scenario plus the length of the filter function. This is also illustrated in Fig. 34 where the user terminals are placed inside the black square. The extension space is needed to avoid filter artifacts at the edges of the map. We initialize the map with random, normal distributed numbers. Then we apply the filter (23) in vertical (running from top to bottom) and in horizontal (from left to right) direction.

$$B^{[1]}_{y,x} = X \quad \text{with} \quad X \sim N(0,1) \tag{25}$$

$$B^{[2]}_{y,x} = \sum_{k=0}^{\lfloor 4 \cdot d_\lambda / d_{\mathrm{px}} \rfloor} a_k \cdot B_{y-k,x} \tag{26}$$

$$B^{[3]}_{y,x} = \sum_{k=0}^{\lfloor 4 \cdot d_\lambda / d_{\mathrm{px}} \rfloor} a_k \cdot B_{y,x-k} \tag{27}$$

Next, we apply the second filter (24) on the diagonals of the map. First, we go from the top left to the bottom right and then we go from the bottom left to the top right.

$$B^{[4]}_{y,x} = \sum_{k=0}^{\lfloor 4 \cdot d_\lambda / d_{\mathrm{px}} \rfloor} b_k \cdot B_{y-k,x-k} \tag{28}$$

$$B^{[5]}_{y,x} = \sum_{k=0}^{\lfloor 4 \cdot d_\lambda / d_{\mathrm{px}} \rfloor} b_k \cdot B_{y+k,x-k} \tag{29}$$

After the autocorrelations are applied, the extension space is removed and values of the remaining map are scaled to have the desired distribution μ, σ. The same procedure is repeated for all seven LSPs. However, the decorrelation distance d_λ as well as μ, σ for each parameter can be different. We account for the cross-correlation of the parameters by assembling a matrix $\mathbf{X}$ that contains all cross-correlation values and multiplying its matrix-square-root with the values of the seven parameter maps $\mathbf{B}_{DS} \ldots \mathbf{B}_{EsD}$. The cross-correlation matrix needs to be positive definite to get a unique, real numbered solution.

$$\begin{pmatrix} B_{y,x,DS} \\ \vdots \\ B_{y,x,EsD} \end{pmatrix} = \mathbf{X}^{\frac{1}{2}} \begin{pmatrix} B^{[5]}_{y,x,DS} \\ \vdots \\ B^{[5]}_{y,x,EsD} \end{pmatrix} \tag{30}$$

Last, the users are placed on the maps and the corresponding values for the LSPs are obtained. In this way, we initialize the second part of the channel model, the generator of the individual channel coefficients, with correlated input values for each user. An example output of the correlation map procedure is shown in Fig. 35. A set of 200 mobile terminals is randomly placed in an urban cellular scenario (blue dots). The transmitter is situated in the scenario center (red cross). The map for the DS is displayed as a background image. The initial values of the LSPs for each user position (link level) serve as an input for calculating the channel coefficients. They are simply generated by reading the map-values around the position of the mobile terminal and interpolating between adjacent pixels.

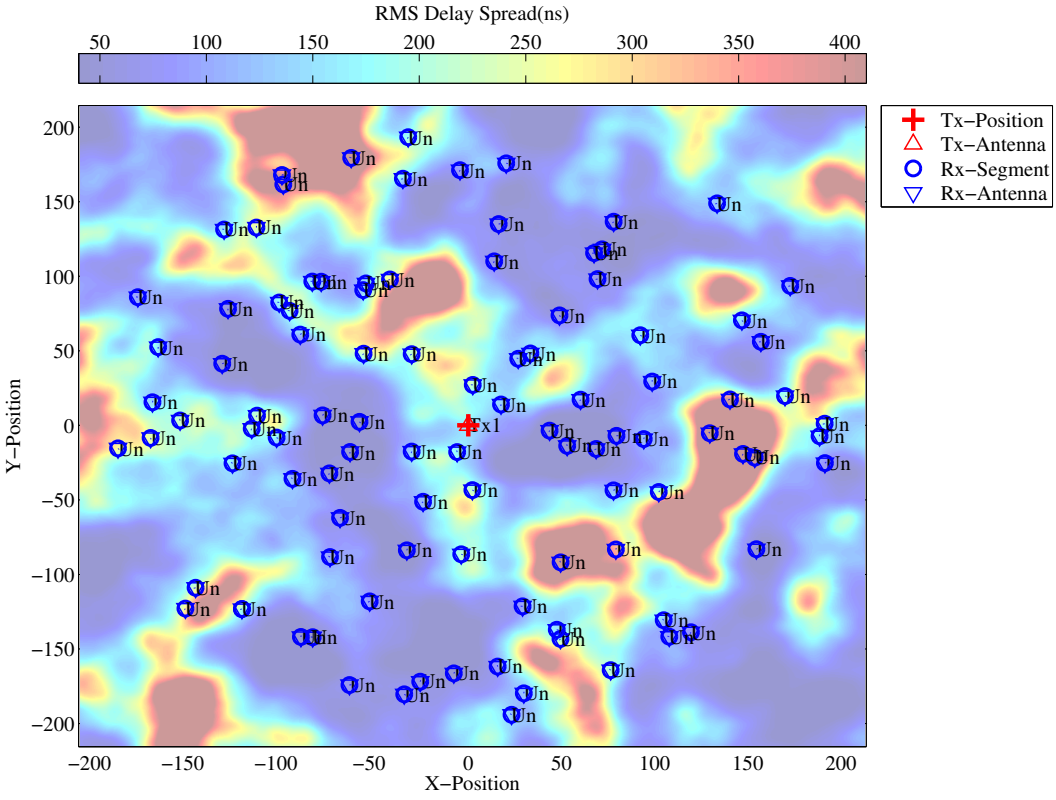

Figure 35: Illustration of the map based generation of the DS

3.3 Calculation of Channel Coefficients

In the model software, the channel coefficients are generated by the *channel builder*. It takes the correlated large scale parameter values as input and calculates the CIR for each user position.

Each scattering cluster is represented by a propagation path which is modeled as a Dirac function in delay domain. A path is made of up of 20 spatially separated *subpaths* according to the sum-of-sinusoids method [PB01]. Path powers, path delays, and angular properties for both sides of the link are modeled as random variables defined through probability density functions (PDFs) and cross-correlations. All parameters, except the fast-fading, are drawn independently in time, in what is termed *drops* (see [3GP05]). Even though a path consists of multiple subpaths in an angular domain, it remains a single tap in delay domain.

3.3.1 Initial Delays and Cluster Powers

Implemented in ⇒ `channel_builder.generate_initial_paths`

Initial delays are drawn randomly from a scenario-dependent delay distribution as

$$\tau_l^{[1]} = -r_\tau \sigma_\tau \ln(X_l) \tag{31}$$

where $X_l \sim \mathrm{uni}(0,1)$ is a uniformly distributed random variable having values in between 0 and 1, σ_τ is the initial DS from the map and r_τ is a proportionality factor. r_τ has been introduced in [3GP11] because σ_τ is influenced by both, the delays τ_l and the powers P_l. r_τ is usually calculated from measurement data. Next, the delays are normalized such that the first delay is zero and then they are sorted in descending order

$$\tau_l^{[2]} = \mathrm{sort}\left\{\tau_l^{[1]} - \min\left(\tau_l^{[1]}\right)\right\} \tag{32}$$

The NLOS cluster powers are drawn from a single slope exponential power delay profile (PDP) depending on the DS σ_τ and and a random component $Z_l \sim \mathcal{N}(0,\zeta)$. ζ is a scenario-dependent coefficient emulating an additional shadowing process among the clusters in one segment. It is normally obtained from measurements.

$$P_l^{[1]} = \exp\left(-\tau_l \frac{r_\tau - 1}{r_\tau \sigma_\tau}\right) \cdot 10^{\frac{-Z_l}{10}} \tag{33}$$

The power of the first cluster is further scaled according to the initial KF from the map and cluster powers are normalized so that their sum power is unity.

$$P_1^{[1]} = K \cdot \sum_{l=2}^{L} P_l^{[1]} \qquad P_l = P_l^{[1]} / \sum_{l=1}^{L} P_l^{[1]} \tag{34}$$

In the last step, we correct the influence of the KF on the DS which has changed due to the scaling. The DS after applying (34) is calculated by

$$\bar{\sigma_\tau} = \sqrt{\cdot \sum_{l=1}^{L} P_l \cdot (\tau_l)^2 - \left(\cdot \sum_{l=1}^{L} P_l \cdot \tau_l\right)^2} \tag{35}$$

The cluster delays are then obtained by

$$\tau_l = \frac{\sigma_\tau}{\bar{\sigma_\tau}} \cdot \tau_l^{[2]} \tag{36}$$

with σ_τ being the initial DS from the map.

3.3.2 Departure and Arrival Angles

Implemented in ⇒ `channel_builder.generate_initial_angles`
and ⇒ `channel_builder.correction_function`

We calculate four angles for each cluster: the azimuth of departure (AoD, ϕ^d), the elevation of departure (EoD, θ^d), the azimuth of arrival (AoA, ϕ^a) and the elevation of arrival (EoA, θ^a). They share the same calculation method but have a different angular spread σ_ϕ. We assume that the power angular spectrum of all clusters follows a wrapped Gaussian distribution [KMH+07, PMF97].

$$P(\phi) = \frac{1}{\sigma_\phi \sqrt{2\pi}} \exp\left(\frac{-\phi^2}{2\sigma_\phi^2}\right) \tag{37}$$

The wrapping is applied later by (40) when the discrete cluster angles are drawn from the statistics. Since the above formula assumes a continuous spectrum and the channel model, on the other hand, uses discrete paths, we need to correct the variance by a function $C_\phi(L, K)$ depending on the number of clusters L and the KF K. This formula is derived in the Appendix. It ensures that the input variance σ_ϕ is correctly reflected in the generated angles.

We obtain the angles ϕ_l by first normalizing the power angular spectrum so that its maximum has unit power. We can thus omit the scaling factor $1/(\sigma_\phi\sqrt{2\pi})$. We also normalize the path powers P_l (34) so that the strongest peak has unit power which corresponds to an angle $\phi = 0$. All other paths get relative departure- or arrival angles depending on their power

$$\phi_l^{[1]} = \frac{\sigma_\phi}{C_\phi(L, K)} \cdot \sqrt{-2 \cdot \ln(P_l / \max(P_l))} \tag{38}$$

The value σ_ϕ is measured in radians here. Next, we create two random variables X_l and Y_l where $X_l \sim \{-1, 1\}$ is the positive or negative sign and $Y_l \sim \mathcal{N}(0, \sigma_\phi/10)$ introduces a random variation on the angle. Then we calculate

$$\phi_l^{[2]} = X_l \cdot \phi_l^{[1]} + Y_l \tag{39}$$

If the power P_l of a path is small compared to the strongest peak, its angle ϕ_l^b might exceed $\pm\pi$. In this case, we wrap it around the unit circle by a modulo operation

$$\phi_l^{[3]} = \left(\phi_l^{[2]} + \pi \mod 2\pi\right) - \pi \tag{40}$$

In case of elevation spreads, the possible range of elevation angles goes from $-\pi/2$ to $\pi/2$. In this case, we have to correct values of ϕ_l^c outside of this range.

$$\phi_l^{[4]} = \begin{cases} \phi_l^{[3]}, & \text{for el. } \left|\phi_l^{[3]}\right| < \frac{\pi}{2} \text{ and all az. angles;} \\ \pi - \phi_l^{[3]}, & \text{for elevation } \phi_l^{[3]} > \frac{\pi}{2}; \\ \phi_l^{[3]} - \pi, & \text{for elevation } \phi_l^{[3]} < -\frac{\pi}{2}. \end{cases} \tag{41}$$

The positions of the transmitter (Tx) and receiver (Rx) are deterministic and so are the angles of the LOS component. We correct the values of the angles to incorporate this position.

$$\phi_l^{[5]} = \phi_l^{[4]} - \phi_1^{[4]} + \phi^{LOS} \tag{42}$$

Finally, the cluster-path is split into 20 sub-paths to emulate intra cluster angular spreads.

$$\phi_{l,m} = \phi_l^{[5]} + c_\phi \cdot \hat{\phi}_m \tag{43}$$

m is the sub-path index, c_ϕ is the scenario-dependent cluster-wise RMS angular spread and $\hat{\phi}$ is the offset angle of the m^{th} sub-path from Table 4. Furthermore, each of the 20 angle pairs $(\phi_{l,m}^d, \theta_{l,m}^d)$ at the Tx gets coupled with a random angle pair $(\phi_{l,m}^a, \theta_{l,m}^a)$ at the Rx (see [KMH+07]).

eMail: quadriga@hhi.fraunhofer.de

Table 4: Offset Angle of the m^{th} Sub-Path from [KMH+07]

Sub-path m	Offset angle $\hat{\phi}_m$ (degrees)	Sub-path m	Offset angle $\hat{\phi}_m$ (degrees)
1,2	± 0.0447	11,12	± 0.6797
3,4	± 0.1413	13,14	± 0.8844
5,6	± 0.2492	15,16	± 1.1481
7,8	± 0.3715	17,18	± 1.5195
9,10	± 0.5129	19,20	± 2.1551

Derivation of the Correction Function The correction function $C_\phi(L,K)$ takes the influence of the K-Factor and the varying number of clusters into account. To approximate the function, we generate the angles as described above. Then we calculate the angular spread from the simulated data and compare the output of the procedure with the given value of σ_ϕ. The angular spread $\tilde{\sigma}_\phi$ is calculated from the given P_l and ϕ_l as [Rap02]

$$\begin{aligned} \tilde{\sigma}_\phi &= 2\pi \cdot \sqrt{1 - \frac{|F_1|^2}{F_0^2}} \\ F_n &= \sum_{l=1}^{L} P_l \cdot \exp(-j \cdot \phi_l \cdot n) \end{aligned} \tag{44}$$

where ϕ_l is the angle calculated by (40) with the correction function set to $C = 1$. F_n is the n-th complex Fourier coefficient. The correction function now follows from comparing $\tilde{\sigma}_\phi$ with σ_ϕ. However, two aspects need to be considered here:

1. Due to the randomization of the angles in (39), we have to take the average angle over a sufficiently large quantity ($\approx$ 1000 realizations) of $\tilde{\sigma}_\phi$. This values is denoted as $\bar{\sigma}_\phi$.

2. Due to the logarithm in (38) and the modulo operation in (40), there is a nonlinear dependency of the angular spread that can be found in the output data and the value given to the model. However, for small values, the relationship can be approximated by a linear function. We define this maximum angular spread $\sigma_\phi^{\max}$ of the linear approximation as the point where the error between the corrected value $\frac{\sigma_\phi}{C_\phi(L,K)}$ and $\bar{\sigma}_\phi$ is 10°.

For each $L \in [2, 42]$ and $K_{[\text{dB}]} \in [-20, 20]$ we now numerically calculate the value of $C_\phi(L,K)$ by

$$C_\phi(L,K) = \frac{1}{\sigma_\phi^{\max}} \cdot \int_0^{\sigma_\phi^{\max}} \frac{\bar{\sigma}_\phi(\sigma_\phi)}{\sigma_\phi} d\sigma_\phi \tag{45}$$

where the σ_ϕ-dependency of $\bar{\sigma}_\phi(\sigma_\phi)$ comes form the individual angles ϕ_l. The function is plotted for different values of L in Fig. 36, left, and tabularized in Tab. 6. Values that are not in the table will be interpolated using linear interpolation.

The plot in Fig. 36, right, compares both, the values given in σ_ϕ and the values calculated by (44) for the final model including the correction function. The parameters for the scatter plot were set to typical values where L ranges from 6 to 30 paths and K ranges from -15 to 15 dB.

The K-Factor has a strong influence on the achievable angular spread. E.g. when the K-Factor is 10, then almost 92% of the energy are focussed in one direction. Thus, it is impossible to get high angular spreads in this case. Tab. 5 gives an overview of the achievable angular spread in azimuth- and elevation direction depending on the K-Factor. The table is valid for realistic path-numbers ranging from 6 to 30 paths.

eMail: quadriga@hhi.fraunhofer.de

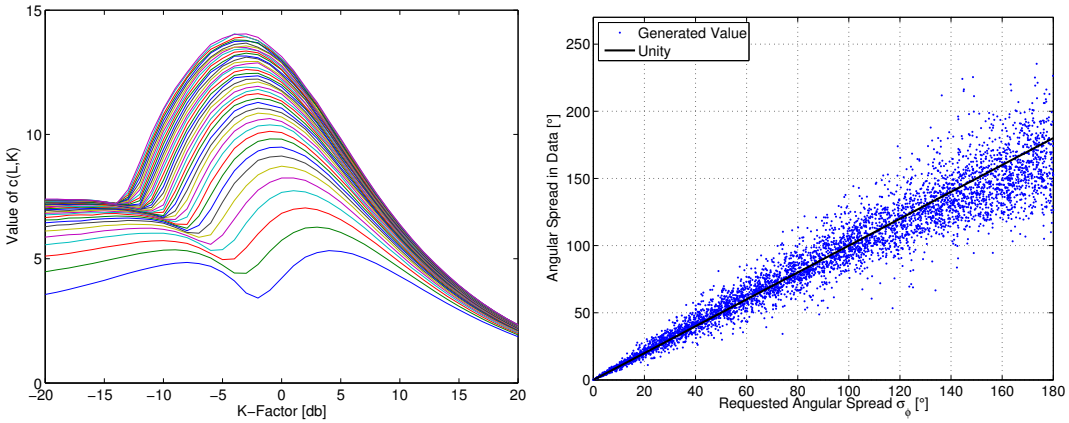

Figure 36: Left: Correction function $C_\phi(L, K)$. Individual lines are for different numbers of paths ranging from 3 (lowest line) to 42 (top line). Right: Comparison of the angular spread σ_ϕ set by the parametrization and the angular spread $\tilde{\sigma}_\phi$ in the data.

Table 5: Maximum Linear Angular Spread vs. K-Factor

K	Az. $\sigma_\phi^{\max}$	El. $\sigma_\phi^{\max}$	K	Az. $\sigma_\phi^{\max}$	El. $\sigma_\phi^{\max}$	K	Az. $\sigma_\phi^{\max}$	El. $\sigma_\phi^{\max}$
-20	206	201	-6	211	209	8	155	151
-18	207	201	-4	209	206	10	143	135
-16	207	202	-2	209	205	12	128	118
-14	205	202	0	200	198	14	113	101
-12	208	203	2	192	190	16	99	84
-10	212	204	4	182	179	18	86	70
-8	213	208	6	170	166	20	74	57

Table 6: Values of $C_\Phi(L, K)$

K/L	3	6	9	12	15	18	21	24	27	30	33	36	39	42
-20	3.59	5.53	6.25	6.62	6.81	6.93	7.04	7.11	7.17	7.13	7.22	7.22	7.25	7.31
-18	3.76	5.63	6.34	6.71	6.78	6.98	7.05	7.07	7.19	7.18	7.23	7.21	7.28	7.26
-16	4.00	5.76	6.36	6.74	6.88	6.96	7.08	7.09	7.18	7.14	7.18	7.24	7.26	7.28
-14	4.24	5.90	6.51	6.78	6.89	6.92	6.99	7.05	7.08	7.16	7.14	7.15	7.06	7.10
-12	4.54	5.98	6.47	6.68	6.74	6.84	6.86	6.92	6.86	7.03	7.38	7.80	8.36	8.77
-10	4.74	5.98	6.38	6.51	6.55	6.66	7.07	7.76	8.54	9.03	9.65	10.12	10.55	10.97
-8	4.83	5.80	5.99	6.27	7.27	8.38	9.12	9.89	10.45	10.90	11.44	11.74	12.10	12.35
-6	4.70	5.30	6.42	7.96	9.13	10.01	10.69	11.36	11.78	12.15	12.60	13.01	13.15	13.47
-4	4.12	5.72	8.00	9.42	10.34	11.09	11.52	12.16	12.57	12.86	13.20	13.39	13.72	14.02
-2	3.42	6.94	8.88	10.01	10.71	11.32	11.90	12.15	12.65	12.95	13.17	13.37	13.53	13.75
0	4.19	7.69	9.07	10.05	10.68	11.09	11.58	11.76	12.12	12.36	12.48	12.84	12.95	13.03
2	5.09	7.66	8.76	9.53	9.98	10.42	10.68	10.99	11.20	11.31	11.45	11.62	11.79	11.87
4	5.33	7.22	8.17	8.67	9.07	9.33	9.53	9.81	9.93	10.01	10.24	10.31	10.44	10.59
6	5.21	6.64	7.26	7.63	7.94	8.10	8.33	8.51	8.62	8.63	8.82	8.89	9.00	9.08
8	4.80	5.85	6.30	6.60	6.83	6.97	7.12	7.23	7.36	7.38	7.43	7.53	7.62	7.67
10	4.29	5.02	5.38	5.59	5.75	5.87	5.97	6.05	6.11	6.21	6.26	6.30	6.33	6.37
12	3.75	4.28	4.54	4.68	4.79	4.90	4.96	5.01	5.10	5.13	5.19	5.22	5.24	5.27
14	3.20	3.59	3.77	3.90	3.97	4.06	4.11	4.17	4.20	4.23	4.26	4.28	4.32	4.35
16	2.70	2.98	3.11	3.21	3.28	3.33	3.37	3.41	3.44	3.46	3.49	3.52	3.54	3.56
18	2.25	2.46	2.56	2.63	2.68	2.72	2.76	2.78	2.80	2.83	2.85	2.86	2.88	2.89
20	1.86	2.01	2.10	2.14	2.18	2.22	2.24	2.26	2.27	2.29	2.31	2.32	2.33	2.34

3.3.3 Drifting of Angles, Delays and Phases

Implemented in ⇒ `channel_builder.get_drifting`

After cluster-delays, powers and angles are known for the initial position, we update their values for each snapshot of the segment. Thus, we get an evolution of the parameters over a short time interval. Since the values of the LSPs and the number of clusters are kept constant, drifting requires that the segment is relatively confined in distance and does not exceed the average autocorrelation distance of the LSPs. A similar concept was already introduced by Baum et. al. in an extension of the SCM [BHS05]. However, it was not incorporated into the WINNER models and no evaluation was reported.

Besides the parameters from steps B and C, drifting requires the position of each antenna element at the Tx and Rx. Additionally, Rx element positions need to be provided for each snapshot separately, depending on the orientation and position of the Rx. The following calculations are then done element-wise where the indices r, t, l, m, s denote the element index of the Rx antenna r and the Tx antenna t, the cluster number l, the sub-path number m and the snapshot number within the current segment s, respectively.

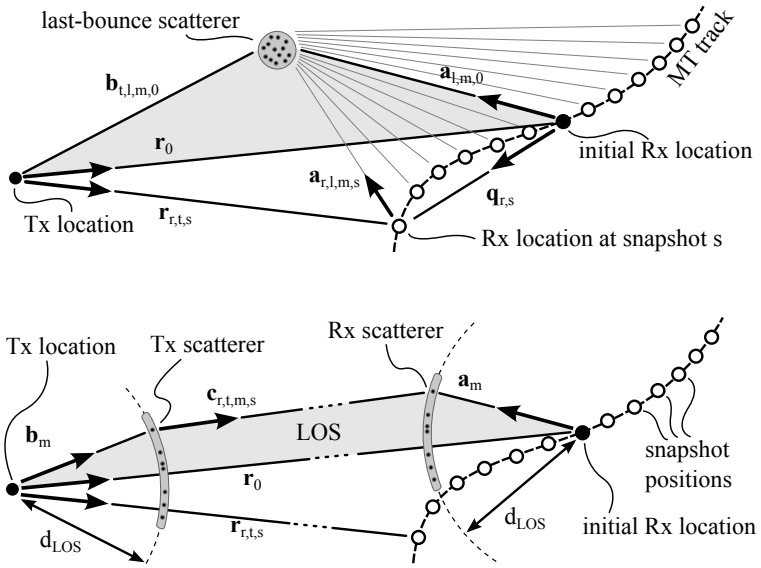

Figure 37: Illustration of the calculation of the scatterer positions and updates of the arrival angles for NLOS (top) and LOS (bottom).

NLOS drifting For the NLOS paths, we calculate the position of the last bounce scatterer (LBS) from the initial arrival angles and the cluster delays. Then we update the angles and path lengths between the last bounce scatterer (LBS) and the terminal for each snapshot on the track. This is done for each antenna element separately. An illustration of the angles and their relations is given in Fig. 37, top.

The first delay is always zero due to (32). Hence, we calculate the total length of the l^{th} path as

$$d_l = \tau_l \cdot c + |\mathbf{r}_0| \tag{46}$$

where $|\mathbf{r}_0|$ is the distance between the Tx and the initial Rx location and c is the speed of light. We assume, that all sub-paths have the same delay and thus the same path length. However, each sub-path has different arrival angles $(\phi^a_{l,m}, \theta^a_{l,m})$. We transform those angles a vector $\hat{\mathbf{a}}_{l,m,0}$ in Cartesian coordinates and obtain

$$\hat{\mathbf{a}}_{l,m,0} = \frac{\mathbf{a}_{l,m,0}}{|\mathbf{a}_{l,m,0}|} = \begin{pmatrix} \cos\phi^a_{l,m} \cdot \cos\theta^a_{l,m} \\ \sin\phi^a_{l,m} \cdot \cos\theta^a_{l,m} \\ \sin\theta^a_{l,m} \end{pmatrix} \tag{47}$$

We approximate the drifting at the Rx by assuming only a single reflection. Hence, Tx, Rx and LBS form a triangle. Since we know d_l, $\mathbf{r}_0$ and $\hat{\mathbf{a}}_{l,m,0}$, we can apply the cosine theorem to calculate the distance $|\mathbf{a}_{l,m,0}|$ between the Rx and LBS[1].

$$\begin{aligned} b_{l,m,0}^2 &= |\mathbf{r}_0|^2 + |\mathbf{a}_{l,m,0}|^2 \\ &\quad -2\,|\mathbf{r}_0|\,|\mathbf{a}_{l,m,0}|\cos\beta_{l,m,0} \\ (d_l - |\mathbf{a}_{l,m,0}|)^2 &= |\mathbf{r}_0|^2 + |\mathbf{a}_{l,m,0}|^2 + 2\,|\mathbf{a}_{l,m,0}|\,\mathbf{r}_0^T\hat{\mathbf{a}}_{l,m,0} \\ |\mathbf{a}_{l,m,0}| &= \frac{d_l^2 - |\mathbf{r}_0|^2}{2\cdot(d_l + \mathbf{r}_0^T\hat{\mathbf{a}}_{l,m,0})} \end{aligned} \tag{48}$$

Now we can calculate the vector $\mathbf{a}_{r,l,m,s}$ for the Rx antenna element r at snapshot s. The element position includes the orientation of the antenna array with respect to the moving direction of the Rx. Hence, the vector $\mathbf{q}_{r,s}$ points from the initial Rx location to the r^{th} antenna element at snapshot s.

$$\mathbf{a}_{r,l,m,s} = \mathbf{a}_{l,m,0} - \mathbf{q}_{r,s} \tag{49}$$

Now, we can obtain an update of the arrival angles by transforming $\mathbf{a}_{r,l,m,s}$ back to spherical coordinates.

$$\phi_{r,l,m,s}^a = \arctan_2\left\{a_{r,l,m,s,y}; a_{r,l,m,s,x}\right\} \tag{50}$$

$$\theta_{r,l,m,s}^a = \arcsin\left\{\frac{a_{r,l,m,s,z}}{|\mathbf{a}_{r,l,m,s}|}\right\} \tag{51}$$

We assume a static scattering environment. Thus, the departure angles at the Tx do not change. We also assume that the distance between the Tx and the first scatterer is large compared to the Tx array dimension. Hence, we use the same departure angles for all Tx elements. The phases and path delays, however, depend on the total path length $d_{r,t,l,m,s}$. To obtain this value, we calculate the vector $\mathbf{b}_{t,l,m,0}$ from the vectors $\mathbf{r}_{r,t,s}$ and $\mathbf{a}_{r,l,m,s}$ at $r = s = 1$.

$$\mathbf{b}_{t,l,m,0} = \mathbf{r}_{1,t,1} + \mathbf{a}_{1,l,m,1} \tag{52}$$

$$d_{r,t,l,m,s} = |\mathbf{b}_{t,l,m,0}| + |\mathbf{a}_{r,l,m,s}| \tag{53}$$

Finally, we calculate the phase ψ and path delays τ.

$$\psi_{r,t,l,m,s} = \frac{2\pi}{\lambda}\cdot(d_{r,t,l,m,s} \bmod \lambda) \tag{54}$$

$$\tau_{r,t,l,s} = \frac{1}{20\cdot c}\sum_{m=1}^{20} d_{r,t,l,m,s} \tag{55}$$

LOS drifting The direct component is handled differently since there are no discrete scatterers. LOS fading, however, can occur if there are objects in the first Fresnel zone of the propagation path. To simplify the calculations, we assume that those objects have a constant distance to the Rx and are only separated by their angular distribution. They are placed on a circle with radius d_{LOS} as depicted in Fig. 37, bottom. We update the departure- and arrival angles based on the vector $\mathbf{r}_{r,t,s}$ which points from the location of the Tx element t to the location of the Rx element r at snapshot s.

$$\phi_{t,1,m,s}^d = \arctan_2\left\{r_{r,t,s,y}, r_{r,t,s,x}\right\} + c_{\text{AoD}}\cdot\hat{\phi}_m \tag{56}$$

$$\theta_{t,1,m,s}^d = \arcsin\left\{r_{r,t,s,z}/\,|\mathbf{r}_{r,t,s}|\right\} + c_{\text{EoD}}\cdot\hat{\phi}_m \tag{57}$$

$$\phi_{r,1,m,s}^a = \arctan_2\left\{-r_{r,t,s,y}, -r_{r,t,s,x}\right\} + c_{\text{AoA}}\cdot\hat{\phi}_m \tag{58}$$

$$\theta_{r,1,m,s}^a = \arcsin\left\{-r_{r,t,s,z}/\,|\mathbf{r}_{r,t,s}|\right\} + c_{\text{EoA}}\cdot\hat{\phi}_m \tag{59}$$

[1] We substitute $\cos\beta_{l,m,0}$ with $-\mathbf{r}_0^T\hat{\mathbf{a}}_{l,m,0}/|\mathbf{r}_0|$ since we are at the Rx position looking towards the Tx.

The phases and delays, are determined by the length of the vector $\mathbf{c}_{r,t,m,s}$ in Fig. 37, bottom. This vector points from a random scatterer at the Tx to a random scatterer at the Rx. For the sake of simplicity, we define the vectors $\mathbf{a}_m$ and $\mathbf{b}_m$ to be position-independent, i.e. their origin is always relative to the Tx and Rx antenna element. The vector $\mathbf{c}_{r,t,m,s}$ and the path length $d_{r,t,m,s}$ then follow from

$$\mathbf{c}_{r,t,m,s} = -\mathbf{b}_m + \mathbf{r}_{r,t,s} + \mathbf{a}_m \tag{60}$$

$$d_{r,t,1,m,s} = 2 \cdot d_{\mathrm{LOS}} + |\mathbf{c}_{r,t,m,s}| \tag{61}$$

Finally, the LOS phase $\psi_{r,t,1,m,s}$ and the delay $\tau_{r,t,1,s}$ can be calculated using (54) and (55).

3.3.4 Geometric Polarization

Implemented in ⇒ `channel_builder.get_channels` and ⇒ `channel_builder.generate_xpr`

As for the angles and the delays, the polarization is calculated in a geometric way. This is done for each (sub-)path, for each snapshot and for each antenna pair (r, t) separately. For the sake of simplicity, we omit the indices l, m, s for the path, subpath and snapshot in the following. Due to the sheer number of computations, calculating the drifting polarization is also the most computing-intense task. To reduce this complexity, the polarization is only updated when the arrival-angle changed more than 0.2 degree since the last update[2].

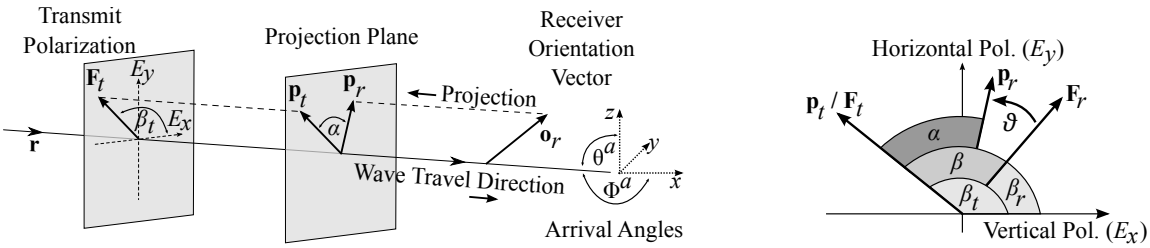

Figure 38: Illustration of the angles and vectors used for the computation of the geometric LOS polarization. Left: Scheme of the projection. Right: Angles on the projection plane.

Model for the LOS component The principle of the model is depicted in Fig. 38. The wave travel direction $\mathbf{r}$ is determined by the AoA at the receiver given in azimuth ϕ^a and elevation θ^a direction. The transmit polarization vector $\mathbf{F}_t$ results from the beam pattern (5) and lies in the plane perpendicular to $\mathbf{r}$. Note here, that our method is only valid for linearly polarized waves. Circular polarization can be obtained by combining two linear elements with a phase offset. The receive antenna can have any orientation in 3D space. Thus, we need additional information on the element orientation which is realized by a vector $\mathbf{o}_r$. $\mathbf{o}_r$ represents the linear receiver polarization. However, this vector does not lie in the same plane as $\mathbf{F}_t$ does. The polarization vector $\mathbf{p}_r$ results from a projection of the orientation vector $\mathbf{o}_r$ on the plane perpendicular to the travel direction. Due to the orientation mismatch between transmitter and receiver, there will be an offset between $\mathbf{p}_r$ and the vector obtained from the receiver beam pattern $\mathbf{F}_r$. This offset is compensated by introducing a virtual polarizer that turns the polarization state of the wave in a way that it matches the orientation of the receiver. Since we do not want to change the amplitude of the wave (this is handled by other parts of the model) nor the type of polarization, we need to compute a rotation matrix. Thus, we have to determine the rotation angle ϑ. This can be done by the following procedure.

1. To simplify the computations, we rotate the coordinate system such that the wave travel direction $\mathbf{r}$ lies in y-direction (i.e. $\mathbf{r}^+ = (0, 1, 0)^T$). Thus, we need to rotate the orientation vector $\mathbf{o}_r$ by $p = -\phi^a - \pi/2$ in

[2] This value can be changed in `simulation_parameters.drifting_update_threshold`

azimuth direction and $q = \theta^a$ in elevation direction.

$$\mathbf{o}_r^+ = \begin{pmatrix} \cos p & -\sin p & 0 \\ \cos q \cdot \sin p & \cos q \cdot \cos p & -\sin q \\ \sin q \cdot \sin p & \sin q \cdot \cos p & \cos q \end{pmatrix} \cdot \mathbf{o}_r \tag{62}$$

2. We calculate the projection of the receiver orientation vector on the projection plane. Since the projection plane lies now in the x-z-plane due to the rotation of the coordinate system, we simply omit the y component of $\mathbf{o}_r^+$, switch the x and z component and normalize the resulting vector to unit length. The switching is done to obtain the same orientation as in (5).

$$\mathbf{p}_r = \begin{pmatrix} o_{rz}^+ \\ o_{rx}^+ \end{pmatrix} / \left| \begin{pmatrix} o_{rz}^+ \\ o_{rx}^+ \end{pmatrix} \right| \tag{63}$$

3. We get the transmit polarization vector $\mathbf{p}_t$ by normalizing the field pattern vector $\mathbf{F}_t$ (5) to unit length. $\mathbf{F}_t$ is already in the same plane as $\mathbf{p}_r$ due to the coordinate rotation.

$$\mathbf{p}_t = \mathbf{F}_t / \left| \mathbf{F}_t \right| \tag{64}$$

4. We calculate the angle α between the two vectors.

$$\alpha = \arccos \left(\mathbf{p}_r^T \cdot \mathbf{p}_t \right) \tag{65}$$

5. We obtain the angles β_t and β_r from the field patterns of the transmitter and receiver, respectively. β is the angle between the x-axis of the polarization plane and the polarization vector. Note that E_x in Fig. 38 is the vertical and E_y is the horizontal polarized component.

$$\beta_t = \arctan_2 \left\{ F_{tH} \left(\phi^d, \theta^d \right), F_{tV} \left(\phi^d, \theta^d \right) \right\} \tag{66}$$

$$\beta_r = \arctan_2 \left\{ F_{rH} \left(\phi^a, \theta^a \right), F_{rV} \left(\phi^a, \theta^a \right) \right\} \tag{67}$$

6. The difference between the angles β_t and β_r is the polarization mismatch β between the receiver and the transmitter if both antenna elements were aligned on the same optical axis. The angle α, however takes the different orientation of the receive antenna into account. We thus need to rotate the polarization of the receiver by an angle of

$$\vartheta_{r,t} = \beta_t - \beta_r - \alpha \tag{68}$$

7. The channel coefficients are now calculated according to (4) where the polarization coupling matrix $\mathbf{M}$ notes

$$\mathbf{M}(\vartheta_{r,t}) = \begin{pmatrix} \cos \vartheta_{r,t} & \sin \vartheta_{r,t} \\ -\sin \vartheta_{r,t} & \cos \vartheta_{r,t} \end{pmatrix} \tag{69}$$

Model for the NLOS components For the NLOS components, the transmitted signal undergoes some diffraction, reflection or scattering before reaching the receiver. Following the common Fresnel formula in electrodynamics, the polarization direction can be changed at the boundary surface between two dielectric media. T. Svantesson [Sva01] provided a method for modeling the polarization of a reflected wave where the polarization coupling is a function of several geometric parameters such as the orientation of the scatterers. However, these parameters are not generally available in the SCM. In addition to that, only metallic reflections keep the polarization unchanged. Reflections at dielectric media can cause changes of the polarization being a function of the complex-valued dielectric constant of the media and of the angle of incidence. Hence, not only the polarization angle might change, but also the polarization type. In order to address this issue,

studies of the polarizations effects in individual scattering clusters in several outdoor- and indoor scenarios were done [MTIO09, QOHDD10, PHL+11]. The published results indicate that, in many cases, scattering preserves the polarization quiet well. However, since only the powers of the elements in the polarization coupling matrix were analyzed, no conclusions can be drawn on how elliptic the polarization of the scattered wave becomes.

We assume that the polarization coupling matrix $\mathbf{M}$ for the NLOS components can be described by a combination of linear transformations. Hence, we can take advantage of the existing findings of the cross polarization ratio (XPR). If the XPR is identical for both polarization directions (such as in the WINNER parameter tables), then we can follow the approach from Zhou et. al. [ZRP+05] and calculate an additional NLOS rotation matrix $\mathbf{M}_\gamma$ as

$$\mathbf{M}_\gamma = \begin{pmatrix} m_{vv} & m_{vh} \\ m_{hv} & m_{hh} \end{pmatrix} = \begin{pmatrix} \cos\gamma & -\sin\gamma \\ \sin\gamma & \cos\gamma \end{pmatrix} \tag{70}$$

Following the notations in [OCGD08], we get

$$\mathrm{XPR} = \frac{|m_{vv}|^2}{|m_{hv}|^2} = \frac{|m_{hh}|^2}{|m_{vh}|^2} = \frac{(\cos\gamma)^2}{(\sin\gamma)^2} = (\cot\gamma)^2 \tag{71}$$

$$\gamma = \operatorname{arccot}\left(\sqrt{\mathrm{XPR}}\right) \tag{72}$$

However, when the XPR is different for the vertical and horizontal component [OCGD08, QOHDD10], then we get three parameters:

$$\mathrm{XPR}_v = \frac{|m_{vv}|^2}{|m_{hv}|^2} \quad \mathrm{XPR}_h = \frac{|m_{hh}|^2}{|m_{vh}|^2} \quad \mathrm{CPR} = \frac{|m_{vv}|^2}{|m_{hh}|^2}$$

In order to fulfill all three, we can combine two rotations, one for the vertical and one for the horizontal component, with a scaling operation. We convert XPR_v and XPR_h to rotation angles γ_v and γ_h using (72) and calculate $\mathbf{M}_\gamma$ to

$$\mathbf{M}_\gamma = \begin{pmatrix} \cos\gamma_v & -\tan\gamma_h \cdot \cos\gamma_v \cdot \frac{1}{\sqrt{\mathrm{CPR}}} \\ \sin\gamma_v & \cos\gamma_v \cdot \frac{1}{\sqrt{\mathrm{CPR}}} \end{pmatrix} \tag{73}$$

Elliptic polarization is obtained, when there is a phase difference κ between the horizontal and the vertical component. This is included by a scaling matrix

$$\mathbf{M}_\kappa = \begin{pmatrix} 1 & 0 \\ 0 & \exp j\kappa \end{pmatrix} \tag{74}$$

The antenna-dependent parameters β_r, β_t and α are handled as in the LOS case using (68) which results in a rotation matrix $\tilde{\mathbf{M}}(\vartheta)$. The transformations are then combined to

$$\mathbf{M} = \frac{\sqrt{2}}{||\mathbf{M}_\gamma||_F} \cdot \tilde{\mathbf{M}}(\vartheta) \cdot \mathbf{M}_\gamma \cdot \mathbf{M}_\kappa \tag{75}$$

The normalization with the Frobenius norm $||\mathbf{M}_\gamma||_F$ ensures that $\mathbf{M}$ does not change the power of the multipath component.

eMail: quadriga@hhi.fraunhofer.de

3.3.5 Calculation of the Channel Coefficients

Implemented in ⇒ `channel_builder.get_channels` and ⇒ `array.interpolate`

Next, we combine antenna patterns, polarization and phases to calculate initial channel coefficients for each snapshot of a segment. The antennas are defined by their polarimetric response **F** containing vertical and the horizontal polarization in spherical coordinates [NKS+07].

$$\mathbf{F}(\phi,\theta) = \begin{pmatrix} F_V(\phi,\theta) \\ F_H(\phi,\theta) \end{pmatrix} \tag{76}$$

Since we already know the arrival- and departure angles of each MPC, we can combine the response from both, the Tx and Rx antenna with the polarization rotation and get the coefficient

$$g^{[\mathrm{pol}]}_{r,t,l,m,s} = \mathbf{F}_r(\phi^a,\theta^a)^T \cdot \mathbf{M} \cdot \mathbf{F}_t(\phi^d,\theta^d) \tag{77}$$

Each MPC has a random initial phase ψ^0. Hence, by summing up the 20 sub-paths in order to get one path per cluster, we get a random cluster power. This is compensated by normalization where we first sum up the complex phases and then average the power over all S snapshots of the segment. We calculate the "raw" channel coefficients as

$$\psi^+_{r,t,l,m,s} = \exp\left(-j\psi^0_{l,m} - j\psi_{r,t,l,m,s}\right) \tag{78}$$

$$P^{[\mathrm{norm}]}_{r,t,l} = \frac{1}{S}\sum_{s=1}^{S}\left(\sum_{m=1}^{20}\psi^+_{r,t,l,m,s}\right)^2 \tag{79}$$

$$g^{[\mathrm{raw}]}_{r,t,l,s} = \sqrt{\frac{P_l}{P^{[\mathrm{norm}]}_{r,t,l}}}\cdot\sum_{m=1}^{20} g^{[\mathrm{pol}]}_{r,t,l,m,s}\cdot\psi^+_{r,t,l,m,s} \tag{80}$$

where P_l is the initial power assigned to each cluster.

3.3.6 Path Gain, Shadow Fading and K-Factor

Implemented in ⇒ `channel_builder.get_channels` and ⇒ `parameter_set.get_sf_profile`

Now, we apply the path gain (PG), the shadow fading (SF) and the KF. A common path gain (PG) model for macro-cellular settings is given by M. Hata [Hat80] where the PG scales with the logarithm of the distance d (in units of meters) between BS and terminal.

$$\mathrm{PG}_{[\mathrm{dB}]} = -A\cdot 10\log_{10} d_{[\mathrm{m}]} - B \tag{81}$$

A and B are scenario-specific coefficients which are typically determined by measurements. A often varies between 2 and 4, depending on the propagation conditions, the BS height and other factors.

The values for the SF and the KF are obtained from the map by an interpolation of the surrounding pixels at the position of the s^{th} snapshot. The KF at the initial position is already included due to the scaling in (34). Thus, we have to take this into account and scale the power accordingly.

$$g_{r,t,l,s} = P^{[\mathrm{MT}]}_s \cdot \begin{cases} \sqrt{\frac{K_s}{K_0}}\cdot g^{[\mathrm{raw}]}_{r,t,1,s} & \text{for } l=1; \\ g^{[\mathrm{raw}]}_{r,t,l,s} & \text{otherwise.} \end{cases} \tag{82}$$

$$P^{[\mathrm{MT}]}_s = \sqrt{10^{0.1\cdot\mathrm{PG}_{[\mathrm{dB}]_s}+0.1\cdot\mathrm{SF}_{[\mathrm{dB}]_s}}}\cdot\sqrt{1+P_1\left(\frac{K_s}{K_0}-1\right)}$$

K_s and $\mathrm{SF}_{[\mathrm{dB}]_s}$ are the interpolated values for the KF and the SF from the map, K_0 is the KF at the initial position, $\mathrm{PG}_{[\mathrm{dB}]_s}$ is the path gain at the MT position (81) and P_1 is the power of the LOS cluster from (34).

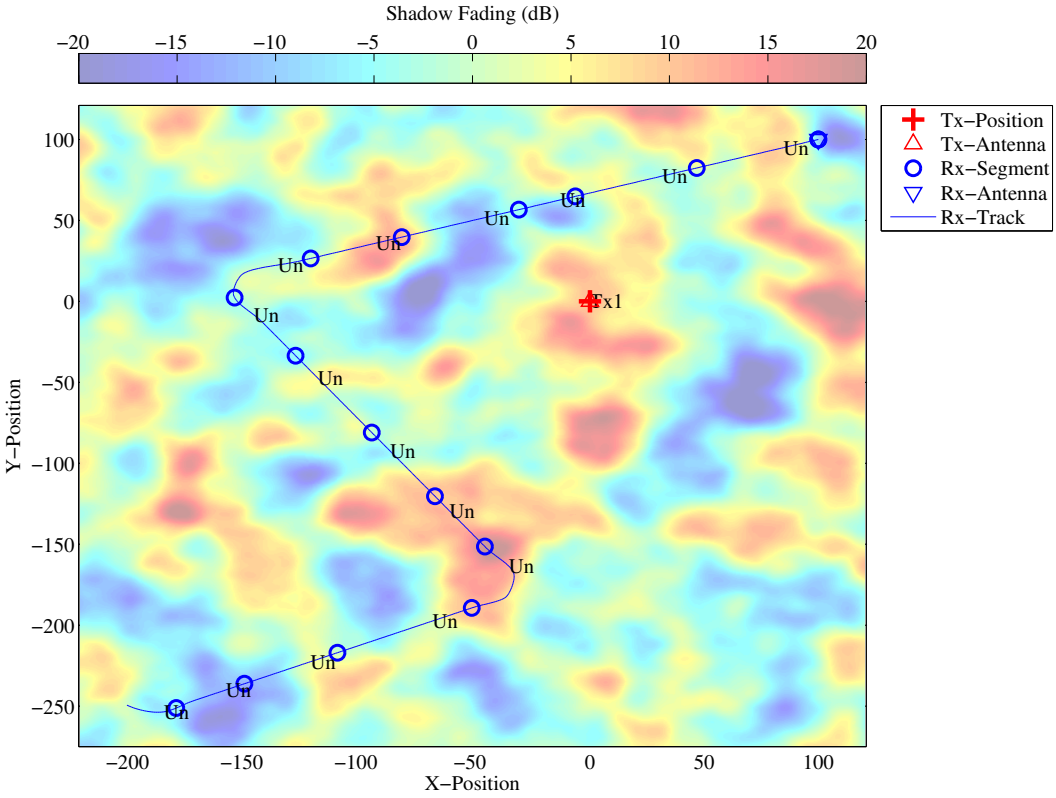

Figure 39: Illustration of the SF drifting along a terminal track

3.3.7 Transitions between Segments

Until now, the calculations were done for each segment of a MT trajectory independently. Longer sequences are created by merging the channels from adjacent segments into one long sequence. The basic idea comes from the documentation of the WINNER II model [KMH+07]. However, it was neither implemented nor tested. Our implementation requires overlapping segments as depicted in Fig. 40, top. Like in a movie, the transition is carried out by ramping down the power of paths in the old segment and at the same time ramping up the power of paths from the new segment. Hence, this process describes the birth and death of clusters along the trajectory. In order to keep the computational overhead low, we split the overlapping part into several sub-intervals equal to the minimum number of clusters in both segments. During each sub-interval, the power of one old cluster ramps down and one new cluster ramps up. We model power ramps by a squared sine function to allow smooth transitions.

$$w^{[\mathrm{sin}]} = \sin^2\left(\frac{\pi}{2} \cdot w^{[\mathrm{lin}]}\right) \tag{83}$$

$w^{[\mathrm{lin}]}$ is a linear ramping function ranging from 0 to 1. $w^{[\mathrm{sin}]}$ is the corresponding sine-shaped ramping function having the advantage of a constant slope at the points 0 and 1, which prevents inconsistencies at the edges of the intervals. If the number of clusters is different in both segments, clusters are ramped up or down without a counterpart from the new/old segment. The ramp is then stretched over the whole overlapping area. For the LOS path, we continuously adjust power and phase over the overlapping area since it has the same delay in both segments.

In order to minimize the impact of the transition on the instantaneous values of the LSPs, paths need to be carefully matched. For example, if a path with a small delay ramps down and a similarly strong path with a longer delay ramps up, then the DS increases. This increase (or decrease) can fluctuate randomly along the merging interval. To balance it out, we pair paths from both segments that minimize the fluctuations. This is done by first determining the values of the DS before and after the transition. Then, we calculate a

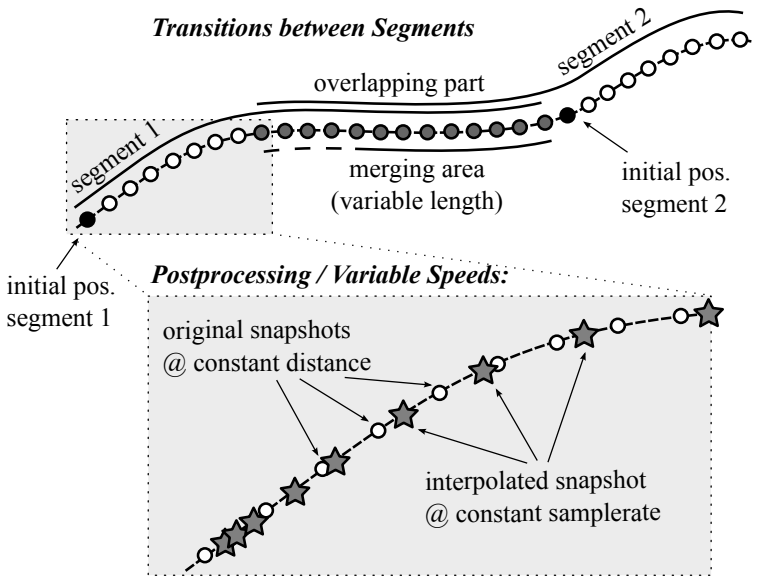

Figure 40: Top: Illustration of the overlapping area used for calculating the transitions between segments (step G); Bottom: Illustration of the interpolation to to obtain variable MT speeds (step H)

target DS for each sub-interval. For example, if the old segment yields a DS of 200 ns and the new segment has 400 ns, then the target-DS will be 220 ns for the first sub-interval, 240 ns for the second and so on. Then we look for a combination of paths to ramp up/down in each sub-interval that best matches the DS along the overlapping area to the target area in a mean square sense.

3.3.8 Postprocessing / Variable Speeds

Realistic channel traces incorporate arbitrary speeds, accelerations and decelerations. Provided that the channel sampling theorem is fulfilled, we can interpolate the coefficients as it is illustrated in Fig. 40, bottom. The white dots represent the snapshots at a constant distance. However, the sample points (gray stars) can have an unequal spacing, e.g. for an accelerated movement. Each sample point in the time domain (given in units of seconds) has a corresponding sample point on the track (in units of meters). The amplitudes and phases of the channel coefficients are interpolated separately using a cubic spline interpolation. The path delays are interpolated with a piecewise cubic hermite interpolating polynomial.

eMail: quadriga@hhi.fraunhofer.de

A Effect of the Simulation Settings on the Delay spread

Here, we performed a set of simulations determining how the delay spread is influenced by the simulations settings. First, a real word scenario in downtown Berlin, Germany, was chosen as reference. Three BS at an ISD of 500 m were equipped with high gain Kathrain antennas. The main beam was pointing at a distance of 450 m. The scenario was split manually into LOS and NLOS segments. The DS for the LOS was fixed to 400 ns (-6.4) and for the NLOS to 900 ns (-6.05). The simulations were then repeated several times using different settings as indicated below.

Settings	CDF	Comment
Off: Antennas SF, KF$_\sigma$, XPR Cluster-AS	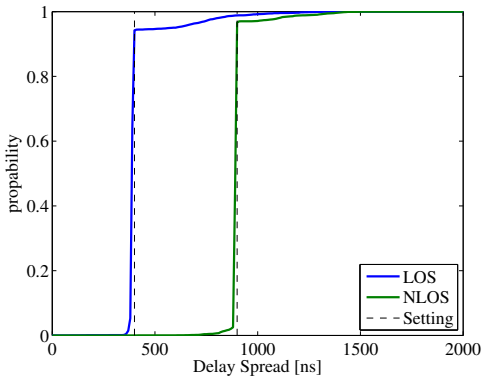	Almost perfect match. The offset in the top of the CDF are due to offsets in the channel merging module. Here, the DS can be increased when strong paths of the other segment ramp up/down. LOS: $\ln\mathcal{N}(-6.40, 0.07)$ NLOS: $\ln\mathcal{N}(-6.05, 0.02)$
On: Antennas **Off:** SF, KF$_\sigma$, XPR Cluster-AS	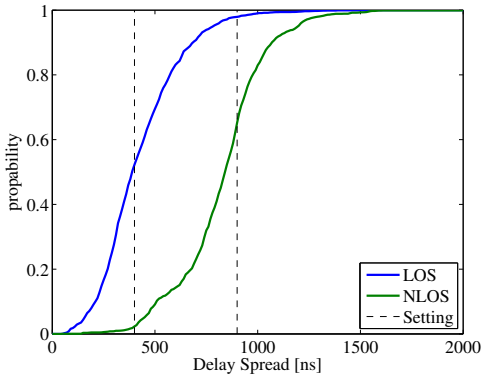	The antennas have a huge impact on the delay spread. The beam patterns at the transmitter and receiver filter the paths. Thus, some paths get more power and other get less. The median stays roughly the same. The STD, however increases significantly. LOS: $\ln\mathcal{N}(-6.40, 0.21)$ NLOS: $\ln\mathcal{N}(-6.07, 0.13)$
On: SF, KF$_\sigma$ **Off:** Antennas, XPR Cluster-AS	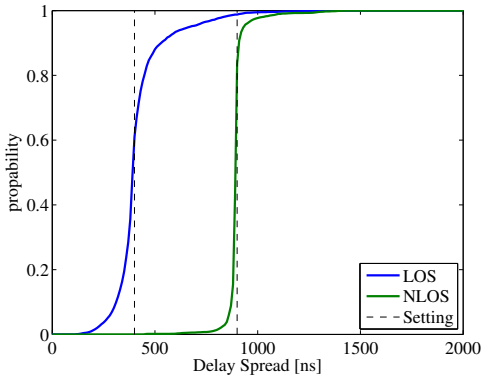	The drifting of the KF and the SF varies the power of the LOS component and the NLOS components along the track. This changes the DS. I.e. high LOS power decreases the DS, lower power increases it. LOS: $\ln\mathcal{N}(-6.40, 0.11)$ NLOS: $\ln\mathcal{N}(-6.05, 0.03)$

eMail: quadriga@hhi.fraunhofer.de

Settings	CDF	Comment
On: Cluster-AS **Off:** Antennas SF, KF$_\sigma$, XPR	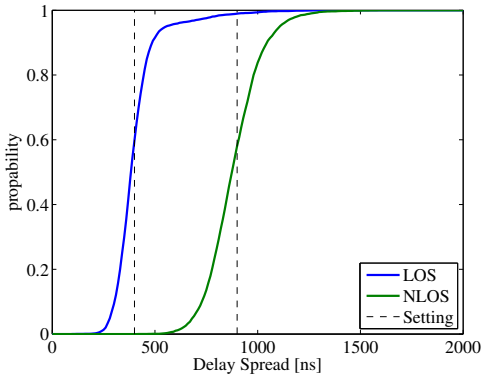	The per-cluster angular spread determines the amount of fading within a path. Fading changes the power of the taps randomly. Thus, some random variation of the DS occurs. LOS: $\ln\mathcal{N}(-6.41, 0.10)$ NLOS: $\ln\mathcal{N}(-6.06, 0.06)$
On: Antennas Cluster-AS **Off:** SF, KF$_\sigma$, XPR	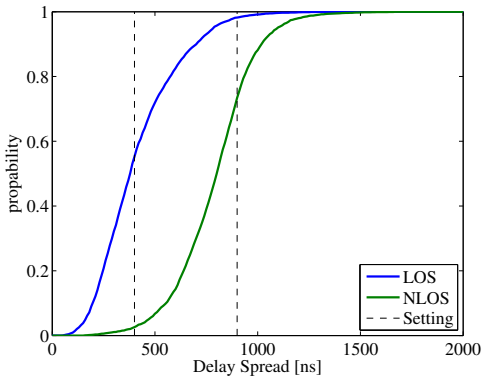	The combination of fading and antennas has no significant impact compared to the antennas-only scenario. LOS: $\ln\mathcal{N}(-6.42, 0.21)$ NLOS: $\ln\mathcal{N}(-6.09, 0.11)$
On: Antennas SF, KF$_\sigma$, XPR Cluster-AS	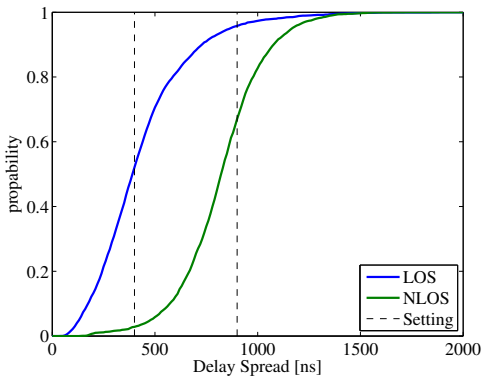	The combination of all effects does not show significant differences compared to the case where only the high gain antennas are used. Thus, it seems that the antennas have the dominant effect on the delay spread. LOS: $\ln\mathcal{N}(-6.40, 0.24)$ NLOS: $\ln\mathcal{N}(-6.08, 0.13)$

eMail: quadriga@hhi.fraunhofer.de